

***"SYNTHESIS, CHARACTERIZATION AND CATALYTIC
ACTIVITY OF GALLIUM AND VANADIUM ANALOGS
OF FERRIERITE TYPE ZEOLITE"***

Mr. SIDDHESH SUDHAKAR SHEVADE

JULY 2000

**"SYNTHESIS, CHARACTERIZATION
AND CATALYTIC ACTIVITY OF
GALLIUM AND VANADIUM ANALOGS
OF FERRIERITE TYPE ZEOLITE"**

A THESIS SUBMITTED TO THE
UNIVERSITY OF PUNE
FOR THE DEGREE OF
DOCTOR OF PHILOSOPHY
(IN CHEMISTRY)

by

Mr. SIDDHESH SUDHAKAR SHEVADE

CATALYSIS DIVISION
NATIONAL CHEMICAL LABORATORY
PUNE - 411008. (INDIA)

JULY 2000



Dedicated to

My Parents and Sister

Certificate

Certified that the work incorporated in the thesis "***SYNTHESIS, CHARACTERIZATION AND CATALYTIC ACTIVITY OF GALLIUM AND VANADIUM ANALOGS OF FERRIERITE TYPE ZEOLITE***" submitted by ***Mr. Siddhesh Sudhakar Shevade***, for the degree of Doctor of Philosophy, was carried out by the candidate under my supervision in the Catalysis Division, National Chemical Laboratory, Pune, India. Materials obtained from other sources have been duly acknowledged in the thesis.

B.S.Rao
(Research Guide)

Acknowledgements

I wish to express my sincere gratitude to Dr. B.S. Rao (Deputy Director, NCL, Pune) for his invaluable guidance and help rendered throughout the course of this investigation without which I would not have completed this thesis successfully.

I am thankful to Dr. A.N. Kotasthane (G.M., R & D, UCIL, Baroda.) for his inspiration to me for selecting research as a mission.

I thank Dr. A.V. Ramaswamy, Head Catalysis Division, for providing me all the facilities to conduct research.

I am grateful to Dr. Shivashankar, Dr. Shiralkar, Dr.(Mrs) V. Ramaswamy, Dr. H.S. Soni, Dr. D. Srinivasan, Dr.(Mrs). Belehkar , Dr. Sathye, Prof. Bhave, Dr.(Mrs) Kashalkar, Dr. Mirajkar, Mr. Kavedia, Dr.(Ms). Awate, Ms. Agashe, Dr. Hegde, Dr. Dongare, , Dr.(Mrs) Chandwadkar and Mrs. Jacob for their help during the study.

I am also thankful to other scientific staff in Catalysis and Inorganic Division for their cooperation.

I wish to thank Dr. Ranjeet Kaur Ahedi, Dr.Suhas Katdare, R. Anand and N.R.Shiju for their unconditional help and encouragement.

I am grateful to all my friends Thomas, Shivanand, Suresh, Satish, Karuna, Sindhu, Sharada, Rajaram, Dr. Jyothi, Dr. Shreekumar, Sabde, Suhas, Sunil, Sudhir, Milind, Ranjeet, Sachin, Deshmukh and Avinash for their moral support and good wishes.

I am very grateful to Prof. Sobalik (Czech Republic) and Prof. Naccache (France) for providing me Characterization data.

I am grateful to my Parents and my sister Girija for their love, unflinching support, patience and encouragement during the course of my research carrier.

Finally I thank Dr. P. Ratnasamy, Director, NCL, Pune for permitting me to work at NCL.

...is?dex

: Contents :

	Pg. No.
Chapter I : Introduction	
1.1 Zeolite	1
1.1.1 General Introduction	1
1.1.2 Historical background	2
1.1.3 Nomenclature	4
1.1.4 Classification	4
1.2 Zeolite Synthesis	8
1.2.1 Natural procedures	8
1.2.2 Hydrothermal	8
1.2.3 Role of template	10
1.2.4 Sol-gel method	13
1.2.5 Mechanism of zeolite crystallization	13
1.2.6 HF and non-aqueous medium	15
1.2.7 Reactors	15
1.2.7.1 Static Autoclave	17
1.2.7.2 Stirred Autoclave	17
1.2.7.3 Teflon Autoclave	17
1.3 Special features of zeolite	17
1.3.1 Acidity	17
1.3.2 Shape selectivity	19
1.3.2.1 Reactant shape selectivity	19
1.3.2.2 Product shape selectivity	19
1.3.2.3 Restricted transition state shape selectivity	19
1.3.2.4 Molecular traffic control	21
1.3.3 Modifications	21
1.3.3.1 Isomorphous substitution	21
1.3.3.2 Cation exchange	22
1.3.3.3 Metal loading	23
1.3.3.4 Dealumination or steaming	23
1.4 Physico-chemical characterization	24
1.4.1 X-ray diffraction	24
1.4.2 Infrared spectroscopy	24
1.4.3 Nuclear magnetic resonance	26
1.4.4 Thermal analysis	27
1.4.5 Sorption and diffusion properties	27
1.4.6 Scanning electron microscopy	28
1.4.7 Electron spin resonance spectroscopy	28
1.4.8 UV-vis spectroscopy	29
1.5 Catalysis over zeolite	29
1.5.1 Acidic reactions	29
1.5.2 Redox reactions	30
1.5.3 Reactors	30
1.6 Application of zeolites	32
1.7 Environmental catalysis	34
1.8 Ferrierite	35

1.8.1	Discovery	35
1.8.2	Structure	36
1.8.3	Uses	38
1.9	Conclusion	38
1.10	Aim of the present work	38

Chapter II : Ga-FER

2.1	Introduction	47
2.2	Synthesis	48
2.3	Characterization	49
2.3.1	XRD	50
2.3.2	Surface area	54
2.3.3	Thermal analysis	55
2.3.4	Framework FT-IR	57
2.3.5	Acidity measurement by IR	59
2.3.6	Scanning electron microscopy	62
2.3.7	Nuclear magnetic spectroscopy	64
2.4	Catalysis	67
2.4.1	Benzene hydroxylation	67
2.4.1.1	Cumene process	68
2.4.1.2	Utilization of N ₂ O	69
2.4.1.3	Effect of temperature	70
2.4.1.4	Effect of W.H.S.V.	72
2.4.1.5	Effect of Benzene/N ₂ O mole ratio	73
2.4.1.6	Effect of gallium content	74
2.4.1.7	Time on stream study	74
2.4.1.8	Comparison between different FER	74
2.4.1.9	Kinetics	75
2.4.2	Benzene alkylation	76
2.4.2.1	Effect of temperature	79
2.4.2.2	Time on stream study	81
2.4.2.3	Influence of benzene to ethanol ratio	82
2.4.2.4	Effect of flow rate	83
2.4.2.5	Comparison between different FER	84
2.5	Conclusions	85

Chapter III : V-FER

3.1	Introduction	89
3.2	Synthesis	89
3.3	Characterization	91
3.3.1	XRD	91
3.3.2	Surface area	94
3.3.3	Thermal analysis	96
3.3.4	Framework FT-IR	97
3.3.5	Acidity measurement by IR	98
3.3.6	Scanning electron microscopy	101

3.3.7	UV-vis spectroscopy	102
3.3.8	Electron spin resonance spectroscopy	103
3.3.9	Nuclear magnetic spectroscopy	104
3.4	Catalysis	107
3.4.1	Toluene oxidation	108
3.4.1.1	Experimental	108
3.4.1.2	Product analysis	109
3.4.1.3	Results and discussion	109
3.4.1.4	Effect of temperature	109
3.4.1.5	Effect of solvent	110
3.4.1.6	Effect of vanadium quantity	110
3.4.2	Styrene epoxidation	112
3.4.2.1	Experimental	112
3.4.2.2	Product analysis	113
3.4.2.3	Results and discussion	113
3.4.2.4	Effect of solvent to styrene	114
3.4.2.5	Effect of solvent polarity	115
3.4.2.6	Effect of temperature and pressure	115
3.4.2.7	Comparison of different molecular sieves	117
3.4.3	Hydrogenation of nitrobenzene	118
3.4.3.1	Experimental	119
3.4.3.2	Product analysis	119
3.4.3.3	Results and discussion	120
3.4.3.4	Effect of temperature	120
3.4.3.5	Time on stream study	121
3.4.3.6	Effect of W.H.S.V.	122
3.5	Redox behavior of vanadium species by ESR spectroscopy	124
3.6	Conclusion	128
Chapter IV : SUMMARY		
4.1	Ga-FER	132
4.1.1	Synthesis	132
4.1.2	Characterization	133
4.1.3	Catalysis	133
4.2	V-FER	134
4.2.1	Synthesis	134
4.2.2	Characterization	135
4.2.3	Catalysis	135
List of publication		137

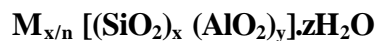
CHAPTER I

INTRODUCTION

1.1 Zeolites

1.1.1 General introduction:

Zeolites are water containing crystalline aluminosilicates of natural or synthetic origin with highly ordered structures [1-8]. They consist of SiO_4 and AlO_4^- tetrahedra, which are interlinked through common oxygen atoms to give a three dimensional network by which long channels are formed. In the interior of these channels, which are characteristic of zeolites, are water molecules and mobile alkali metal ions, the latter can be exchanged with other cations. These compensate for the excess negative charge in the framework resulting from the aluminum content. The interior of the pore system, with its atomic-scale dimensions, is the catalytically active surface of the zeolites. The inner pore structure depends on the composition, the zeolite type, and the cations. Thus, zeolites are represented by the general formula:



where \mathbf{M} is the charge compensating cation with the valency \mathbf{n} . \mathbf{M} represents the exchangeable cation (eg. Alkali or alkaline earth metals or an organic cation). The ratio x/y can have the value 1 to ∞ . According to Lowenstein's rule no two aluminum tetrahedra can exist adjacent to one another. The Si/Al molar ratio corresponds to the acid sites in the zeolites. \mathbf{z} represents the number of water molecules, which can be reversibly adsorbed or desorbed in the pores. Zeolites are also popularly known as *molecular sieves*' due to their ability to differentiate between molecules of different shapes and size.

Zeolites have found widespread application as adsorbents, ion exchange materials, detergent builders and catalysts, especially in petroleum refining, petrochemicals, and as Fluidized

Cracking Catalysts (FCC) [7]. Furthermore, zeolite functionality has also been compared with catalytic antibodies [9] and metalloenzymes [10].

The characteristic features of zeolites, which make them effective catalysts, are:

- High surface area and adsorption properties.
- Active acid sites; to use as solid acid.
- Shape selectivity (due to uniform pores and channels),
- Easy regeneration
- High thermal stability.
- Eco friendly.

1.1.2 Historical background:

Axel Fr. Cronstedt [11] (1756), a Swedish mineralogist, observed that certain rock minerals, when heated sufficiently, appeared as were boiling. He named them '*Zeolites*' (**zeo** means to boil and **lithos** means stone). Damour [12] observed that zeolites could be reversibly dehydrated without alteration in the structure or morphology. The role of water as a mineralizing agent, aided by alkaline conditions, drew the attention of mineralogists towards hydrothermal reaction conditions for the synthesis. The first claim, to have synthesized a zeolite named levynite, was made by St. Claire Deville and Thompson in 1862 [13,14]. In 1962, the commercialization of natural zeolites namely chabazite, erionite, mordenite and clinoptillolite started for a number of applications [15]. McBain introduced the term *Molecular Sieves* to describe a class of materials that exhibited selective adsorption properties [16]. Molecular sieves separate components of a mixture on the basis of molecular size and shape differences.

However, Barrer [17] was the first to demonstrate the molecular sieve behavior of zeolites and their potential in separation techniques (Fig. 1.1). Since 1940, systematic studies on zeolites were undertaken. ZK-5 [18,19,20] was the first known synthetic zeolite (no natural counterpart) crystallized under hydrothermal conditions. Hydrogen forms of zeolites were also made for the first time in the year 1949, by heating ammonium-exchanged forms of mordenite [21]. Special features of molecular sieves and zeolites are mentioned below.

Molecular Sieve	Zeolite
<ul style="list-style-type: none"> ➤ It covers all the porous materials which can separate molecules by their size. ➤ AIPO's and their metal analogs, TS-1, VS-1 and all the metallosilicates etc. 	<ul style="list-style-type: none"> ➤ A particular class of molecular sieves containing Aluminosilicates. ➤ ZSM-5, X, Y, Beta, L, Ferrierite, Mordenite etc.

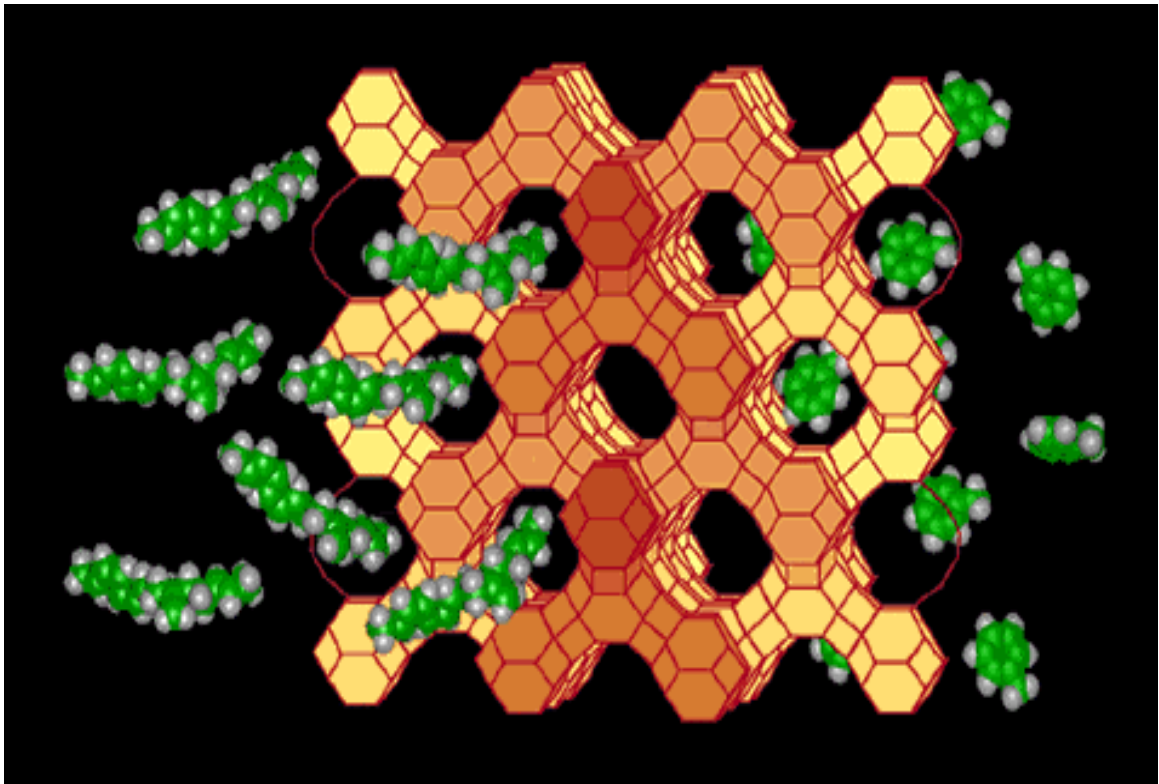


Fig. 1.1.: ZEOLITE : MOLECULAR SIEVE

1.1.3 Nomenclature:

Although, there is no systematic nomenclature for molecular sieve materials, the Structure Commission of International Zeolite Association and IUPAC has assigned structural codes to synthetic and natural zeolites [22,23]. Designations consisting of three capital letters have been used to identify structure types (Table 1.1). The codes for zeolite identifications have generally been derived from the names of the type of species, and do not include numbers and characters other than Roman letters. Structure type codes are independent of chemical composition, distribution of various possible T atom, (e.g. Si⁴⁺, Al³⁺, P⁵⁺, Ti⁴⁺, etc.), cell dimension or crystal symmetry.

Table 1.1 : Structural Codes and Zeolites

Structural Code	Zeolites
FAU	Faujasite, X and Y
MFI	Mobil Five : ZSM-5
MEL	Mobil Eleven : ZSM-11
MOR	Mordenite
FER	Ferrierite, ZSM-35, ZSM-21
MCM's	Mobil Carbon Materials

1.1.4 Classification:

Zeolites have been classified in accordance with the morphology [24], crystal structure [1,3,25], chemical composition [26] and effective pore diameter [27,28].

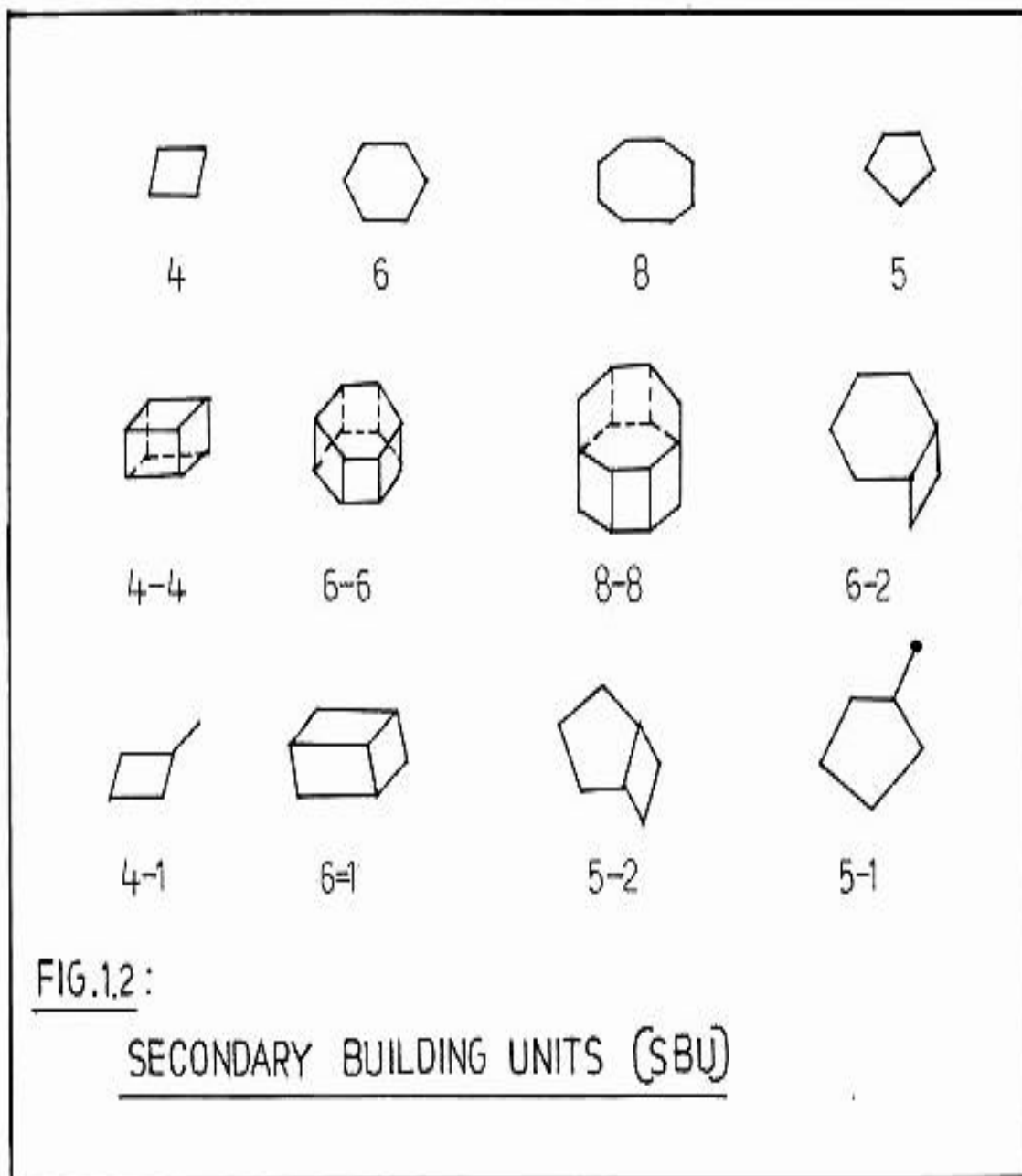
Table 1.2 : Classification of zeolite on the basis of Morphology

The tetrahedra are linked more numerous in one crystallographic Fibrous
--

direction

Zeolites have structural linkages more numerous in one plane and are characterized by a platy cleavage **Lamellar** (open framework materials)

Smith [29], Fischer [30] and Breck [31] have structurally classified zeolites on the basis of differences in the secondary building units (SBU). SBU [Fig.1.2] are the aluminosilicate oligomers having chain, ring and cage like structures which are basic building units of zeolite framework structure.



Flanigen [26] has also classified zeolites according to their chemical composition as shown below and some of their salient features are described.

Table 1.3: Classification of Zeolites on the basis of Chemical Composition.

Low silica zeolites	Si/Al = 1- 1.5	A, X, sodalite, etc.
intermediate silica zeolites	Si/Al = 2.0 - 5.0	erionite, chabazite, mordenite, X,Y,L, Ω , etc.
high silica zeolites	Si/Al = 5 – 500	MFI, FER, BEA, etc.
pure silica zeolites	Si/Al = ∞	Si-MFI (silicalite-1), Si-MEL (silicalite - 2), Si-TON, Si-MTW, Si-ZSM-48, Si-NCL-1, Si-FER, Si-UTD-1, etc.

- The thermal stability increases from low silica zeolites to high silica zeolites.
- The high silica zeolites are hydrophobic in nature while low silica zeolites are more hydrophilic.
- The acidity tends to increase in strength with increase in Si/Al ratio.
- The cation concentration and ion exchange capacity (which is directly proportional to the aluminum content) decreases with the increase in Si/Al ratio.
- Low silica zeolites are formed predominantly with 4-, 6- and 8- rings of tetrahedra while in case of intermediate silica zeolites there is an onset of 5- rings and in case of high silica zeolite 5-ring tetrahedra predominate in the structure.

Zeolites are also classified according to their effective pore diameter, which is dependent on the number of tetrahedra present in the ring aperture, which circumscribes the pore. Barrer [27] has classified zeolites into five groups. Sand [28] has further modified the classification into three groups, as shown in Table 1.4. In 1988, Davies *et al.* discovered a very large pore aluminophosphate molecular sieve VPI-5 containing 18 membered ring pore openings [32]. Recently, an extra large pore gallophosphate molecular sieve containing 20 membered ring pore opening called cloverite has been synthesized [33]. A 14- membered ring structure called UTD-1 has also been reported [34].

Table 1.4 : Classification of zeolites on the basis of the effective pore diameter [28]

Small pore (8 MR)	Medium pore (10 MR)	Large pore (12 MR)
Li-A	Dachiardite	cancrinite
MTN	Epstilbite	Linde X,Y, L.
NU-1	Ferrierite (FER)	gmelinite
bikitaite	heulandite	mazzite
brewsterite	laumontite	mordenite
chabazite	ZSM-5 (MFI)	offretite
clinoptilolite	ZSM-11 (MEL)	ZSM-12 (MTW)
edingtonite	EU-1 (ZSM-50)	omega
erionite	Stilbite	Beta (BEA)
gismondine	ZSM-23	
ZK-5	theta-1 (ZSM-22)	
Levynite	ZSM-48 (EU-2)	
Linde A		
merlonite		
natrolite		
Paulingite		
phillipsite		
Rho		
thomsonite		

1.2 Synthesis of zeolites

1.2.1 Natural zeolites :

The crystallization of natural zeolites involve geological timescale. Large crystals of zeolite minerals grow in cavities in basic volcanic or metamorphic rocks in the presence of mineralizing solutions. Vast sediments of natural zeolite microcrystallites originate from an alteration of volcanic glass and occur in chemical sedimentary rocks of marine origin. The formation of these natural zeolites from volcanic glass and saline water as reactants must have occurred in the temperature range 300-350 K and at $\text{pH} \geq 13$, requiring several years for crystallization [35,36]. Huge deposits of natural zeolites are present in all oceans. The natural zeolites find many applications but are less suitable as catalysts due to the presence of impurities. In the following table some of the well known natural zeolites with the year of discovery has been shown.

Table 1.5 : Natural Zeolites and the year of discovery [37]

Zeolite	Year of Discovery	Zeolite	Year of Discovery
Stilbite	1756	Erionite	1890
Chabazite	1772	Ferrierite	1918
Faujasite	1842	Barrerite	1974
Mordenite	1864	Merlinoite	1976

1.1.2 Hydrothermal synthesis :

Morey and Ingerson [38] have already documented reports of zeolite synthesis up to 1937. Barrer[39], in 1940 initiated systematic study on the hydrothermal synthesis of zeolites and also demonstrated the use of zeolites on separations by molecular action and sorption.

Zeolites are synthesized under hydrothermal conditions by the reaction of certain basic oxides (e.g. K_2O and Na_2O) with silica and alumina. Zeolites with various structures as well as varied compositions and properties can be synthesized by varying the reactants. Zeolite crystallization is mainly a nucleation-controlled process, occurring in homogenous alkaline aqueous gels, in the temperature range of 348 to 523K. A number of silica and alumina sources [1] can be utilized in the synthesis for gel formulation and the final product is generally source dependent.

Inorganic cations (like alkali / alkaline earth metals) play a major role in directing a particular structure. Structural sub-units of zeolites such as double four membered ring (D_4R), double six membered ring (D_6R) and cancrinite, gmelinite and sodalite cages are thought to be formed by way of clathration of an alkali cation with silica and alumina [1,40,41,42]. Na^+ and hydrated sodium ions were suggested to be responsible for the formation of D_4R , D_6R , gmelinite and sodalite cages [1,43]. K^+ , Ba^{+2} and Rb^+ ions were believed to be responsible for directing cancrinite cages [1,43].

The major drawback of the above synthesis procedures was that the zeolites with high silica to alumina ratios could not be synthesized using inorganic cations alone. Furthermore, these materials possessed low thermal stability.

Introduction of organic ammonium cations (e.g. tetramethyl ammonium cation) called templates, in zeolite synthesis led to a major breakthrough in zeolite science and as a result more siliceous materials i.e. zeolites with high silica to alumina ratios could be crystallized.

1.2.3 Role of Template:

The utilization of quaternary ammonium cation and their inherent capacity to “template” the formation of zeolite structures had two major impacts on zeolite science. The first impact relates to larger size of the organic cation. Template cations being larger cannot be placed close packed in zeolite pore system as their alkali / alkaline earth counter parts. Preservation of charge neutrality, therefore, forced the anionic aluminum sites to be equivalently spaced at larger intervals and hence zeolites with higher silica to alumina ratios could be synthesized. Furthermore, it led to the synthesis of ultrastable species.

The second major advantage of the addition of quaternary ammonium and other organic ions to hydrothermal synthesis was that the structure directing functions contributed by these ions could influence the silica polymerization procedure in such a way that many unique zeolite structure types were found to crystallize in presence of certain organic bases and in combination with alkali and / or alkaline earth salt [1].

The structure-directing role of a quaternary ammonium compound appears to influence the variety of SBU's (Secondary Building Unit) present in the hydrothermal magma. The result of this is that a particular organic base does not lead to the formation of specific zeolite structure type but rather a variety of structure types, which can be compiled from the various combinations of secondary building units. An example of this is evident in the systems employing TMA as quaternary amine e.g. gismondine, sodalite, zeolite P, N-A, NU-1, ZSM-5, Ferrierite, etc. while certain zeolite structures tend to be preferentially crystallized in the presence of certain organic bases as reported by Lok et al [44]. The next generation of molecular sieves was the synthesis of AlPO_4 molecular sieves wherein phosphate substitutes silica. More than 20 unique three dimensional aluminophosphate molecular sieve structures could be crystallized from more

than 45 amines and quaternary ammonium ions [44]. Substituted aluminophosphates [45,46] and zinc (or beryllio-) phosphates (or arsenates) [47,48] have also been reported. Tetrahedrally coordinated atoms in some of these structures can be substituted by other metal ions, which give rise to other similar type of structures such as gallophosphates [49,50].

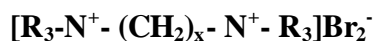
Although zeolites have desirable catalytic properties they become inadequate when reactants with dimensions larger than the pore diameter of the zeolite have to be processed. As a result scientists diverted their efforts towards synthesis of mesoporous type materials using large template molecules (e.g. surfactants). This family was termed as M41S and had large channels from 1.5 to 10 nm ordered in a hexagonal (MCM-41), cubic (MCM-48) and lamellar (MCM-50) manner with surface areas above 700 m²/g [51-61]. Isomorphous substitution of heteroatoms such as Ti⁴⁺, V⁴⁺, Zr⁴⁺, Cr³⁺ etc. in M41S type materials is now well known [62].

Recently a number of di-quaternary ammonium salts also have been used as templates for the synthesis of high silica molecular sieves. (Table 1.6)

Table 1.6: Diquaternary ammonium salts and corresponding synthesized zeolites.

No.	diquaternary ammonium salt	Zeolite
1.	trimethylene bis (trimethyl ammonium bromide)	ZSM-39 [63], EU-1 [64]
2.	pentamethylene bis(trimethyl ammonium bromide)	EU-1 [65]
3.	hexamethylene bis(trimethyl ammonium bromide)	ZSM-48 [66] , EU-1 [67]
4.	heptamethylene bis(trimethyl ammonium bromide)	ZSM-23 [68] , MCM-10 [69]
5.	tetramethylene bis(ethyl dimethyl ammonium bromide)	ZSM-12 [70]
6.	hexamethylene bis(ethyl dimethyl ammonium bromide)	ZSM-12 [71]
7.	hexamethylene bis(tripropyl ammonium bromide)	ZSM-5 [72]
8.	hexamethylene bis(tributyl ammonium bromide)	ZSM-5 [73]
9.	hexamethylene bis(triethyl ammonium bromide)	NCL-1 [73,74]

The di-quaternary salts may be represented by the general formula:



Where **R** may be methyl, ethyl, propyl, butyl, benzyl or a combination of these and **x** may have values in the range 3 to 10. In the case of bis quaternary ammonium cations, both the chain length and terminal alkyl group determine the particular structure that may be crystallized. By systematically increasing the chain length in bis quaternary salts and keeping their terminal alkyl groups constant e.g. methyl, a number of zeolite structures can be crystallized. Recently, a high silica, large pore, ZSM-12 zeolite has been synthesized using mixed alkali quaternary salt of the formula: $[(\text{C}_2\text{H}_5) (\text{CH}_3)_2\text{-N}^+ \text{- (CH}_2\text{)}_6\text{-N}^+ (\text{CH}_3)_2(\text{C}_2\text{H}_5)]2\text{Br}^-$ and $[(\text{CH}_3)_2(\text{C}_6\text{H}_5\text{CH}_2)\text{-N}^+ \text{- (CH}_2\text{C}_6\text{H}_5)(\text{CH}_3)_2]2\text{Br}^-$ [71]. A novel, high silica zeolite, NCL-1 has been reported using a new di-quaternary ammonium salt [73,74].

1.2.4 Sol-Gel synthetic Route (Wetness Impregnation Method) :

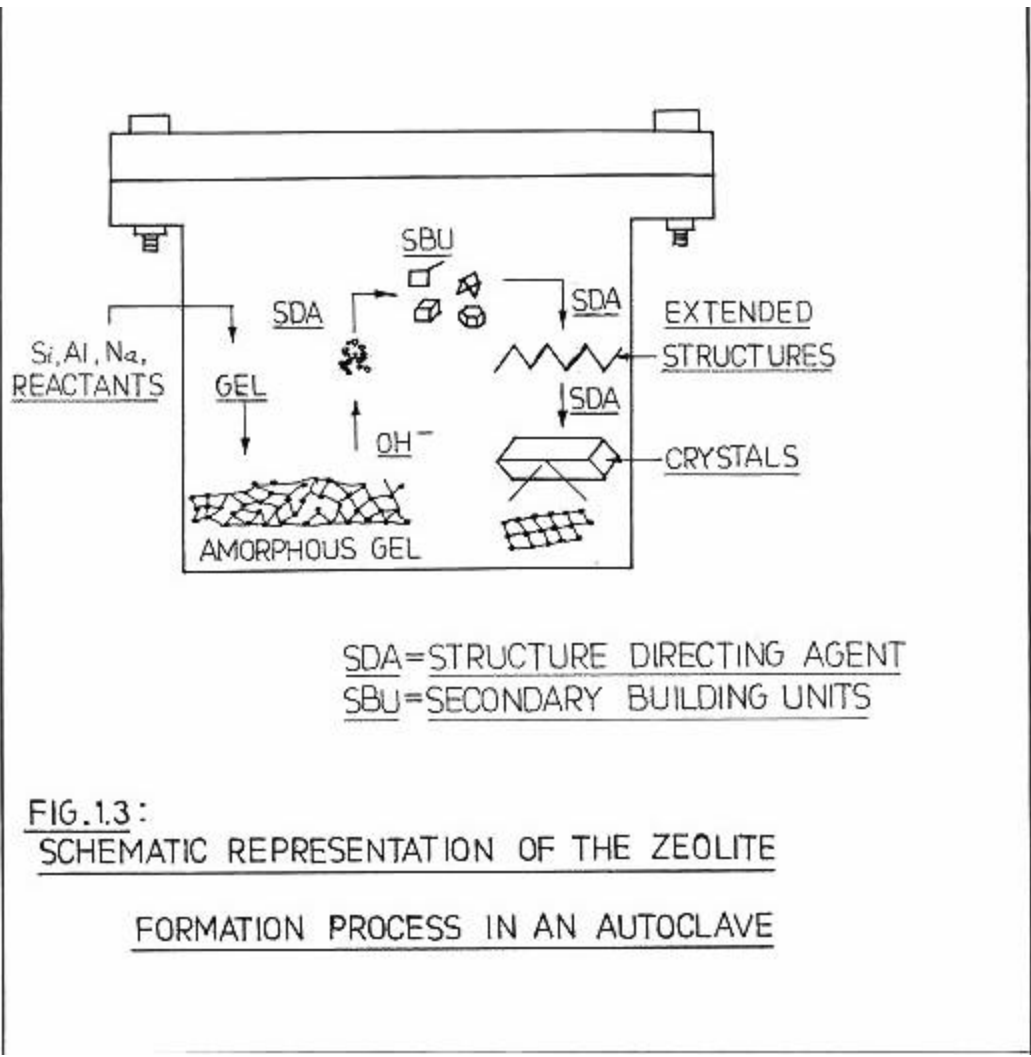
This synthesis procedure was developed to overcome the problems in metal incorporation in the molecular sieve framework. During TS-1 synthesis, TiO_2 precipitation was the major problem. Pandovan et.al. [74a] and Uguina et.al. [74b] have developed an alternative route for its synthesis using wetness impregnation method. In this process silica-metaloxide ($\text{SiO}_2\text{-MO}_2$) cogel (prepared by sol-gel method) is impregnated with a quantity of the template solution similar to the pore volume of the solid. The crystalline molecular sieve is obtained under autogenous pressure at high temperature. Presently research in this field is oriented towards the development of many new materials which can't be synthesized by the conventional methods.

1.2.5 Mechanism of zeolite crystallization:

The actual mechanism of zeolite crystallization is yet a mystery due to the complex interactions occurring in the hydro-gel. Sand [75] in brief has described the reactions that can occur during the synthesis as follows:

1. precipitation of a gel phase,
2. dissolution of the gel,
3. nucleation of zeolite,
4. continued crystallization and crystal growth of the zeolite,
5. Dissolution of the initial meta stable phase,
6. Nucleation of the more stable metastable phase or phases,
7. Continued crystallization and crystalline growth of the new crystalline phase while the initial crystals are dissolved,
8. Dissolution of the metastable phase,
9. Crystallization and crystal growth of the final crystalline phase.

Weitkamp [76] has described the zeolite synthesis diagrammatically [Fig. 1.3].



Two mechanisms have been suggested for the zeolite formation. Kerr [77,78] postulated crystal growth from a solution for zeolites A and X. McNicol et al [79] suggested that the nucleation and crystal growth of zeolite takes place within the gel phase. It was evidenced by crystallizing zeolites from clear solutions under hot conditions with the help of microscope [80]. The nucleation and subsequent crystallization can occur readily in the solution. Culfaz and Sand [81] proposed that the nucleation occurs at solid liquid interphase wherein it was suggested that nucleation, mass transfer of species by diffusion and zeolite crystallization occur in the boundary layer at the solid-liquid interface. There are other physical variables affecting the zeolite

formation such as order of mixing, rate of addition of aluminate to silicate solution and vice-versa and also agitation rate.

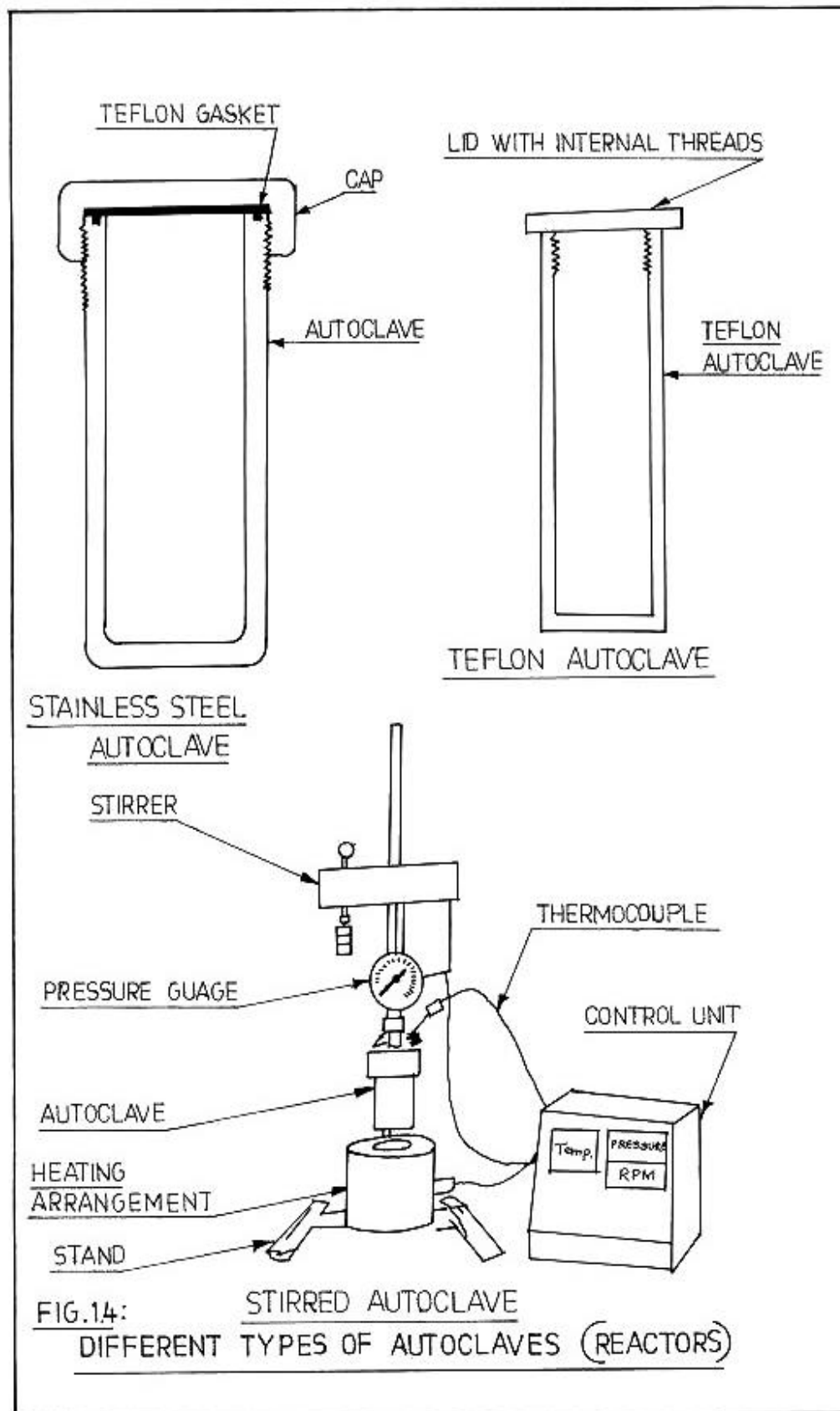
1.2.6 HF and Non-aqueous medium

Due to solubility problem certain metal analogs of zeolite cannot form in aqueous medium. In such cases F⁻ anions can fulfil the catalytic function of OH⁻ ions, allowing zeolite formation in acid (HF) medium. The use of F⁻ anions increases the solubility of certain tri- and tetravalent elements (e.g. Ga^{III}, Ti^{IV} and V^V) [82,83] through complex formation. The crystal formed in these solutions contain less structural defects. A disadvantage of this process is the longer crystallization period and large size crystal formation.

Alcohols are known as non-aqueous medium for zeolite crystallization. Recently Kuperman et.al [84] utilized pyridine, triethylamine and polyethylene glycol as non-aqueous media. HF-pyridine and HF-alkylamines are claimed to be novel mineralizers by acting as reservoirs for anhydrous HF in the organic solvent, thereby allowing the amount of reactant water to be controlled.

1.2.7 Reactors for zeolite synthesis :

Various types of reactors are employed in the synthesis of zeolites. They range from static autoclaves to stirred reactors at temperatures around 200 with autogenous pressure. [Shown in the Fig.1.4]



1.2.7.1 Static Autoclave: It is a stainless steel cylindrical vessel with capacities varying from 100 ml to 5000 ml. The top portion, closed with a lid provided with nuts and bolts or self threaded lid, is to withstand and maintain the in built hydrothermal pressure of the reactant materials generated during the synthesis. Such type of reactors are heated by laboratory ovens maintained at the desired temperature.

1.2.7.2 Stirred Autoclave : This is similar to the above mentioned stainless steel reactor having additional stirring arrangement with controlled heating.

1.2.7.3 Teflon Autoclave : This is special type of reactor used for zeolite synthesis in HF medium. A Teflon vessel of the dimensions little lesser to the stainless steel autoclave is fitted inside the static autoclave. For heating it is being kept inside a oven.

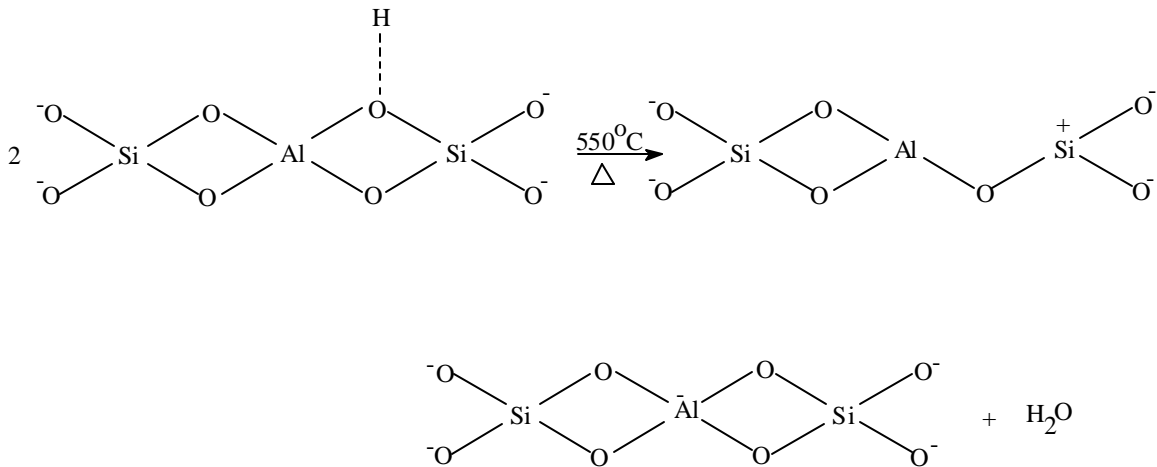
1.3 Special Features of Zeolites

1.3.1 Acidity :

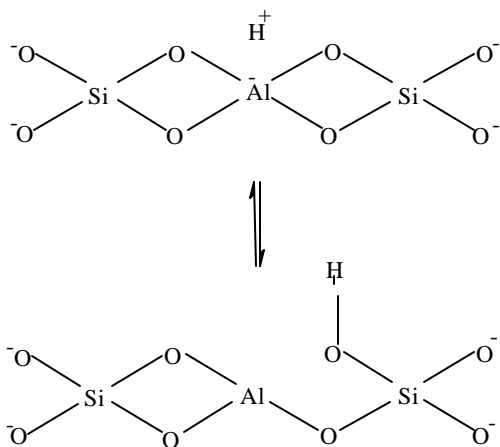
When the cationic form of any zeolite is converted into its H-form or proton form, the zeolite is said to be active or acidic. Acidity is dependent upon the number of Al^{3+} present in the framework or in other words zeolites with low silica to alumina ratios are highly acidic and their acidity decreases with increase in silica to alumina ratio. Substitution of trivalent metal atoms such as Ga^{3+} , Fe^{3+} , B^{3+} , etc. modifies the acidity within the zeolite.

When hydrogen (proton) of the zeolite framework exhibits the property to act as a proton donor it is referred to as Brönsted acid [85-87].

When the zeolite is heated to 823 K, Si—O—Al bond breaks giving rise to Lewis acid site and water.



Generally, in zeolites both Brönsted and acid Lewis sites exist simultaneously.



From the dissociation energy calculations it was shown that the bridging hydroxyl groups are more acidic than the terminal hydroxyl groups [88]. These results were further supported by the lower vibrational frequency of the bridging hydroxyl groups [89]

1.3.2 Shape selectivity:

Shape selectivity plays an important role in molecular sieve catalysis. Highly crystalline and well-defined uniform channels are the key features that molecular sieves (zeolites) offer over other materials. Weiz and Friette [90] were the first to describe the shape selectivity. The pore size and shape may affect the selectivity of a reaction in four 4 ways:

1.3.2.1 Reactant shape selectivity:

This results from limited diffusivity of some of the reactants, which cannot effectively enter and diffuse inside the crystal. The zeolite pore is such that it admits only certain smaller molecules from the reactants and excludes larger molecules and hence in the reaction mixture only the smaller molecules react effectively [Fig. 1.5a]. In catalytic cracking, activity of n-heptane is more than any other bulkier molecule (2 methyl hexane).

1.3.2.2 Product shape selectivity:

When certain bulkier compounds are formed or produced within the zeolite pores during a reaction they can't diffuse out due to large dimensions. These will either be converted to smaller products and diffuse out or they may block the pores resulting in the deactivation of the catalyst. For example in toluene methylation, p-xylene is the major product in modified zeolites as compared to bulky o- and m- isomers due to pore diameter restrictions [Fig. 1.5b].

1.3.2.3 Restricted transition state shape selectivity:

This type of shape selectivity is observed when certain reactions are prevented because of restrictions in the inner pore space for the corresponding transition state. Diffusion of reactants and products in this situation are not hindered nor are the reactions involving smaller transition state [Fig. 1.5c].

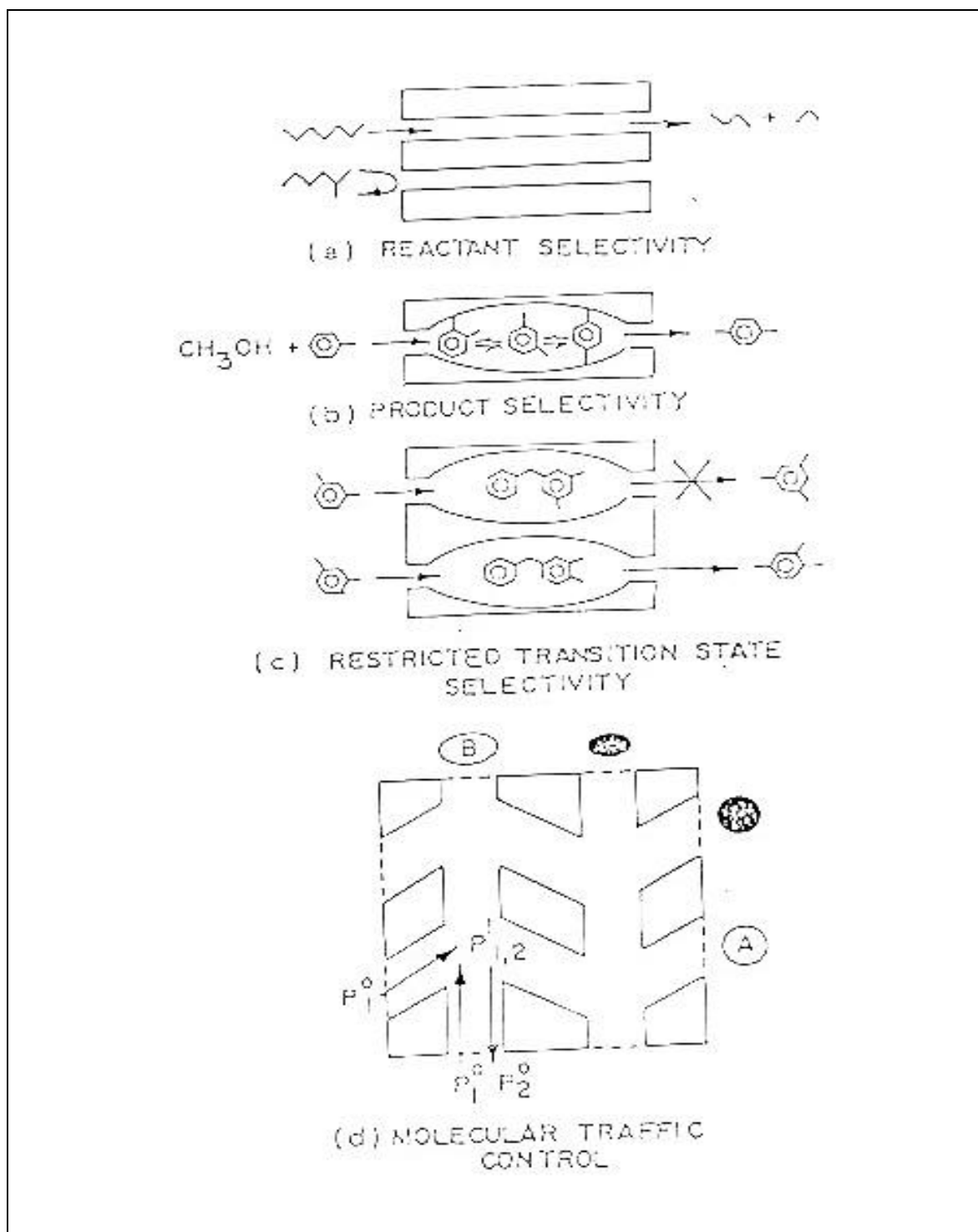


Fig. 1.5 : Shape selectivity in the Zeolite structure

1.3.2.4 Molecular traffic control:

Derouane and Gabelica [91] proposed a new type of shape selectivity in zeolites containing intersecting channel of different diameters. According to them, in cases where zeolites contain more than one type of intersecting channels, the reactants preferentially enter through one set of channels and the products diffuse out through the other, thus minimizing counter diffusion [Fig. 1.5d].

Several model reactions viz. constraint index [92], refined constraint index [93], spacious index [94], o-p index [95], DEB distribution in EB disproportionation [96] have been used to determine the shape selectivity of the zeolites quantitatively.

1.3.3 Modifications :

The use of zeolites can further be enhanced by altering the properties. Properties of zeolites can be modified either by isomorphous substitution or by cation exchange, metal loading or dealumination.

1.3.3.1 Isomorphous substitution:

Modification of zeolites by isomorphous substitution induces variation in acidic properties and changes in unit cell volume, which may lead to interesting catalytic properties. Goldsmith [97] was the very first to report isomorphous substitution of Si^{4+} by Ge^{4+} in the lattice. This was followed by isomorphous substitution of Si^{4+} or Al^{3+} by elements such as B [98-102], Fe [99,100], Ga [99,101], Ti [103], V [104], etc. It has been well established [105] that isomorphous substitution of Si and Al by P, Ge, B, Ga and Al modify the acid strength and catalytic properties of various zeolites. This was followed by synthesis of a number of new aluminophosphate molecular sieves containing Al^{3+} and P^{5+} in lattice. Further, the isomorphous

substitution of Co^{2+} , Fe^{3+} , Mg^{2+} , Zn^{2+} , Be^{2+} , B^{3+} , Ga^{3+} , Cr^{3+} , Ti^{4+} , Si^{4+} and Mo^{3+} in AIPO structure is also well established [85,105].

Barrer [106] classified four types of isomorphous substitution in zeolites namely, (i) cation exchange, (ii) framework substitution, (iii) isomorphous substitution of isotopes and (iv) substitution of intracrystalline salts and molecular water. Isomorphous substitution can be achieved by direct hydrothermal synthesis or by post synthesis methods. Using characterization techniques such as XRD, IR, MASNMR, ESR, UV-VIS, XPS and by catalytic test reactions, the tetrahedral occupancy of the substituted metal cation can be verified.

1.3.3.2 Cation exchange:

The ion exchange capacity of a zeolite is dependent upon the amount of aluminum present in the framework of zeolite. Majority of the zeolites synthesized, are in their cationic forms, wherein, positively charged cations neutralize the charge created by the aluminum tetrahedra on the framework. These extra framework cations are exchangeable and the degree of cation exchange depends on:

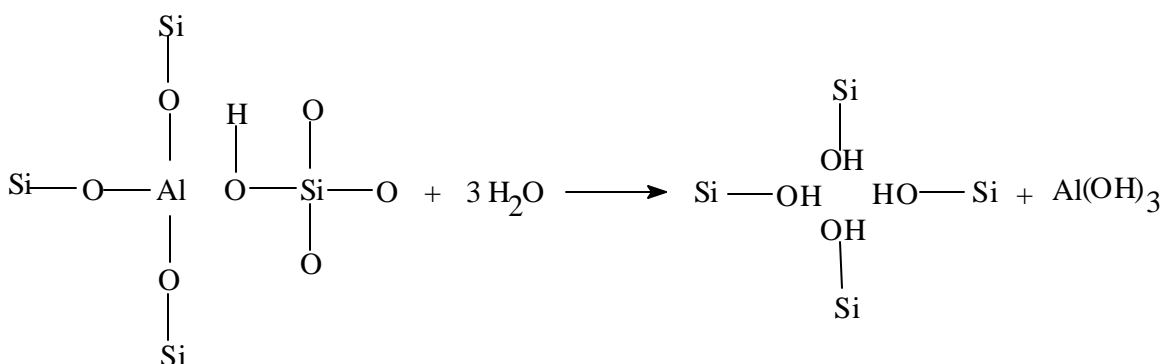
- The type of cation being exchanged, its size as well as its charge.
- The nature, size and strength of any cation coordination complex.
- The temperature of the ion-exchange treatment.
- The thermal treatment of the parent zeolite before and after exchange.
- The structural properties of the zeolites and its silica to alumina ratio.
- The location of the cations in the zeolite structure.
- The concentration of the cation exchange solution
- The prior treatment of the zeolite.

1.3.3.3 Metal Loading:

In certain reactions, it is necessary to have additional components in the catalyst to perform the total or partial catalytic functions. Such components are mainly metals, their oxides or sulphides similar to those used in non-zeolite amorphous catalyst systems. Loading may be achieved by ion exchange (solution), impregnation, adsorption from the gas phase (silylation) or co-mulling during the catalyst formation of the solid metal component in its solution. Ni, Pt, Co, Pd, Ag, W etc. are the metals, which are generally loaded on a zeolite.

1.3.3.4 Dealumination or steaming:

Dealumination or steaming generally involves removal of some surface and framework aluminum to make the zeolitic material more stable. Dealumination can be done by a number of techniques for example steam treatment, acid treatment, EDTA treatment or chemical vapor deposition (silylation). The dealumination process is generally represented as follows:



Due to this treatment the Si/Al can be increased and a defect site (nest) can be formed in the Zeolite framework. It helps to reduce the acidity of the catalyst and to increase the stability. The main advantage of dealumination is that the variation in crystallite size does not take place, which is common in the direct synthesis of zeolites with high and low silica alumina ratios.

1.4 Physico-Chemical Characterization of zeolites:

X-ray powder diffraction and adsorption measurements are the important techniques employed in the zeolite characterization. Infrared spectroscopy, Ultra violet spectroscopy, Nuclear Magnetic Resonance spectroscopy and Electron spin resonance spectroscopy have also been applied in obtaining structural information about zeolites.

1.4.1 X-ray diffraction:

Among the various spectroscopic techniques employed for structural evaluation of zeolites, x-ray diffraction is one of the most important and useful technique to identify zeolite structure [107], and determining phase purity, percent crystallinity, unit cell parameters, crystallite size and further in understanding the kinetics of crystallization. As the powder pattern is the finger print of the individual zeolite structure, phase purity and percent crystallinity of the synthesized zeolite can be ascertained by comparing with the standard pattern for the zeolite under investigation. Isomorphous substitution of a heteroatom in zeolitic framework results in changes in the unit cell parameters, unit cell volume. This is one way of confirming isomorphous substitution [108].

1.4.2 Infrared spectroscopy:

Infrared spectroscopy can yield information about the structural details of the materials. In addition, it can be used to confirm acidic characteristics and isomorphous substitution as well as aid in relating different zeolite materials by their common structural features. Flanigen [109] and Ward [110] discussed IR studies in the hydroxyl group region. Maroni et al. [111] and Janin et al. [112] have used different probe molecules to study the acidity of zeolites by diffuse

reflectance and transmission techniques. The IR spectrum in the range 200 - 1300 cm^{-1} is used to characterize and to differentiate various zeolite framework structures. The framework vibrations can be classified as structure sensitive (vibrations related to the external linkage of TO_4 units in the structure) and *structure insensitive* (internal vibrations of framework TO_4). No distinction can be made between the SiO_4 and AlO_4 tetrahedral vibrations because the masses of the two T atoms are the same. Flanigen [109] reported the general zeolite infrared assignments for the structure insensitive (internal tetrahedra) and structure sensitive (external tetrahedra) vibrations, they are:

<i>Internal tetrahedra:</i>	
Asymmetric stretch	1250 - 950 cm^{-1}
Symmetric stretch	720 - 650 cm^{-1}
T— O bend	420 - 500 cm^{-1}
<i>External linkages:</i>	
Double ring	650 - 500 cm^{-1}
Pore opening	300 - 420 cm^{-1}
Symmetric stretch	750 - 820 cm^{-1}
Asymmetric stretch	300 - 420 cm^{-1}

Shifts in the band positions in the symmetric and asymmetric stretching vibrating models can be observed with change in silica to alumina ratio in the material though no distinct band can be assigned to either group.

Isomorphous substitution of the metal ions such as B, Fe, Ga, etc for Aluminum and Ti, Ge, V etc. for Silicon, also lead to a shift in band position or an appearance of an additional band at 960 cm^{-1} (viz Ti or V substituted zeolites). The IR bands around 3600 - 3700 cm^{-1} confirm

the presence of the silanol groups [113,114] and or bridged hydroxyl groups in the zeolites. Their Brönsted acidities can be compared. IR spectroscopy has also been used to determine the crystal purity of the samples of ZSM-5. Contamination with amorphous silica can be evaluated by comparing the optical density ratio of 550 and 450 cm^{-1} bands. A ratio of 0.8 for samples containing pure ZSM-5 materials has been suggested [115-117].

1.4.3 Nuclear Magnetic Resonance spectroscopy:

Lipmaa et al.[118] were the first to demonstrate the use of ^{29}Si MAS-NMR (Magic Angle Spinning Nuclear Magnetic Resonance) spectra in determining the nature and chemical environment of the atoms. Since then this technique was found to be very useful in understanding the structural and physicochemical properties of the zeolites. Nagy and Derouane [119] reported the application of a number of NMR nuclei to study zeolites. Attention had been focused mainly on ^{29}Si and ^{27}Al MAS-NMR spectra which provided information on Si/Al ordering [120], such as crystallographic equivalent and non-equivalent Si and Al ions in various sites [121,122], framework silica to alumina ratio [123], coordination of Si and Al [124,125], spectral correlation with Si—O—T bond angles [126] and Si—O bond lengths [127].

Solid state MAS-NMR spectroscopy for ^{29}Si and ^{27}Al can confirm tetrahedral coordinated atoms in the zeolite lattice [120,121] and also indicate octahedral aluminum which may be present in the pores of the zeolites. Thirteen more NMR nuclei have been utilized in obtaining information on structural features of zeolites [128,129].

1.4.4 Thermal Analysis:

Generally zeolites are thermally stable, but heating at elevated temperatures may lead to structure breakdown and therefore decrease in crystallinity. Thermo analytical data obtained from TG, DTA and DTG study are useful in evaluating the thermal properties of zeolites [130]. The shape and splitting of the endotherms (low temperature) helps to identify the location of water molecules and also helps in studying kinetics of dehydration of water molecules. Zeolites are known to possess high thermal stability, which increases with increase in silica to alumina ratio [131,132]. Ferrierite zeolite is found to be stable up to 1273 K.

1.4.5 Sorption and Diffusion properties:

As zeolites are microporous with channels and cavities they are able to selectively sorb certain molecules. Generally in zeolites, intracrystalline surface area is higher and constitutes to about 97 % of the total surface area. Damour (1846) demonstrated that water could be reversibly removed from a zeolite without altering its structure. Later on a number of reports on sorption of gases and vapors by dehydrated zeolites started appearing [133,134]. Furthermore, Barrer and his co-workers studied sorption of various gases and vapors on natural as well as synthetic zeolites [135,136]. The selective adsorption of molecules depends on molecular size of adsorbate, polarizability and polarity of the adsorbate, organophilicity and hydrophilicity of the host zeolite structure, degree of unsaturation of organic adsorbate and polarizing power of the host cation. Sorption studies on zeolites can provide information about their void volumes, pore size, percentage crystallinity, surface area, acidity, diffusion properties and pore blockage if any. Low temperature (77 K) nitrogen sorption isotherms help in determining pore volume, pore size distribution as well as the surface area of zeolite under study [137,138]. Adsorption and

diffusion properties of zeolite play an important role on the rate of chemical reaction at the active sites. Barrer et al [139] studied in detail the diffusion process in zeolites. Diffusion in zeolites has been categorized as Configurational, Knudsen and Bulk diffusion.

1.4.6 Scanning Electron Microscopy

The crystal morphology of zeolite samples are investigated using Scanning Electron Microscopy (SEM JEOL, JSM-5200). Cathode rays are bombarded on the sample and the scattered Secondary Electrons are used to form image. A thin layer (~ 0.1 mm) of the sample was mounted on a carrier made from alumina and was coated with a film of Gold to prevent surface charging and to protect the zeolite material from thermal damage by the electron beam. The major advantage of the SEM is that bulk samples can be studied by this technique.

1.4.7 Electron Spin Resonance spectroscopy

Electron Spin Resonance is widely used in catalysis to study paramagnetic species (species having one or more unpaired electrons). This technique is sensitive and is used for investigating and characterizing low-abundance active sites at catalyst surface. Anomalous oxidation states have been observed and numerous hypothetical paramagnetic intermediates in catalytic reactions have been detected and identified by means of ESR. It is mainly useful in the transition metal containing heterogeneous catalyst samples [140,141].

1.4.8 UV-Vis

UV-Vis spectroscopy allows the study of electronic transitions between orbitals or bands in the case of atoms, ions and molecules in gaseous, liquid or the solid state [142,143]. In metal

substituted zeolites d-d transitions give information on oxidation states and co-ordination of the metal species and thus used to find out the position of metal species in the zeolite framework.

1.5 Catalysis over Zeolite

Zeolites offer advantages over conventional catalysts in acid, acid-base, oxidation and reduction reactions. The major properties such as well defined structure, uniform pores, high thermal stability, high surface area, easy regeneration, well defined micro-pore system (enhances selectivity), etc make zeolites unique as heterogeneous catalysts.

1.5.1 Acidic reactions:

The catalytic sites for acid catalyzed reactions in aluminosilicate zeolites are mainly the Brønsted acid centers associated with protons. The as-synthesized form of zeolite can be converted into catalytically active protonic form (H form) by a number of techniques. The first and the simplest one being ion exchange of cations by protons from acidic solution. However, presence of acid leads to dealumination and finally may result into structural collapse, hence the above method is not practiced for all zeolites. The second method involves the replacement of cations (e.g. Na) by ammonium ions, from a solution containing ammonium salts followed by thermal decomposition of ammonium form to produce protonic form of the zeolite. The strength and the concentration of the acidic sites can also be modified by isomorphous substitution of trivalent Al and tetravalent Si by other metal ions. All the alkylation [144-148] and Isomerization [149-152] reaction carried out on zeolites are due to acidity of the zeolite. Zeolites are used as solid acids

in many conventional acid catalysed reactions where hazardous and corrosive chemicals like mineral acids, AlCl_3 are utilized in the reactions.

1.5.2 Oxidation reduction reactions :

The redox property of the zeolite is due to the modifications discussed earlier. The metal centers are acting as active sites for the specific reaction. The oxidizing or reducing behavior of the metal depends upon the oxidation state of the substituted metal. In oxidation reaction the active centers of the incorporated metal are supported by oxidizing agents such as H_2O_2 [153], N_2O [154], molecular Oxygen [155], TBHP etc. Zeolites have been used in reduction reactions with H_2S [156], C_3 [157] hydrocarbons as reducing agents.

1.5.3 Catalytic reactors :

For investigating the catalytic activity, specific reactions are studied. A reactor is chosen on the basis of the reaction to be studied. Thus several types of reactors are in use. In this study mainly three types of reactors are used.

Liquid Phase reactors : Liquid Phase reactions were carried out at atmospheric pressure in a 50 ml thermostated flask equipped with a condenser and a magnetic stirrer.

Liquid phase high pressure reactors : Liquid phase high pressure reactions were carried out in pressurized and stirred autoclaves. These are similar to those used for the zeolite synthesis.

Fixed-bed atmospheric reactors : Catalytic studies were carried out at atmospheric pressure, in a fixed bed, down flow, integral silica reactor.[Fig.1.6] All heating and temperature measurements were carried out using Aplab temperature controller and indicator. About 3.0 g.

of catalyst (10-20 mesh) was placed at the center of the silica reactor supported by porcelain beads, which was placed vertical in the heating shell (Geomechanique, France). Liquid reactants were fed with a syringe pump (Sage instruments, USA), and carrier gas was used at a desired rate using a mass flow controller (Matheson, USA). Reaction products were condensed by passing through cold water condenser and samples were collected at various intervals. Samples were analysed on gas chromatograph (Shimadzu, model GC 15A).

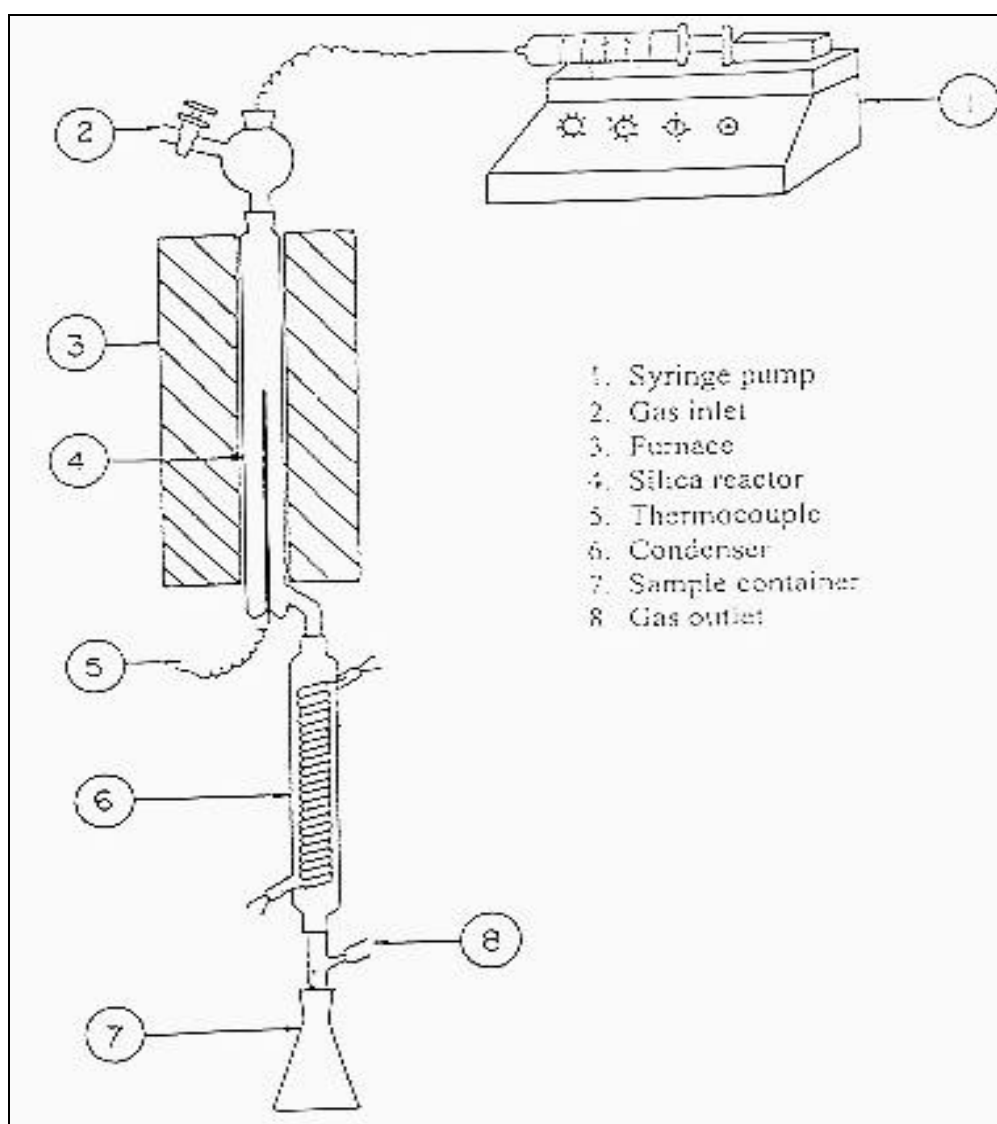


Fig. 1.6 : Fixed-bed down flow reactor

1.6 Applications of zeolites:

Zeolites have been used within home appliances as moisture adsorbents, water and gas purifiers due to the ion exchange capacity and porous structure [158].

Zeolite catalysts play an important role in the synthesis of organic intermediates and a number of reviews have appeared on the application of zeolites as catalysts in organic synthesis [159-161].

The usefulness of zeolites as catalysts in organic reactions like alkylation [162-165], isomerization [166-171], electrophilic substitution of arenes [172,173], cyclization reactions (including heterocyclic ring formation), nucleophilic substitution and addition [174] is well documented.

Zeolites act as excellent catalysts in petrochemical and petroleum conversion processes [175,176]. Processes like selectofforming [177], M-forming [178], M-2 forming [179], Cylar [180] and Aromax [181a] have been developed using zeolite catalysts and commercialized by Mobil Oil Co. and British Petroleum Co. A list of commercial processes based on zeolites is given in Table 1.7.

Table 1.7 : Industrial processes based on shape selective zeolite catalyst [181b]:

Process	Starting Material	Zeolite	Products
Catalytic cracking	Crude oil	Faujasite	Gasoline, heating oil
Hydrocracking	Crude oil + H ₂	Faujasite	Kerosene
Dewaxing	Middle distillate	ZSM-5, Mordenite	Lubricants
Benzene alkylation	Benzene , ethene	ZSM-5	Styrene
Toluene disproportionation	Toluene	ZSM-5	Xylene , benzene

Xylene isomerization	mixed xylenes	ZSM-5	p-xylene
MTG	Methanol	ZSM-5	Gasoline
MTO	methanol	ZSM-5	Olefins
SCR process	Power station flue gases	Mordenite	NO _x free off-gas

1.7 Environmental Catalysis

The role of catalysis in environmental improvement is crucial [182]. The term "Environmental Catalysis" encompasses a variety of different applications of modern catalysts. Very recently Weitkamp has classified the environmental catalysis into the following five categories [183].

1. Control of emissions of environmentally unacceptable compounds, especially in flue gases and automobile exhaust gases.
2. Conversion of solid or liquid waste into environmentally acceptable products.
3. Selective manufacture of alternative products which can replace environmentally harmful compounds, such as some chlorofluorocarbons (CFCs)
4. Replacement of environmentally hazardous catalysts in existing processes.
5. Development of catalysts which enable new technological routes to valuable chemical products without the formation of polluting by-products.

Zeolites are useful in many of these categories. The metal exchanged zeolites such as Cu/ZSM-5 are very much useful in controlling the flue gases and automobile exhausts [184]. Zeolites convert the hazardous CFCs into the less harmful products [185] and thus prevent Ozone layer depletion. The use of X, Y zeolites as solid acids replacing corrosive AlCl_3 and mineral acids in many alkylation, acylation reactions, is well known [162]. Some modified zeolites (Fe/ZSM-5, Ga-FER) are useful in the replacement of hazardous and costly chemical processes by single step green technology [186].

1.8 Ferrierite:

1.8.1 Discovery

Ferrierite (FER) is a natural zeolite mineral, which occurs near Kamloops Lakes, British Columbia. Staples [187] in 1955 reported the unit cell composition as



Vaughan [188] and Kerr [189] solved its crystal structure. Breck [190] classified ferrierite zeolite along with mordenite, dachiardite, epistilbite and bikatite.

Barrer and Marshall [191] demonstrated the first synthesis of ferrierite under hydrothermal conditions in 1964. This procedure involved the use of strontium as the inorganic cation; the synthesis temperature was 613 K and the product crystallized after 10 days. Since then a number of reports [192-196] on synthesis of ferrierite appeared. Most of them required high crystallization temperatures and FERs were of low $\text{SiO}_2/\text{Al}_2\text{O}_3$ ratios. Winquist [197]

synthesized ferrierite from gels containing Na_3PO_4 and KF , with $\text{SiO}_2/\text{Al}_2\text{O}_3$ ratio of 11 in the temperature range 448 - 483 K. These temperatures are significantly lower than those reported earlier.

More than a decade ago Kibby et al [198] reported synthesis of ferrierite using quaternary ammonium cations namely tetramethyl ammonium hydroxide. Since then a number of N- containing molecules and also oxygenated hydrocarbons have been used in FER synthesis.

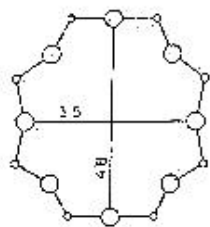
Gies and Gunawardane [199] first synthesized the siliceous form of ferrierite from aqueous medium. On the contrary a non aqueous route in presence of fluoride ions has been reported by Kuperman et al.[200]. Kim et al.[201] succeeded in synthesizing FER in the absence of inorganic cations using pyrrolidine, 1,4-diaminobutane and ethylene diamine as structure directing agents.

Number of studies reflect several isomorphous substitutions in FER framework. Ga^{3+} has been successfully incorporated in the ferrierite structure [202,203] and recently Borade and Clearfield [204] described the synthesis of iron ferrierite, while TS-FER titanosilicate system has been reported by Ahedi and Kotasthane [205]

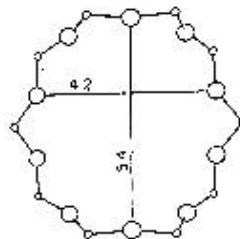
1.8.2 Structure

Synthetic ferrierite is a medium pore, high silica zeolite. The FER framework is based on the chains of 5 rings, which are linked to form five membered $\{5^4\}$ polyhedral units [Fig. 1.7]. There are two types of perpendicular channels in the structure, which intersect one another. The main channels are parallel to orthorhombic 'c' axis of crystal and are outlined by elliptical 10 membered rings ($4.3 \times 5.5 \text{ \AA}$); while the side channels parallel to 'b' axes are formed by 8

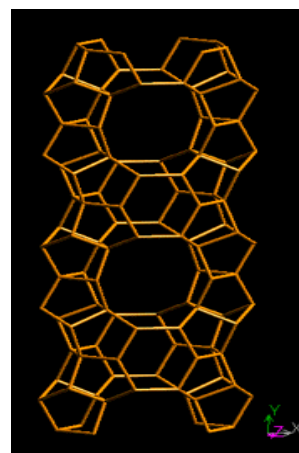
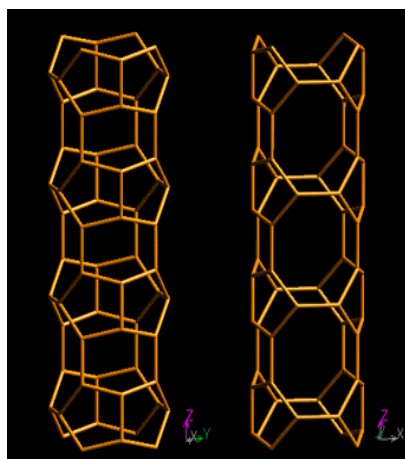
membered rings ($3.4 \times 4.8 \text{ \AA}$). The ferrierite structure type is abbreviated to FER and its crystal has orthorhombic (Fig.1.7) symmetry with $a = 1.92$, $b = 1.41$ and $c = 0.75 \text{ nm}$ [188,206] as unit cell dimensions. The unit cell contains 36 T atoms [206].



8 Membered Ring



10 Membered Ring



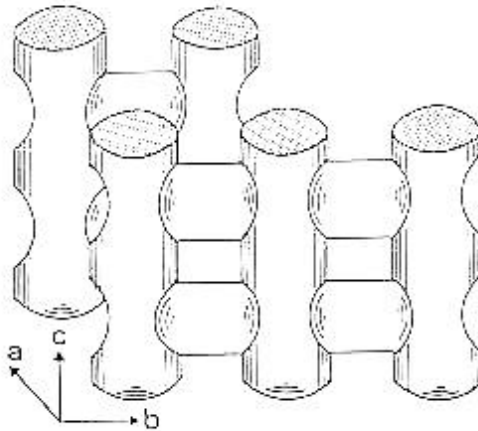


Fig. 1.7 : Ferrierite Structure

1.8.3 Uses

Ferrierite exhibits excellent selectivity for the skeletal isomerization of 1-butene [207,208]. In addition, cobalt-exchanged ferrierite is reported to be active for the selective reduction of NO_x , which remains a serious environmental problem [209,210].

1.9 Conclusion:

As evident from the literature survey, it can be seen that zeolite science developed very rapidly in the past decade. However, it can be observed that although a large number of zeolites are synthesized, only few (Na-Y, ZSM-5, etc.) have been in the commercial use. Number of other potential zeolites and related molecular sieves are reported as selective catalysts in several reactions and are for future commercialization.

In subsequent chapters, systematic study on a modified medium pore zeolite Ferrierite (Ga-FER and V-FER), has been described.

1.10 Aim of the present work:

Zeolite ferrierite (FER) belongs to high silica medium pore class of zeolites. The silica to alumina ratio is in the range 15 - 60. These zeolites are thermally stable and acid resistant. Isomorphous substitution of Al^{3+} by Ga^{3+} and Si^{4+} by V^{4+} modifies the physico-chemical as well as catalytic properties of the FER. The aim of the present work is to synthesize Ga and V analogs of ferrierite (FER) type zeolites by hydrothermal and organothermal methods followed by their characterization and evaluation of their catalytic properties. The present study includes:

- Synthesis of Gallium (Ga-FER) analogs of Ferrierite by hydrothermal route.
- Synthesis of Vanadium (V-FER) analogs of Ferrierite by organothermal synthetic route.
- Detailed characterization of the above samples by XRD, TG/DTA, FT-IR, ESR, MAS-NMR, SEM, UV-Vis and Sorption techniques.
- Testing of Ga-FER for ethylation and hydroxylation reactions of benzene.
- Testing of V-FER catalysts for oxidation of toluene, styrene epoxidation and Nitrobenzene reduction reactions.

1.References:

- 1 Barrer, R.M.; “*Hydrothermal Chemistry of Zeolites*” academic press, New York (1982).
- 2 Barrer, R.M.; *J. Chem. Soc.*(1961) 971.
- 3 Breck, D.W.; “*Zeolites Molecular Sieves*” Wiley, New York (1974).
- 4 Chen, N.Y., Kaedly, W.W. and Dwyer, F.G.; *J. Am. Chem. Soc.* **101** (1979) 6783.
- 5 Liebau, F.; *Zeolites* **3** (1983) 191.
- 6 Szostak, R.; “*Molecular Sieves: Principles of Synthesis and Identification*” Van Nostrand Reinhold, New York (1989).
- 7 Rees, L.V.C.; *Nature* **296** (1992) 492.
- 8 McBain, J.W.; “*The Sorption of gases and vapours by solids*”, Ritledge and Sons, London; (1932) Ch. 1.
- 9 Szhultz, P.G.; *Angew Chem. Int. Ed. Engl.* **28** (1989) 1283.
- 10 Davis, M.E. ; *Acc. Chem. Res.* **26** (1993) 111.
- 11 Cronstedt, A.F.; *Kongl Vetenskaps Acad. Handl.* Stockholm **17** (1756) 120.
- 12 Damour, A.; *Ann. Mines* **17** (1840) 191.
- 13 Deville, St. Claire; *Compt. Rend.* **54** (1862) 324.
- 14 Thomson, H.S.; *J. Roy. Agric. Soc.* **11** (1862) 68.
- 15 Breck, D.W., “*Molecular Sieves Zeolites*”, Adv. Chem. Ser. (American Chemical Society, Washington DC) **101** (1971) 251.
- 16 McBain, J. W.; “*The Sorption of gases and vapors by solids*” Pub. Rutledge and Sons London (1932) Ch. 5.
- 17 Barrer, R.M.; “*Proc. Roy. Soc.*” (London) **162** A (1938) 393; *Trans. Far. Soc.* **40** (1944) 559.
- 18 Barrer, R.M.; *J. Chem. Soc.* (1984) 127.
- 19 Barrer, R.M. and Marcilly, C.; *J. Chem. Soc. A* (1970) 2735.
- 20 Barrer, R.M. and Robinson, D.J.; *Zeit. Krist.*, **135** (1972) 374.
- 21 Barrer, R.M.; *Nature* **164** (1949) 112.

- 22 Barrer, R.M.; *Pure and Appl. Chem.*; **51** (1979) 1091.
- 23 Meier, W.M. and Olson, D.H.; *Atlas of Zeolite Structure Types*, Butterworths (1987).
- 24 Bragg, W.L.; *The Atomic Struc. of Miner.* Cornell University Press, Ithaca, New York (1937).
- 25 Meier, W.M.; "Molecular Sieves" *Soc. of Chem. Ind.* London (1968) 10.
- 26 Flanigen, E.M.; "In Proceedings of the fifth Interanational Conference of Zeolites", (L.V.C Rees Eds.) Naples, Italy, June 2-6, (1980) 760.
- 27 Barrer, R.M., "Molecular Sieves" *Soc. of chem. Ind.* London (1968) 10.
- 28 Sand, L.B.; *Econ. Geol.* (1967) 161.
- 29 Smith, J.V., *Mineral Soc. Amer. Spec.* paper # 1 (1963).
- 30 Fischer, K.F.; Meier, W.M.; *Fortschi Mineral* **42** (1965) 50.
- 31 Breck, D.W.; "Molecular Sieves Zeolites", *Adv. Chem. Ser.*, Amer. Chem. Soc., Washington DC, **101** (1971) 1.
- 32 Davis, M.E.; Saldarriaga, C.; Montes, C.; Graces, J. and Crowder, C.; *Nature* **331** (1988) 968.
- 33 Estemann, M.; McCusker, L.B.; Baeloche, C.; Merrouche, A. and Kessler, H.; *Nature* **352** (1991) 320.
- 34 Freyharett, C.C.; Tsapatsis, M.; Lobo, R.F.; Balkus Jr., K.J. and Davis, M.E.; *Nature* **381** (1998) 295.
- 35 Mumpton, F.A.; *Min. Soc. Am.* Washington (1977).
- 36 Sand, L.B. and Mumpton, F.A. (Eds.) "Natural Zeolites: Occurance, Properties, Use" Pergamon press, Oxford (1978).
- 37 Barrer R.M., in "Zeolites and Clay Minerals as Sorbents and Molecular Sieves", 'Academic Press' (1978).
- 38 Morey, G. and Ingerson, E.; *Econ. Geol.* **32** (1937) 607.
- 39 Barrer, R.M. and Balchetz, L.; *J. Soc. Chem. Ind.* London, **64** (1941) 132.
- 40 Barrer, R.M. and Denny, P.J.; *J. Chem. Soc.* (1961) 971.
- 41 Breck, D.W.; Flanigen, E.M.; "Molecular Sieves", Society of Chemical Industry, London (1968) 47.
- 42 Flanigen, E.M. *Adv. Chem. Ser.*; **121** (1973) 119.
- 43 Flanigen, E.M.; *Ibid* 153.
- 44 Lok, B.M.; Cannan, T.R. and Messina, C.A.; *Zeolites* **3** (1983) 282.
- 45 Flanigen, E.M.; in "Introduction of Zeolite Science and Practice" (Eds.) Van Bekkum, H.; Flanigen, E.M. and Jansen, J.C.; Elsevier, New York (1991) 13-34.
- 46 Flanigen, E.M.; Patton, R.L. and Wilson, S.T.; in "Innovation in Zeolite Material Science" (eds. Grober, P.I., Mortier, W.J., Vasant, E.F. and Schulz-Ekloff, G.) 13-27 (Elsevier, New York 1988).
- 47 Gier, T.E. and Stucky, G.D.; *Nature* **349** (1991) 508.
- 48 Harvey, G. and Meier, W.M.; in *Stud. Surf. Sci. Catal.* (Eds. Jacobs, P.A. and VanSanten, R.A., Elsevier, Amesterdam) **49** A (1989) 411.
- 49 Marten, J.A. and Jacobs, P.A.; in "Advanced Zeolite Science and Applications" (eds. Jansen, J.C.; Stocker, M.; Karge, H.G. and Weitkamp, J.; Elsevier, Amesterdam) (1994) 653.
- 50 Meier, W.M.; Olson, D.H. and Baerlocher, C.H.; *Atlas of Zeolite Structure Types*, Elsevier Boston, (1996).
- 51 Kresge, C.T.; Leonowicz, M.E.; Roth, W.J. and Vartulli, J.C.; US Pat. 5, 098, 684 (1992).
- 52 Kresge, C.T.; Leonowicz, M.E.; Roth, W.J.; Vartulli, J.C. and Beck, J.S.; *Nature* **359** (1992) 710.

- 53 Beck, J.S.; Chu, C.T.; Johnson, I.D.; Kresge, C.T.; Leonwicz, M.E.; Roth, W.J. and Vartulli, J.C.; US Pat. 5, 108, 725 (1992).
- 54 Beck, J.S.; Calabro, D.C.; McCullen, S.B.; Pelrine, B.P.; Schmitt, K.D. and Vartulli, J.C.; US Pat. 5, 145, 816 (1992).
- 55 Beck, J.S.; Kresge, C.T.; Leonwicz, M.E.; Roth, W.J. and Vartulli, J.C.; US Pat. 5, 264, 203 (1993).
- 56 Beck, J.S.; Schmitt, K.D. and Vartulli, J.C.; US Pat. 5, 334, 368 (1994).
- 57 Beck, J.S.; Kresge, C.T.; McCullen, S.B.; Roth, W.J. and Vartulli, J.C.; US Pat 5, 370, 785 (1994).
- 58 Beck, J.S.; Vartulli, J.C.; Roth, W.J.; Leonwicz, M.E.; Kresge, C.T.; Schmitt, K.D.; Chu, C.T.; Olson, D.H.; Sheppard, E.W.; McCullen, S.B.; Higgins, J.B. and Schlenker, J.L.; *J. Am. Chem. Soc.* **114** (1998) 10834.
- 59 Vartulli, J.C.; Kresge, C.T.; Leonwicz, M.E.; Chu, A. S.; McCullen, S.B.; Johnson, I.D. and Sheppard, E.W.; *Chem. Mater.* **6** (1994) 2070.
- 60 Beck, J.S.; Vartulli, J.C.; Kennedy, G.J.; Kresge, C.T.; Roth, W.J. and Schramm, S.E.; *Chem. Mater.* **6** (1994) 1816.
- 61 Vartulli, J.C.; Schmitt, K.D.; Kresge, C.T.; Roth, W.J.; Leonwicz, M.E.; McCullen, S.B.; Hellring, S.D.; Beck, J.S.; Schlenker, J.L.; Olson, D.H.; Sheppard, E.W.; *Stud. Surf. Sci. Catal.* **84** (1994) 53.
- 62 Carvalho, W.A.; Varaldo, P.B.; Wallau, M. and Schuchardt, U.; *Zeolites* **18** (1997) 408.
- 63 Casci, J.L.; *Stud. Surf. Sci. Catal.* **28** (1986) 215.
- 64 Valyocsik, E.W.; US Pat. 4, 585, 786 (1986).
- 65 Whittam, T.V.; EP Appl. 54, 363 (1982).
- 66 Rollmann, L.D. and Valyocsik, E.W.; EP Appl. 15, 132 (1980).
- 67 Casci, J.L.; Lowe, B.M. and Whittam UK Pat. Appl. 2, 077, 709 (1982).
- 68 Valyocsik, E.W.; US Pat. 4, 481, 177 (1984).
- 69 US Pat. 4, 623, 527 (1987).
- 70 Szostak, R.; US Pat. 4, 585, 639 (1986).
- 71 Bhaumik, A. and Kumar, R.; *Microporous Materials* **5** (1995) 173.
- 72 EP 174, 121 (1986).
- 73 Kumar, R.; Reddy, K.R. and Ratnasamy, P.; US Pat. 5, 219, 813 (1993).
- 74 Reddy, K.R.; Kumar, R.; Ramaswamy, V. and Ramaswamy, A.V.; *Zeolites* **4** (1994) 326.
- 74a Podovan M., Leofanti. G., and Roffia. P.; Eur. Pat. Appl.; 0311983, (1989).
- 74b Uguina. M.A., Ovejero. G., Grieken R.V, Serrona. D.P. and Camacho. M.; *J.C.S.Chem. Commun.*; (1994), 27
- 75 Sand, L.B.; *Pure and Appl. Chem* **52** (1980) 2105.
- 76 Feijes. E.J.P., Martines J.A. and Jacobs P.A. in "Handbook of Heterogeneous Catalysis" by Weitkamp (Eds), (1999), 312.
- 77 Kerr, G.T.; *J. Phys. Chem* **70** (1966) 1047.
- 78 Kerr, G.T.; *J. Phys. Chem* **72** (1968) 1385.
- 79 McNicol, B.D.; Pott, G.T. and Loos, R.K.; *J. Phys. Chem* **76** (1972) 3388.
- 80 Guth, J.L. and Cullet, P.; *J. Chim. Phys.* **83** (1986) 155.
- 81 Culfaz, A. and Sand, L.B.; *Adv. Chem. Ser.* **121** (1973) 152.
- 82 Guth J.L., Gullet P., Seive A., Patarin J., Delprato F.; *Nato ASI Ser.*; **221** (1990) 69.

- 83 Jensen J.C.; in "Introduction to Zeolite Science and Practice "; (Eds) H.Van Bakkum et.al.; Elsevier Science, Amsterdam, (1991), 77.
- 84 Kuperman A., Nadimi S., Oliver S., Ozin G.A., Graces J.M., Olken M.M.; *Nature*; **365** (1993) 239-42
- 85 Ward, J.W.; "Zeolite Chemistry and Catalysis", [C. Rabo, J.A. Eds.], ACS monograph. Chp. 2 **171** (1976) 118.
- 86 Breck, D.W., "Zeolite Molecular Sieves", John Wiley and Sons, New York (1974) 449
- 87 Jacobs, P.A.; "Carboniogenic activity of zeolites", Chp. II, Elsevier Sci. Pub. Co. ,Amsterdam, Oxford, New York **168** (1977) 33.
- 88 Mortier, W.J.; Saur, J. ; Lercher, J.A. and Noller, H.J.; *J. Phys. Chem.* **88** (1984) 905.
- 89 Hegde, S.G.; Kumar, R.; Bhat, R.N. and Ratnasamy, P.; *Zeolites* **9** (1989) 231.
- 90 Weisz, P.B. and Frilette, V.S.; *J. Phys. Chem.* **64** (1960) 382.
- 91 Derouane, E.G. and Gabelica, Z.; *J. Catal.* **65** (1980) 218.
- 92 Frilette, V.J.; Haag, W.O. and Lego, R.M.; *J. Catal.* **67** (1981) 218.
- 93 Mortens, J.A.; Tielen, M.; Jacobs, P.A. and Weitkamp, T.; *Zeolites* **4** (1984) 98.
- 94 Weitkamp, J.; Ernst, S. and Karge, H.G.; *Erdol Kohle-Erdgas-Petrochem.*, **37** (1984) 457
- 95 Dewing, J.J; *J. Mol. Catal.* **61** (1990) 173.
- 96 Weitkamp, J.; Ernst, S.; Jacobs, P.A. and Karge, H.G.; *Erdol Kolhe-Erdgas-Petrochem*, **39** (1984) 33.
- 97 Goldsmith, T.R.; *Min. Mag.* **29** (1952) 952.
- 98 Becker, K.; John, H; Steinburg, K; Weber, M. and Nestler,K.; "Catalysis on Zeolites" (Kallo. D and Minachev, Kh. M., Eds.), Akademia Kiado, Budapest (1988) 515.
- 99 Naccache, C. and Ben Tarrit, Y. "Zeolite Science and Technology", (Riberio, F.R.; Rodrigues, A.E.; Rollmann, L.D. and Naccache, E. Eds.) Martinus Nijhoff, The Haque (1984) 373.
- 100 Kotasthane, A.N.; Shiralkar, V.P.; Hegde, S.G. and Kulkarni, S.B.; *Zeolites* **6** (1986) 233.
- 101 Rao, G.N.; Shiralkar, V.P.; Kotasthane, A.N. and Ratnasamy, P.; *Molecular Sieves; Synthesis of Microporous Materials*, Vol 1, Ed. M.L. Occelli and H.E. Robson, Van Nostrand Reinhold-New York.
- 102 Minachev, Kh. M; Khariamov, V.V. and Garanin, V.I. "Catalysis on Zeolites" (Kallo. D and Minachev, Kh. M., Eds.), Akademia Kiado, Budapest (1988) 489.
- 103 Pergo, G.; Bellusi, G.; Corono, C.; Taramasso, M. and Buonomo, F.; *Stud. Surf. Sci. Catal.* **28** (1986) 129.
- 104 Kornatowki, J.; Sychev, M.; Goncharuk, V. and Bauer, W-H.; *Stud. Surf. Sci. Catal.* **65** (1991) 581.
- 105 Tielen, M.; Geelen, M.; Jacobs, P.A.; *J. Catal.* **91** (2) (1985) 352.
- 106 Barrer, R.M.; Bayhans, J.W.; Bultitude, F.W. and Meier, W.M., *J. Chem. Soc.* (1995) 195.
- 107 Von Ballmoos R.; "Collection of Simulated XRD Powder Patterns for Zeolites", Butterworths London (1984).
- 108 Meyer, B.L.; S.R. Ely; Kutz, N.A.; Kuduk and Bossche, E.V.; *J. Catal.* **91** (1985) 352.
- 109 Flanigen, E.M.; "Zeolite Chemistry and Catalysis", ACS monograph (Rabo, J.A. Eds.) **171** (1976) 118.
- 110 Ward, J.W.; "Zeolite Chemistry and Catalysis", ACS monograph (Rabo, J.A.. Eds.) **171** (1976) 118.
- 111 Maroni, V.A.; Martin, K.A. and Johnson, S.A.; *ACS Sym. Ser.* **368** (1988) 85.
- 112 Janin, A.; Lovally, J.C.; Macedo, A. and Raatz, F.; *ACS Sym. Ser.* **368** (1988) 85.
- 113 Topsoe, N.; Pedersen, R. and Derouance, E.G.; *J. Catal.* **70** (1984) 369.
- 114 Jacobs, P.A. and Martier, W.Y.; *Zeolites* **2** (1982) 226.
- 115 Jansen, J.C.; vander Gaag; van Bekkum, H.; *Zeolites* **4** (1984) 369.

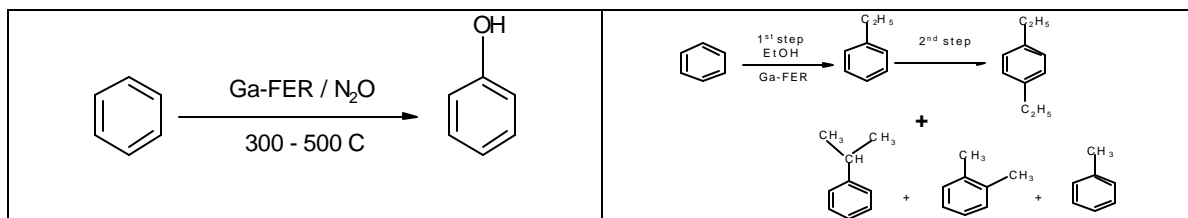
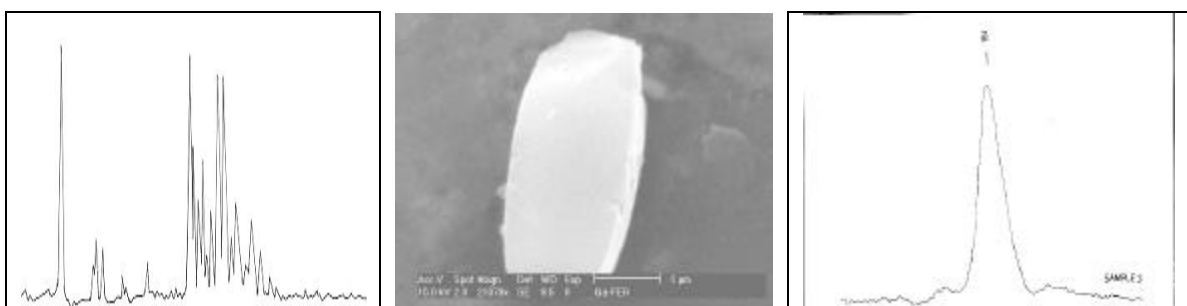
- 116 Jacobs, P.A.; Beyer, H.K.; Valyon, J.; *Zeolites* **1** (1981) 161.
- 117 Von Ballmoos, R.; Ph.D thesis, E.T.H. Zurich (1981).
- 118 Lippmaa, E.; Magi, M.; Samoson, A.; Engelhardt, G. and Gummer, A.R.; *J. Am. Chem. Soc.* **102** (1980) 4889.
- 119 Nagy, J.B. and Derouane, E.G., *ACS Symp. Ser.* **368** (1988) 2.
- 120 Lippmaa, E.; Magi, M.; Samoson, A.; Tarmak, M. and Engelhardt, G.; *J. Am. Chem. Soc.* **103** (1981) 4992.
- 121 Fyfe, C.A.; Gobbi, G.C.; Klinowski, J.; Thomas, J.M. and Ramdas, S.; *Nature* **296** (1982) 530.
- 122 Fyfe, C.A.; Gobbi, G.C.; Klinowski, J. and Thomas, J.M.; *J. Phys. Chem.* **86** (1982) 1247.
- 123 Engelhardt, G.; Lohose, U.; Lippmaa, E.; Tarmak, M. and Magi, M.; *Z. Anorg. Allg. Chem.* **482** (1981) 49.
- 124 Mastikim, V.M. and Zamarev, K.I. *J. Phys. Chemie.* **152** (1987) 332.
- 125 Muller, D.; Gessnev, W.; Behrens, H.S. and Schelev, G.; *Chem. Phys. Lett.* **79** (1981) 159.
- 126 Thomas, J.M.; Fyfe, C.A.; Ramdas, S.; Klinowski, J. and Gobbi, G.C.; *J. Phys. Chem.* **86** (1982) 3061.
- 127 Ramdas, S. and Klinowski, J.; *Nature* **308** (1984) 521.
- 128 Fyfe, C.A.; Thomas, J.M.; Klinowski, J. and Gobbi, G.C.; *Angew Chem.* **95** (1983) 257.
- 129 Nagy, J.B. Gabelica, Z. and Derouane, E.G.; *Chem. Lett.* **7** (1982) 1105.
- 130 Barrer, R.M. and Langley, D.A.; *J. Chem. Soc.* (1958) 3804, 3811, 3817.
- 131 Rabo, J.A.; "Zeolite Chemistry and Catalysis", Eds. Beringer, F.M.; Am. Chem. Soc. Washington D.C. (1976) pg 285.
- 132 Bremer, H.; Marke, W.; Schodel, R. and Vogt, F.; *Adv. Chem. Ser.* **121** (1973) 249.
- 133 Friedel, G.; *Bull. Soc. Fr. Mineral Crystallogr.* **19** [14] (1986) 96.
- 134 Rabinowitch, R. and Wood, W.C.; *Trans. Faraday Soc.* **32** (1936) 947.
- 135 Barrer, R.M.; *Proc. Roy. Soc. A* **167** (1938) 39Z.
- 136 Barrer, R.M.; *Quart. Rev.*, London, (1949) 3239.
- 137 Hong -Xin. Li; Martens, J.A.; Jacobs, P.A.; "Innovation in Zeolite Material Sci.", Gribit, P. J. (Eds.) (1985) 75.
- 138 Tapp, N.J.; Milestone, N.B.; Bibby, D.M.; *Ibid* pg 393.
- 139 Barrer, R.M.; *Adv. Chem. Ser.* **102** (1971) 41.
- 140 Delgas W.N., Haller G.H., Kellerman R., Lunsford J.H.; "Spectroscopy in Heterogeneous Catalysis "; Academi Press, New York; (1979) ; Chapter 4 and 6.
- 141 Che M., Giamello E., in " Spectroscopic Characterization of Heterogeneous Catalysts"; (Eds. Fierro J.L.G.) ; Elsevier Science Pub., Amsterdam; **57** (1990) 265-332.
- 142 Delannay F.; in "Characterization of Heterogeneous Catalysts "; Dekker, New York, (1984) Chapter 4.
- 143 Imelik B. and Vedrine J.C.; in "Catalyst Characterization : Physical Techniques for Solid materials"; Plenum Press, New York, (1994), Chapter 4.
- 144 Pradhan A.R. and Rao B.S.; *J.Catal.*; **132** (1991) 79.
- 145 Witcherlova B. and Jiri Cejka; *J.Catal.*; **146** (1994) 523.
- 146 Siddhesh Shevade, Ahedi R.K., Kotasthane A.N. and Rao B.S.; "Recent Trends in Catalysis", (Eds.) Murugesan et.al.; Narosa Publishing House, (1999) 383.
- 147 Becker K.A., Karge H.G. and Streubel W.D; *J.Catal.*; **28** (1973) 403.
- 148 Barrer R.M., Bultitude F.W. and Sutherland J.W.; *Trans Faraday Soc.*; **53** (1957) 1111.

- 149 Martens J.A., Perez Pariente J., Sastre E., Corma A., Jacobs P.A.; *Appl. Catal.*; **45** (1988) 85.
- 150 Csicsery S.M.; *J.Catal.*; **108** (1987) 433.
- 151 Kim M.H., Chen C.Y., Devis M.E.; *ACS Symp. Ser.* ; **517** (1993) 222.
- 152 Weitkamp J., Newber N.; *Stud.Surf. Sci. Catal.*; **60** (1991) 291.
- 153 Hoelderich W.F. and VanBakkum H.; *Stud. Surf. Sci. Catal.*; **58** (1991) 631.
- 154 Ono Y., Tohmori K., Suzuki K., Nakashiro and Suzuki E.; *Stud. Surf. Sci. Catal.*; **41** (1988) 75.
- 155 Walsh D.E., Han S. and Palermo R.E.; *J.C.S.Chem.Commun.*; (1991) 1259.
- 156 Venuto P.B. and Landis P.S.; *Advances in Catalysis* ; Academic Press, New York, NY ; **18** (1968) 259.
- 157 Kikuchi E., Ihava M., Hishiki T. and Yogo K. in Higgis J.B., Ballmoss R.V. and Treacy M.M.J (Eds.); 9th International Zeolite Conference, Butterworth-Heinemann, Boston, MA (1992) RP 40 (Abstract).
- 158 Nishino A.; *Catal. Today* ; **10** (1991) 107.
- 159 Holderich, W.; Hesse, M. and Naumann, F; *Angew Chemie* **27** [2] (1988) 226.
- 160 Van Bekkum, H. and Kouwenhoven, H.W.; *Red. Trav. Chim. Pays-as* **108** (1989) 283.
- 161 Veneto, P.B.; *Microporous Materials* **2** (1994) 283.
- 162 Pradhan, A.R. and Rao, B.S.; *J.Catal.* **132** (1991) 79.
- 163 Prasad, S. and Rao, B.S.; *J. of Mol. Catal.* **62** (1990) L17-L22.
- 164 Blanka, Witcherlova and Jiri Lcjka.; *J. Catal.* **146** (1994) 523.
- 165 Reddy, K.S.N.; Rao, B.S. and Shirikar, V.P.; *Appl. Catal. A: General*, **95** (1993) 53.
- 166 Martens, J.A., Perez-Pariente, J.; Sastr, E.; Corma, A. and Jacobs, P.A.; *Appl. Catal.* **45** (1988) 85.
- 167 Csicsery, S.M.; *J. Catal* **108** (1987) 433.
- 168 Kim, M.H.; Chen, C.Y. and Davis, M.E.; *ACS Symp. Ser.* **517** (1993) 222.
- 169 Matsuda, T.; Yogo, K.; Mogi, Y.; Ki Ku Chi, E.; *Chem Lett.* (1990) 1085.
- 170 Weitkemp, J. and Neuber, N.; *Stud. Surf. Sci. Catal.* **60** (1991) 291.
- 171 Jacobs, P.A. and Martens, J.A.; *Stud. Surf. Sci. Catal.* **58** (1981) 445
- 172 Schumacher, I. and Wang, K U.S. Pat. 4 426 543 (1984).
- 173 Wortel, Th. M.; Oudijn, D.; Vleugel, C.J.; Rielofsen, D.P. and van Bekkum, H.; *J. Catal.* **60** (1990) 110.
- 174 Hatada, K.; Ono, Y.; Keii, T.; *Adv.Chem. Ser.* **121** (1973) Chp 4.
- 175 Weisz, P.B.; *Pure Appl. Chem.* **52** (1980) 2091.
- 176 Chen, N.Y. and Garwood, W.E.; *Catal. Rev. Sci. Engg.* **28** (1986) 185.
- 177 Chen, N.Y.; Mazink, J.; Schwartz, A.B. and Weisz, P.B.; *Oil Gas J.* **66** (1968) 154.
- 178 Heinemann, H.; *Catal. Rev. Sci. Engg.* **15** [1] (1977) 53.
- 179 Chen, N.Y. and Yan, T.Y. *Ind. Eng. chem. Proc. Res. Dev.* **25** (1986)151.
- 180 Johnson, J.A.; Weiszmann, J.A.; Hider, G.R. and Hall, A.P.H.; Paper presented ar NPRA Annual meeting, San Antorio, Texas, March (1984).
- 181a Tamm, P.W.; Mohr, D.H. and Wilson, C.R.; *Catalysis* (1987), [Ward, J.W. Eds] Elsevier Sci. Pub., Amsterdam, The Netherlands (1988) 395.
- 181b Hagen J. in " Industrial Catalysis : A Practical Approach ", Wiley-Vch, (1999) 242.
- 182 Weitkamp J., Karge H.G., Pfeifer H. and Holderich W. (Eds.); Iwamoto M. ; *Stud. Surf. Sci. Catal.* ; **84**

- (1994) 1395.
- 183 Weitkamp J. ; Proc. Inter. Symp. Environ. Catal., Tokyo (1993).
- 184 Iwamoto M. in " Future Opportunities in Catalytic and Separation Technology "; by Misono et.al (Eds.) ; Elsevier, Amsterdam, (1990) 121.
- 185 Kobayashi K. et.al. 58th Annal Meet. Chem. Soc. Japan (1989).
- 186 Shevade S.S., Rao B.S.; Catalysis Letters ;
- 187 Stapes, L.W.; *Amer. Min.* **40** (1955) 1095.
- 188 Vaughan, P.A.; *Acta. Cryst.* **21** (1966) 983.
- 189 Kerr, I.S. *Nature* **210** (1966) 294.
- 190 Breck, D.W.; " *Molecular Sieve Zeolites* " J. Wiley (1974) 219.
- 191 Barrer, R.M. and Marshall, D.J.; *J. Chem. Soc.* (1964) 2296.
- 192 Coombs, D.S.; Ellis, A.J.; Fyfe, W.S. and Taylor, A.M.; *Geochem Cosmochim Acta* **17** (1959) 53.
- 193 Sanderov, E.E.; *Geokimiya* **9** (1959) 820
- 194 Sands, L.B.; Int. Conf. Mol. Sieves (1967) p 71.
- 195 Hawkins, D.B.; *Mater. Res. Bull.* **2** (1967) 951.
- 196 Vaughan, D.E.W. and Edwards, G.C.; USP 3, 966, 883 (1976) assigned to W.R. Grace.
- 197 Winqvist, B.H.C.; USP 3, 933, 974 (1976) assigned to Shell Oil Corp.
- 198 Kibby, C.L.; Perotta, A.J. and Massoth, J.; *J. Catal.* **35** (1974) 256.
- 199 Gies, H. and Gunawardane, R.; *Zeolites* **7** (1987) 442.
- 200 Kuperman, A; Nadami, S.; Oliver, S.; Ozin, G.A.; Graces, J.M. and Olken, M.M, *Nature* **365** (1993) 239.
- 201 Kim, T.J.; Ahm, W.S.; Hong, S.B.; *Microporous Materials* **7** (1996) 35.
- 202 Sulikowsler, B and Klinnowski, J.; *J. Chem. Soc. Chem. Commun.* (1989) 1289.
- 203 Jacob, N.E.; Joshi, P.N.; Shaikh, A.A. and Shiralkar, V.P.; *Zeolites* **13** (1993) 430.
- 204 Borade, R.B. and Clearfield, A.; *J. Chem. Soc. Commun.* (1996) 2267.
- 205 Ahedi. R.K. and Kotasthane A.N.; *J. Mat. Chem.* **8** (1998) 1685.
- 206 Meier, W.M. and Olson, D.H.; "Atlas of Zeolite Structure Types, IZA, 1978 Polycrystal books pg. 39.
- 207 Natarajan S., Wright P.A. and Thomas J.M., *J.C.S. Chem. Comm.* (1993) 1861.
- 208 Grandvalet P. Mooiweer N.H., Kortbeck A.G.T., Kraushaar B., Czarnetzki,; European Patent 92 200 516.0 (1992).
- 209 Mooiweer, H.H.; de Jong, K.P.; Kraushaar-Czarnetzki, B.; Stork, W.H.J. and Krutzen, *Stud. Surf. Sci. Catal.* **84** (1994) 2327.
- 210 O'Young, C.-L.; Pellet, R.J.; Casey, D.G.; Ugolini, J.R. and Sawicki, R.A.; *J. Catal.* **151** (1995) 467.

CHAPTER II

Ga-FER



2.1 Introduction :

Advances in the preparation of zeolite and zeolite like substances have led to know new molecular sieve materials. These advances kept the basic identities of the modified materials such as thermal stability, ion exchange nature, shape selectivity and many other properties intact. The replacement of metal ions in the framework of the molecular sieve with others, is one of such modifications. This is known as Isomorphous substitution. In the case of zeolites, there are methods of introducing the trivalent ion in place of Al^{+3} and tetravalent ion in place of Si^{+4} .

Although there is a difference in the ionic radii of Al^{+3} (0.53 Å) and Ga^{+3} (0.61 Å), the gallium substitution in place of aluminum is possible. The gallium analogs of many zeolites [1,2,3] including faujasite [2,4,5], ZSM-5 [6] have been already synthesized. Sulikowsler [7] reported the gallium Ferrierite for the first time. Jacob et.al. [8] have also synthesized Gallium substituted Ferrierite. As gallium is moderately acidic than aluminum it will be a milder acid catalyst in acid catalysed reactions [9]. In the synthesis of the gallosilicate, the interaction between gallium ions and the silicate gel appears to be similar to the aluminum ion interactions with the gel [10]. In aqueous solution, however, the free gallate ions are more stable than aluminates [11]. Under the alkaline conditions used in zeolite synthesis, sodium gallate solution is found to be extremely stable. Thus a true solution of gallic acid can be formed, which is not true for the aluminate acid, as it forms dimeric and polymeric species in solution [12]. The presence of monomeric gallate ions in solution thus should not impede gallium's ability to be incorporated into a crystallizing silicate structure, as dissolution of a secondary gallium oxide (hydroxide) phase does not occur. Irreversible formation of metal oxide

(hydroxide) species, prohibiting incorporation into a silicate framework, occurs for other elements with amphoteric hydroxides such as the transition metals, iron and chromium, but it is not a factor in the gallosilicate system.

2.2 Synthesis of Ga-FER :

The reagents used for the synthesis of gallium analog of ferrierite are listed in Table 2.1

Table 2.1: Reagents used in synthesis of Ga-FER.

Reactants	Suppliers	Analysis
Pyrrolidine	SRL	99%
Sodium silicate	-	28% SiO ₂ ; 9.0 % Na ₂ O
Gallium sulphate [Ga ₂ (SO ₄) ₃ .16 H ₂ O]	Aldrich	99%
Sulphuric acid	BDH	98%
D.M.Water		

In a typical synthesis, addition of a solution prepared by mixing 1.625 g. of Ga₂(SO₄)₃ [99%, Aldrich] in 30 g. of distilled water and 1.8 g. of concentrated H₂SO₄ (98% S.D.Fine Chemicals) in 10 g. of distilled water to 52.5 g. of Na₂SiO₃ (28% SiO₂, 9% Na₂O) in 40 g. distilled water leads to the formation of a gel. Then, 10 g. of template pyrrolidine was added to the gel mixture and the gel was stirred for approximately 1 h. The final gel pH was 11.5 ± 0.2. The gel was transferred to a 300 ml stainless steel autoclave (Parr 4861, 300 ml) and heated at 433 K for 40 hours. After this period, the autoclave was quenched with cold water. The material was filtered, washed and dried at 373 K. Utmost care was taken to clean the autoclave to avoid any seeding effect from the previous batches. The samples with different SiO₂/Ga₂O₃ ratios were synthesized by varying the gel composition. The initial gel composition was :

27.18 Na₂O : 32 Py : (30-100) SiO₂ : 1 Ga₂O₃ : 4.97 H₂SO₄ : 1798 H₂O

where Py = pyrrolidine.

The as synthesized Ga-FER samples were calcined at 773 K for 10-12 h. to convert them into the sodium form and then into the ammonium form by multiple exchanges with 2M ammonium nitrate solution at 363 K. The ammonium form was dried at 383 K and then calcined in a step wise controlled way at 753 K to obtain the H⁺ form.

Three different Ga-FER samples were prepared with Si/Ga input ratio varying from 15 to 50. The samples were analysed by XRF (Rigaku 3070 X-ray spectrometer) technique to determine the chemical composition of the Ga-FER. The chemical analysis of the input gel and the final products are shown in Table 2.2.

Table 2.2 : Physico chemical properties of Ga-FER samples

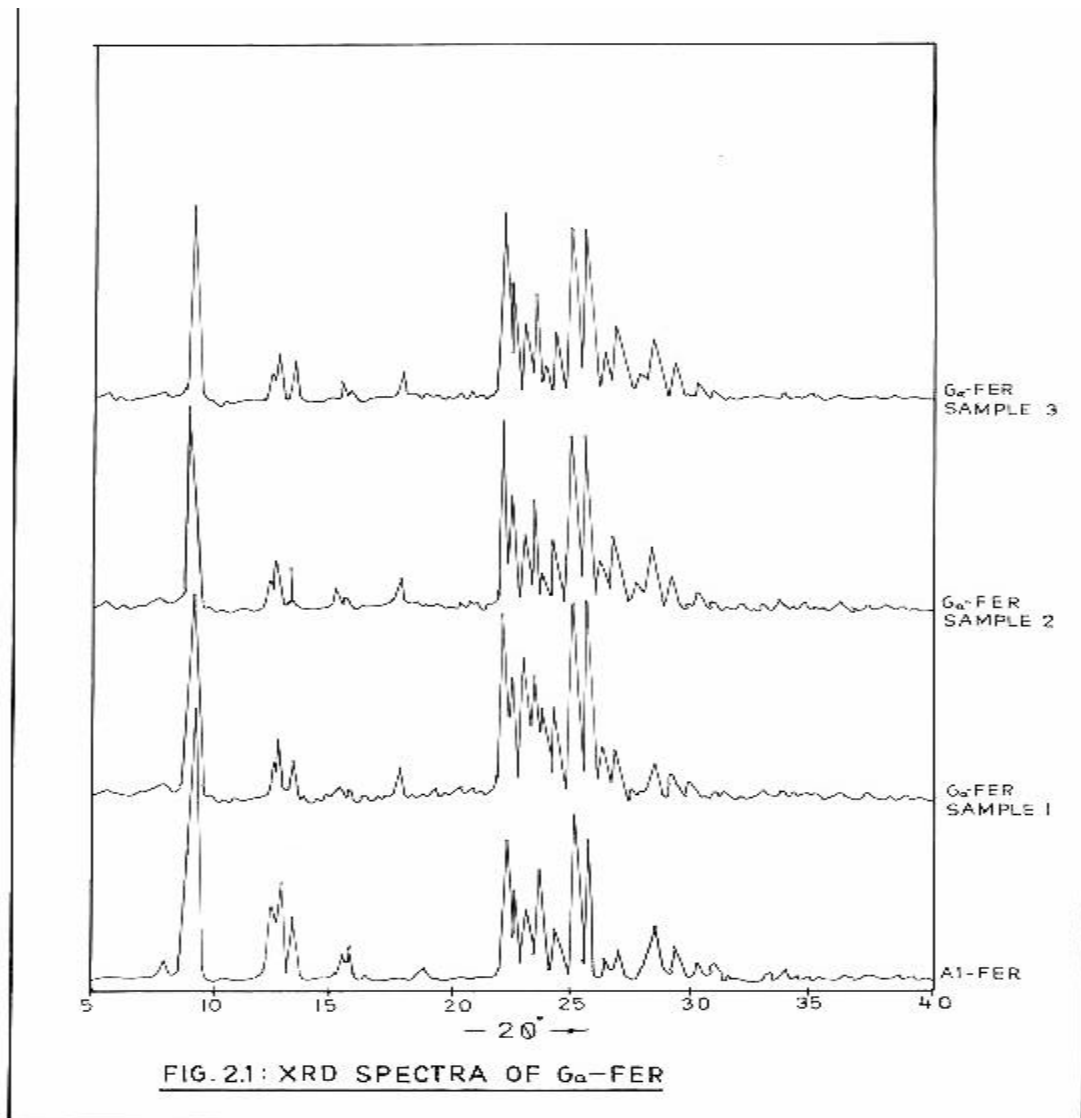
Sample	Si/Ga		Ga (wt %) by XRF
	Input	Output	
Sample 1	15	9.85	10.14
Sample 2	32	19.80	5.44
Sample 3	50	20.92	5.20

2.3 Characterization :

The Ga-FER samples were characterized by using various spectroscopic and non-spectroscopic techniques. The main aim of all the characterization was to find out the gallium incorporation in the Ferrierite structure and its effect. For this purpose, following characterization techniques have been used.

2.3.1 X-Ray Diffraction (XRD):

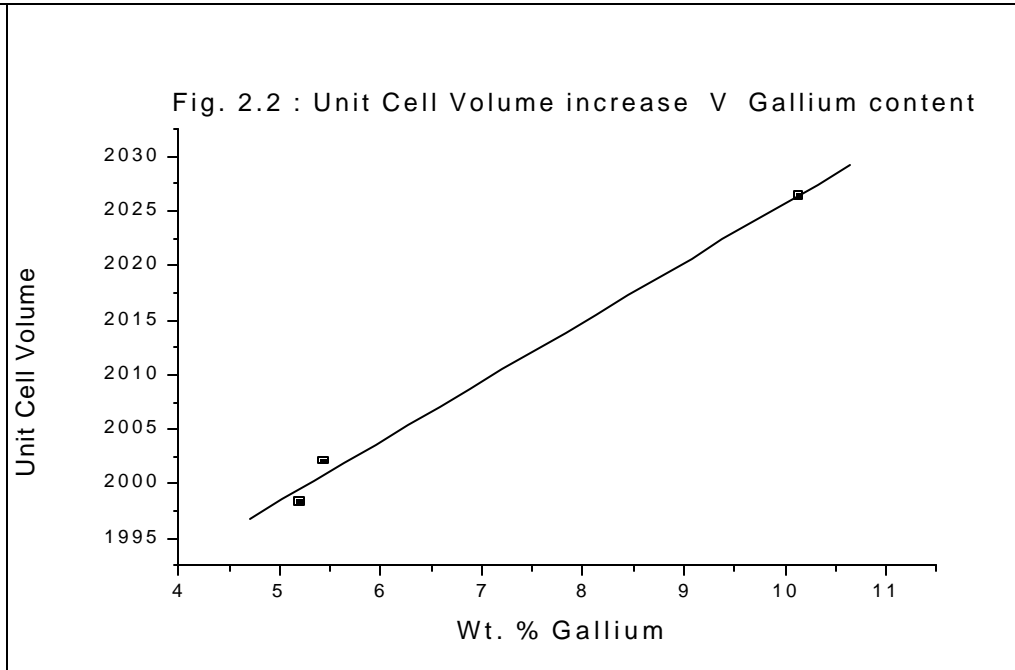
XRD was carried out on Rigaku D max II VC spectrometer. The main aim of employing this technique is to determine phase purity and percent crystallinity of the Ga-FER samples. This also gave information about the unit cell parameters of the Zeolite and Isomorphous substitution, which is revealed by the unit cell expansion. This expansion in unit cell volume is due to replacement of bulkier gallium ions in place of aluminum ion in the Ferrierite structure. In Fig.2.1 XRD patterns of three different gallium containing samples along with the Al-FER pattern were shown.



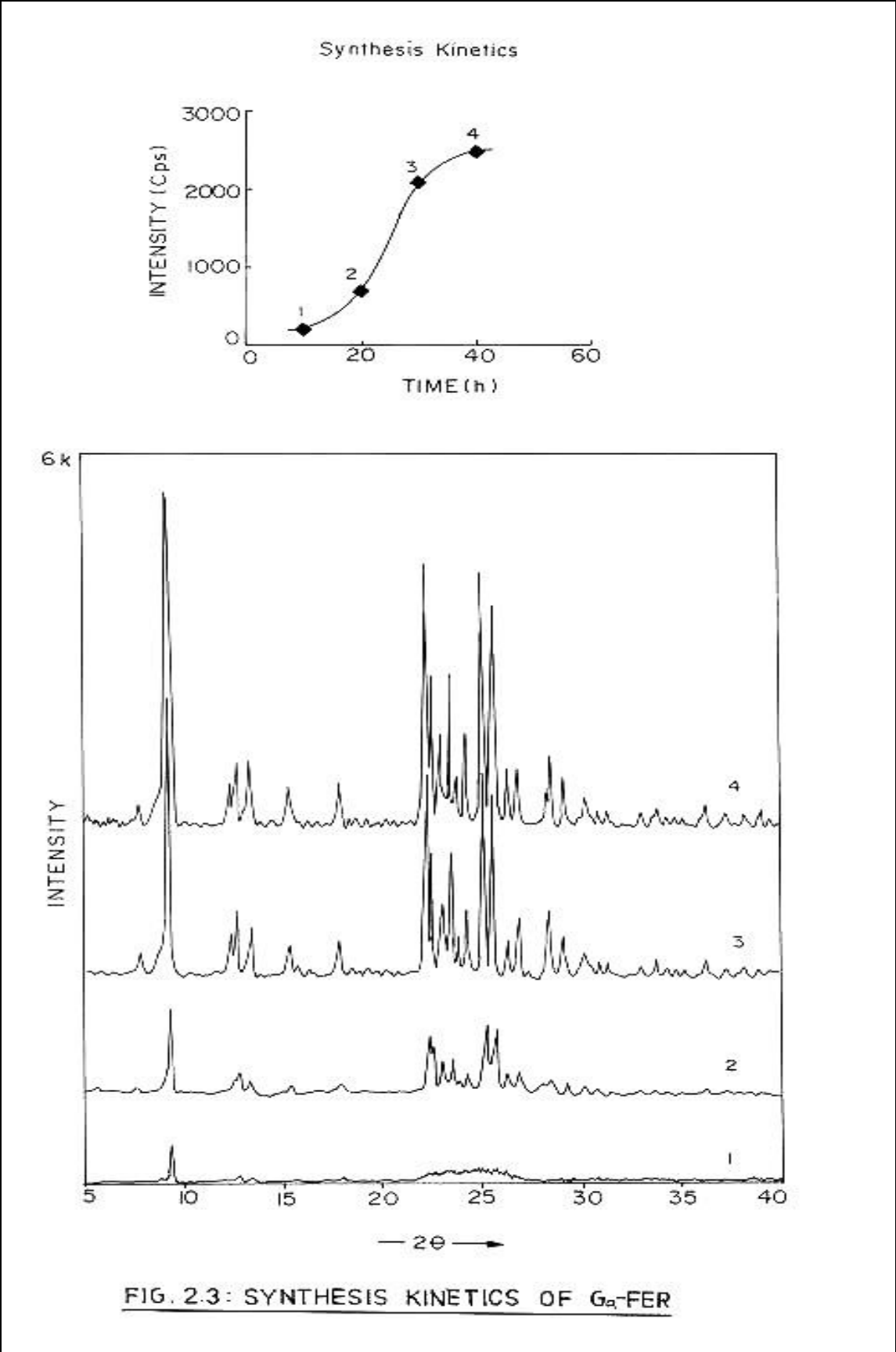
The XRD patterns of the Ga-FER samples were similar to those of aluminum ferrierite. The positions of the peaks were not changed by gallium incorporation which confirms the phase purity after gallium incorporation. The incorporation of Ga⁺³ ions into the framework caused a unit cell volume expansion as expected [13]. In case of Al-FER the unit cell volume was found as 1958.00 Å³. After incorporation of gallium it was increased to 1998.29 Å³, 2002.12 Å³ and 2026.40 Å³ in three Ga-FER samples (Table 2.3). It can be seen that the unit cell volume increased with the gallium content in the FER structure (Fig. 2. 2).

Table 2.3 : Unit cell parameter data of various Ga-FER samples.

Sample (Ga-FER)	Ga wt% (XRF)	a ₀ Å	b ₀ Å	c ₀ Å	unit cell volume Å ³
Sample 1	10.14	18.99	14.19	7.52	2026.40
Sample 2	5.44	18.96	14.14	7.47	2002.12
Sample 3	5.20	18.97	14.11	7.47	1998.29
Al-FER	--	18.69	14.06	7.40	1958.00

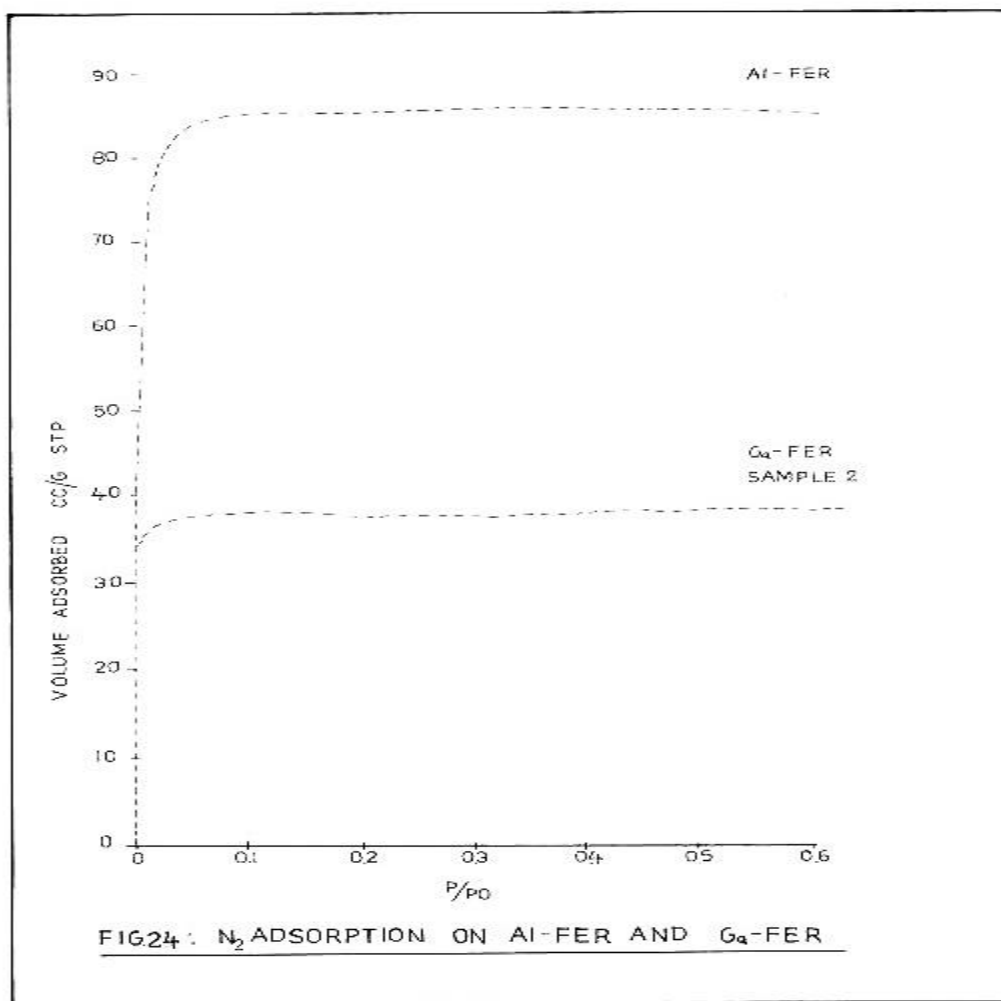


The synthesis kinetics of the Ga-FER zeolite is shown in Fig. 2.3 . During synthesis of Ga-FER, 4 different sets of experiments have been carried out using above mentioned synthesis procedure. Each synthesis experiment was stopped after 10 hours of the previous experiment. The four samples varied in crystallinity. The multiple plot of XRD spectra are plotted in Fig 2.3. The graph of Time verses Highest peak intensity has been drawn. An exact "Sigmoid" shape curve is observed which is characteristic of that of zeolite synthesis [14,15,16].



2.3.2 Surface area measurement :

An Omnisorp 100 CX (COULTIER, USA) analyzer was used for the measurement of low pressure nitrogen adsorption to determine the surface area and micro-pore volume. The sample was activated at 673 K for 2 h. in a high vacuum (10^{-6} Torr). After the treatment, the anhydrous weight of the sample was taken at room temperature. The samples were then cooled to 78 K using liquid nitrogen. After that, the samples were allowed to adsorb nitrogen gas. The BET surface area was calculated. Fig 2.4 shows the comparative graph (adsorption isotherms) of nitrogen adsorbed on the Al-FER and it's gallium analog Ga-FER.



Surface area and micro-pore volume were calculated by using BET equation from the above isotherms and the values are given in Table 2.4 .

Table 2.4 : Surface area and Micropore volume of Ga-FER sample.

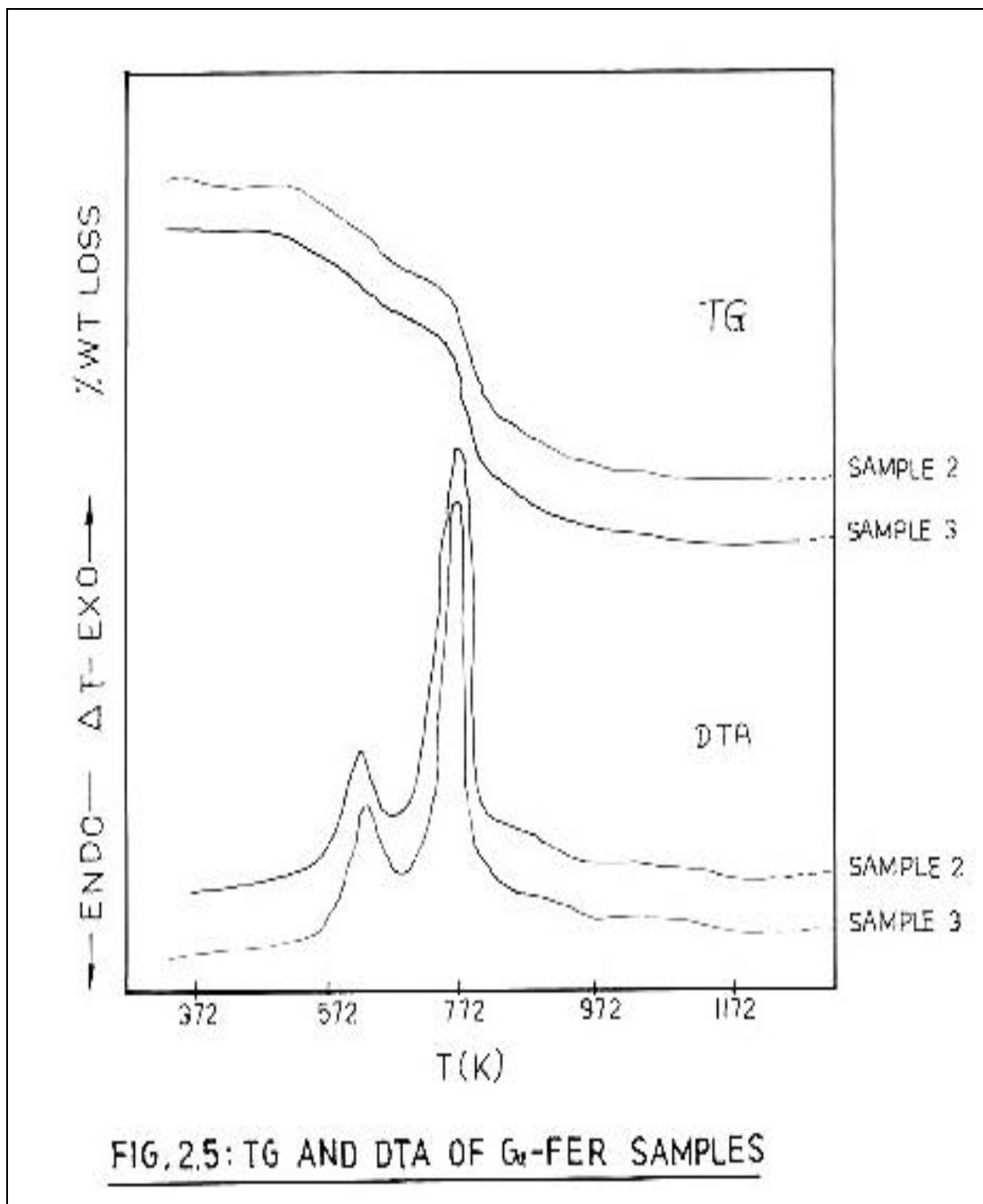
Sample	Surface Area m ² /g.	Micropore Volume ml/g.
Ga-FER (Sample 2)	148.4	0.07
Al-FER	351.3	0.14

It can be seen that due to incorporation of gallium in the Ferrierite framework, the surface area and micro-pore volume decreased significantly. It is surprising that even though there is an increase in unit cell parameters with gallium incorporation, the adsorption of N₂ is decreased. This is due to the extraframework gallium oxide occupying the zeolite pores and decreasing the adsorption capacity.

2.3.3 Thermal analysis and structural stability :

Figure 2.5 represents thermo-analytical curves of samples 2 and 3 in their as-synthesized forms. The TG curves indicate continued weight loss (~ 2.0 wt %) mainly due to the dehydration occurring from the FER zeolite cavity in the low temperature range up to 573 K. The DTA curves obtained in air for the as-synthesized products of varying SiO₂/Ga₂O₃ ratios, reveal significant changes, which are mainly due to oxidative decomposition of the occluded pyrrolidine template. The curves exhibit two characteristic exotherms at T_{max} 622 K and 775 K. The existence of two exothermic peaks in case of other high silica zeolites e.g. ZSM-5 [17], Silicalite [18], EU-1[19], have been reported in the literature. According to Parker *et al.*[18] these low temperature peaks (622K) arise mainly due to templating species (R = pyrrolidine) which are not adjacent to an aluminum ion (≡ SiOR defect groups) and weakly bonded to the frame work. These favour early

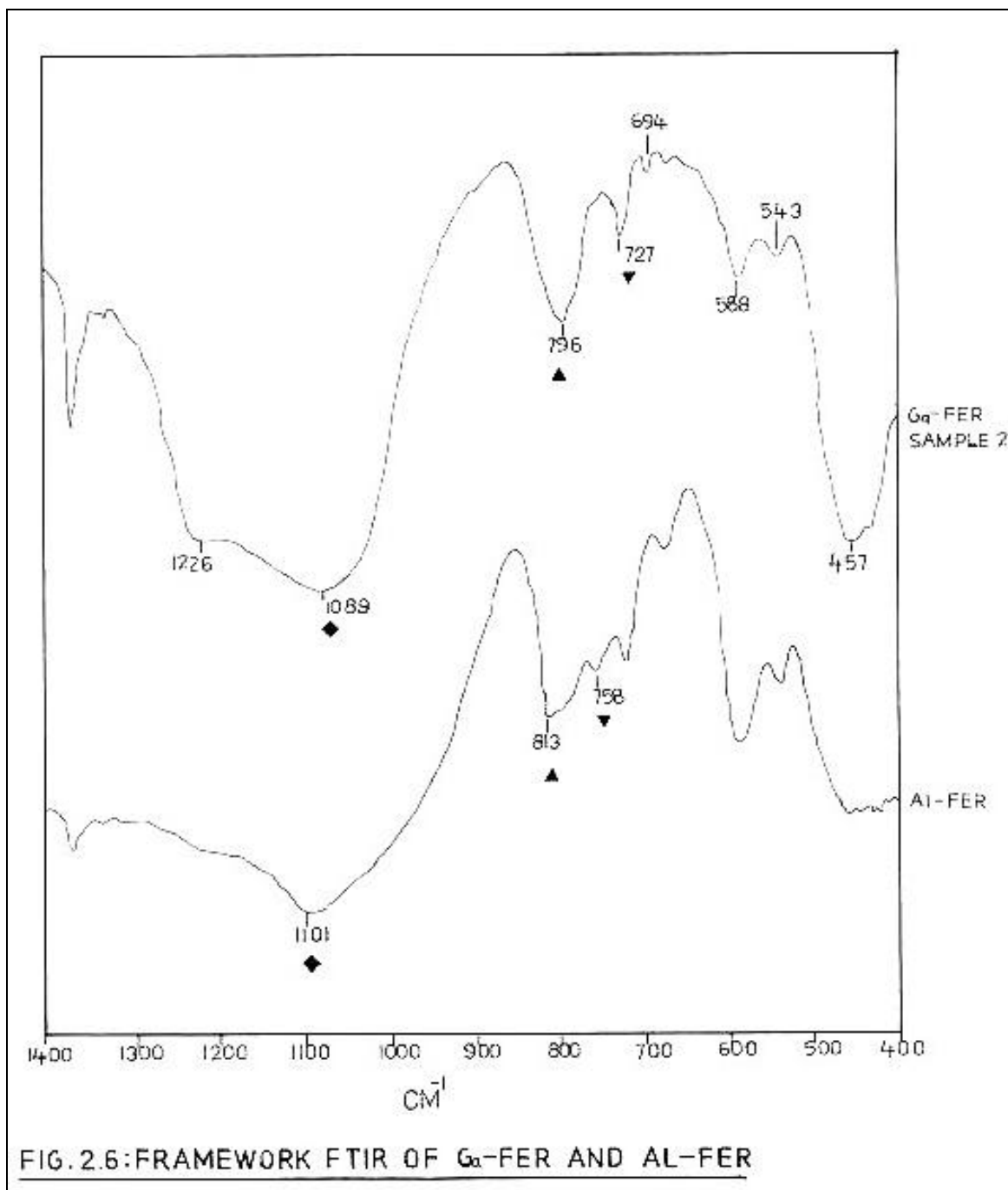
decomposition. On the other hand strongly bonded species near the aluminum site acting as charge compensating (AlO_4^- tetrahedra) ion decompose at higher temperature ($T_{\text{max}} 775 \text{ K}$). There are no major changes or transformations observed in the temperature range $775 - 1273 \text{ K}$ which indicates that the Ga-FER samples maintain structural integrity upto 1273K (1000°C).



2.3.4 Framework IR spectra :

These spectra were recorded in the framework region 1300-400 cm^{-1} with Nujol mull.

Figure 2.6 shows the framework region infrared spectra of gallium ferrierite and Al-ferrierite samples.



Ga-FER spectrum shows two characteristic absorption bands around 1226 cm^{-1} and 694 cm^{-1} . These bands can be attributed to the vibrations within the ferrierite framework [20]. The absorbance around 588 cm^{-1} confirms the presence of distorted five membered double ring (DDR-5) present in the high silica ferrierite framework. The IR spectra shows strongest band at $\sim 1089 \text{ cm}^{-1}$ due to asymmetric stretching of internal Si-O-Ga vibrations. The decrease in this band position from 1101 cm^{-1} was due to introduction of heavier atom in the Ferrierite framework [21].

Table 2.5 shows the framework region vibrational frequencies for FER system.

Table 2.5 : Framework vibration frequencies for Gallium ferrierite (Ga-FER) zeolite.

Wave number (cm^{-1})	Assignment
457.1	Si — O bending.
543.9, 588.2	Distorted double five membered rings (5-DDR).
694.3	Internal tetrahedral symmetrical stretch.
727	External link symmetric stretch.
1089.7	Internal tetrahedral asymmetric stretch.
1226.6	Internal asymmetric stretching.

When compared with Al-FER spectrum the bands at 813.9 and 758 cm^{-1} (from Al-FER) were found to be shifted to 796.5 and 727.1 cm^{-1} (Ga-FER) resp.. This is due to the replacement of heavier gallium ion in place of aluminum ion in the Ferrierite framework and thus increasing the reduced mass which reflected in decreasing the frequency [22].

2.3.5 Acidity measurements using IR spectroscopy :

Pyridine is largely used as a probe molecule to study the acid sites but this can't fully penetrate the channels of 8 and 10 membered rings of Ferrierite [23]. Nitrile has a promising functional group and is of low basicity. It is possible to determine the acidity from the wave number shift of this molecule. Acid site distribution of Ga-FER sample was studied by using d_3 -acetonitrile as a probe molecule. The concentration of Bronsted and Lewis acid sites was calculated by using the reported extinction coefficients [23]. FTIR spectra of Ferrierite samples were recorded on wafers of thickness ca. 10 mg/cm^2 . The Nicolet Magne-550 FTIR spectrometer was used with a DTGS KBr detector and a vacuum cell with CaF_2 windows attached to the vacuum arrangement and dosing system for acetonitrile. The sample was activated at 670 K and adsorption of d_3 acetonitrile (Aldrich) (13 mbar) on evacuated zeolite was carried out at 298 K for 30 min. followed by further evacuation at 298 K for 10 min. Spectra were recorded at ambient temperature with 2 cm^{-1} resolution by collecting 200 scans for a single spectrum. IR spectra are normalized on a sample thickness of 10 mg/cm^2 . IR bands of adsorbed d_3 -acetonitrile was deconvoluted using a procedure consisting of identification of a band position in a second derivative mode of the spectrum and the least square minimization routine approximating the band by a gaussian profile. Extinction coefficients of Bronsted and Lewis acid sites of Al-Ferrierite were used for calculating acid sites. Pelmenchikov [23a] have suggested following species of trivalent and tetravalent metal ions after CD_3CN adsorption. Bands at 2278 cm^{-1} , 2300 cm^{-1} , $2332\text{-}2323 \text{ cm}^{-1}$ correspond to the terminal silanol group, Bronsted acid site (bridging OH) and Lewis alumina site respectively. This is shown in Fig. 2.7.

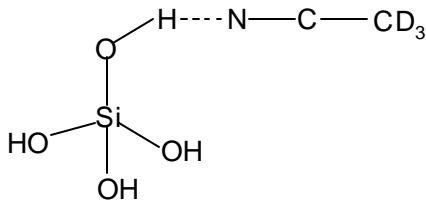
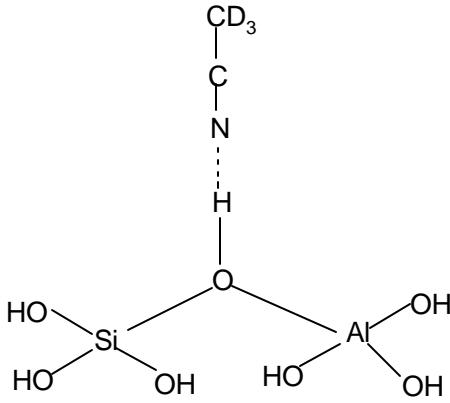
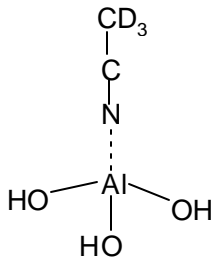
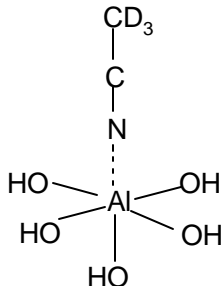
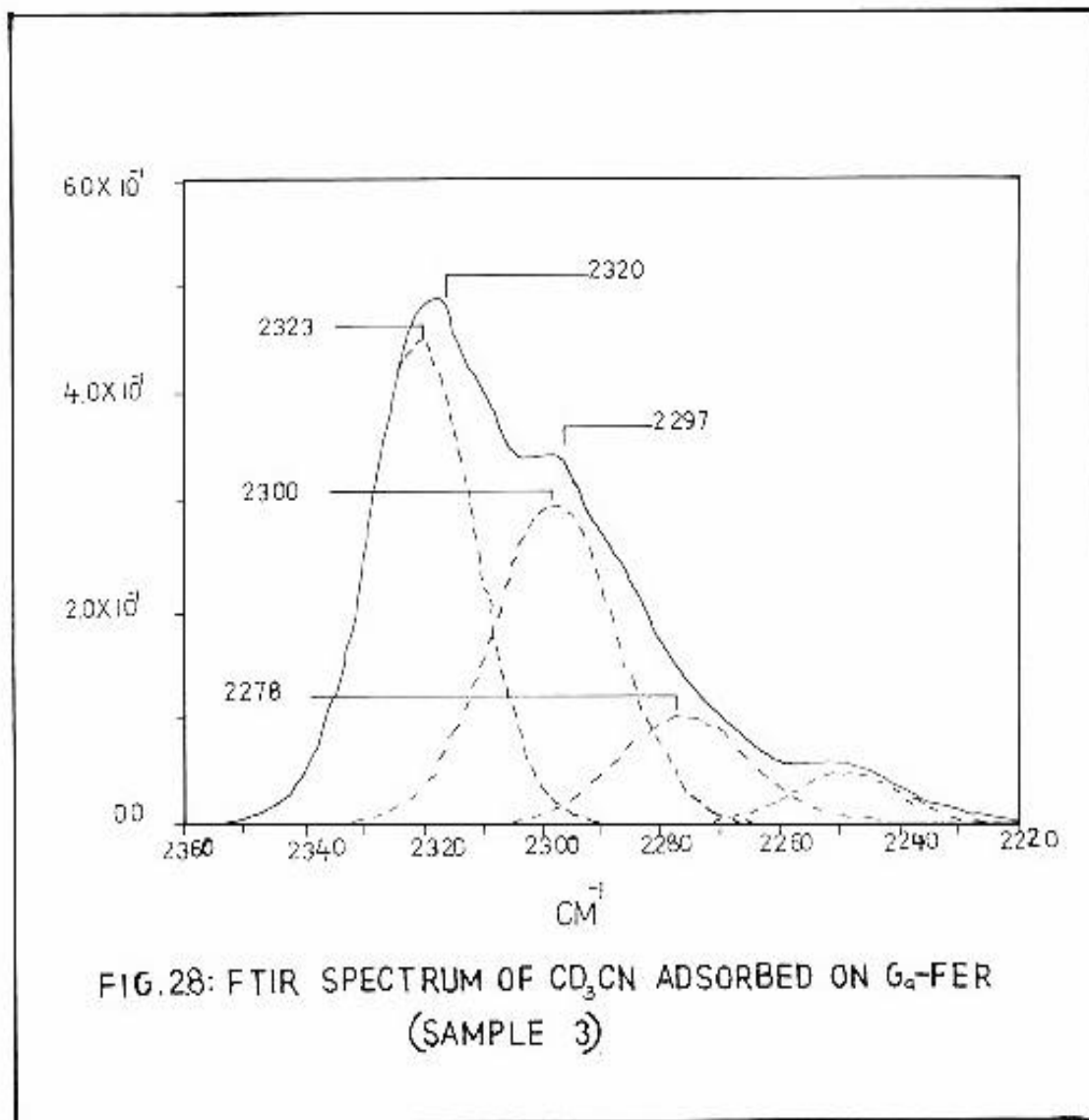
Peak Position cm ⁻¹	Species	Species Description
2278		Terminal Si--OH group
2300		Bridging OH group (Bronsted Acid Sites)
2332		Lewis Alumina site
2323		Lewis Alumina site

Fig. 2.7 : Different species after CD₃CN adsorption

Fig.2.8 shows the cumulative spectra of d_3 -acetonitrile adsorbed on the Ga-FER sample.



The deconvolution procedure yields bands at 2320 cm^{-1} and 2297 cm^{-1} corresponding to Lewis sites and Bronsted sites resp. (Table 2.6). In Ga-FER the amount of Lewis acid sites are little more than Al-FER but that of Bronsted sites are much less than Al-FER. The total acidity is less than Al-FER. This confirms that Ga-FER is moderately acidic.

Table 2.6 : d₃-Acetonitrile Adsorption (cm⁻¹)

Sample	Position (cm ⁻¹)	Area	Position (cm ⁻¹)	Area	Conc. (mmol/g)	
	L-site	L-site	B-site	B-site	L-site	B-site
Al-FER	2323	8.5	2296	11.4	0.24	0.55
Ga-FER (Sample 1)	2320	10.3	2297	7.9	0.28	0.39

2.3.6 Scanning Electron Microscopy :

Fig 2.9 displays the scanning electron micrographs of Ga-FER (Sample 2). The crystal size of the Ga-FER material is ~2-3 μm and is of rectangular plate type morphology.

The shape and size of the crystals are not uniform. The size varies from 1 μm to 5 μm.

The rectangular plate shape of Ga-FER sample is similar to that of Al-FER sample.

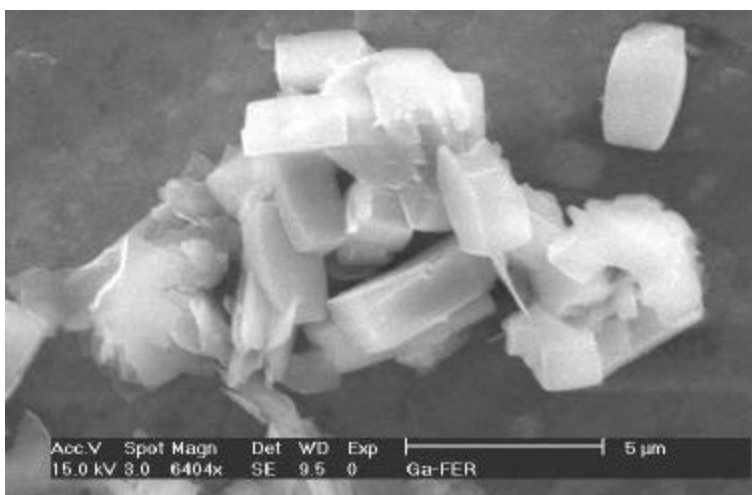
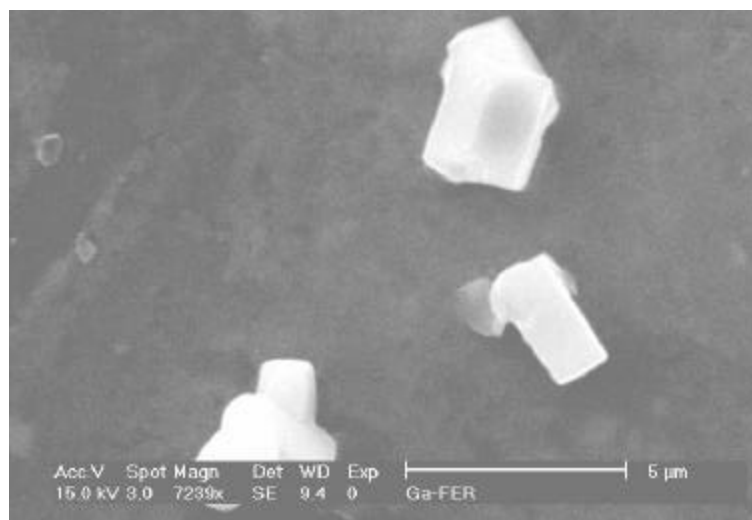
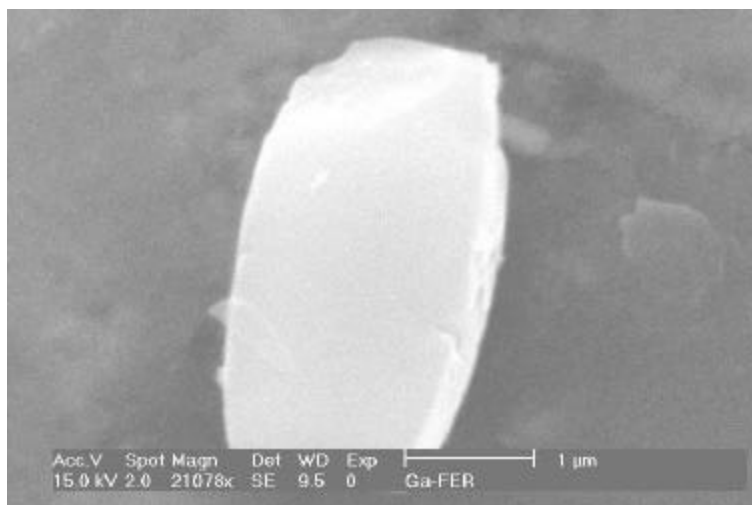
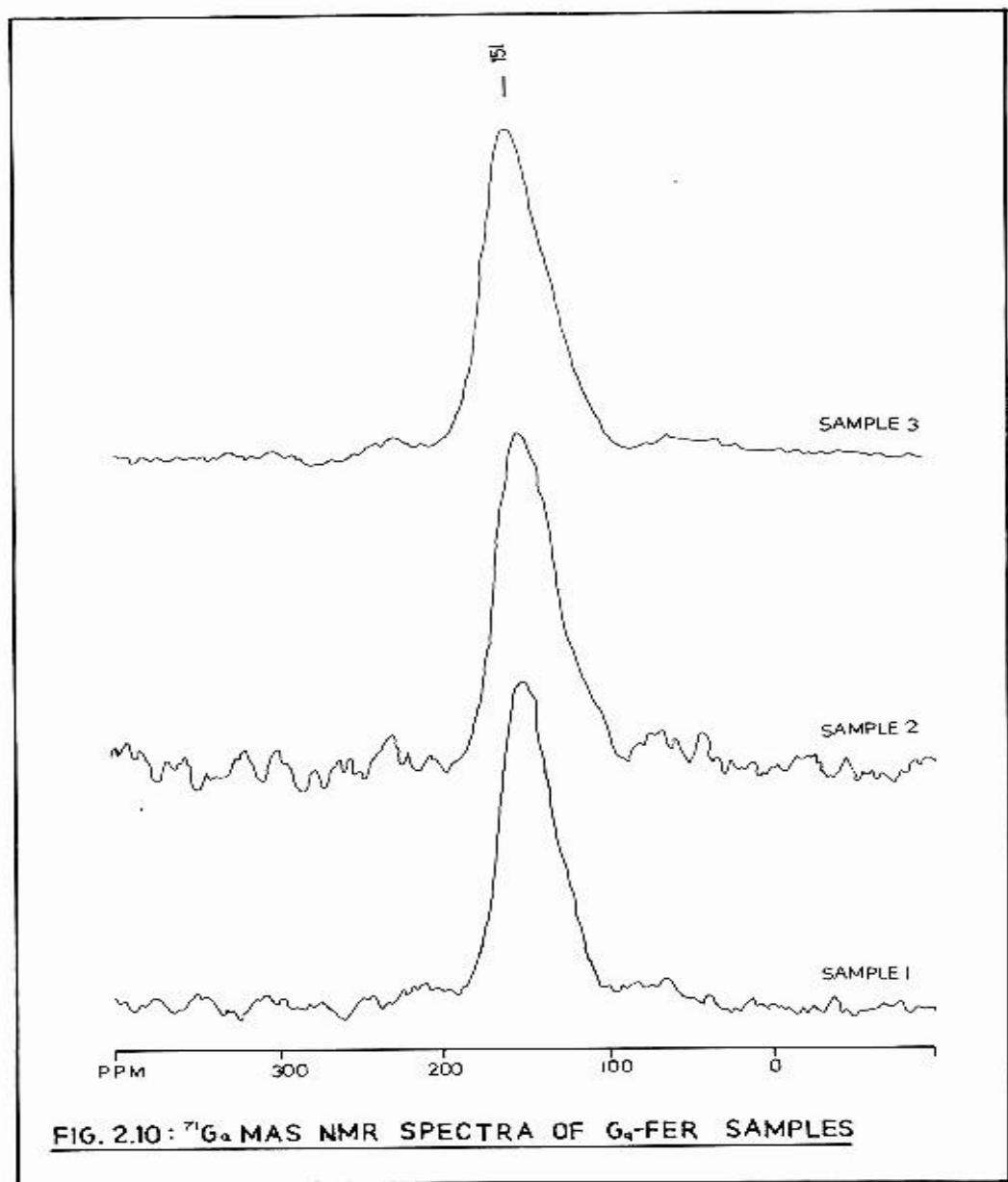


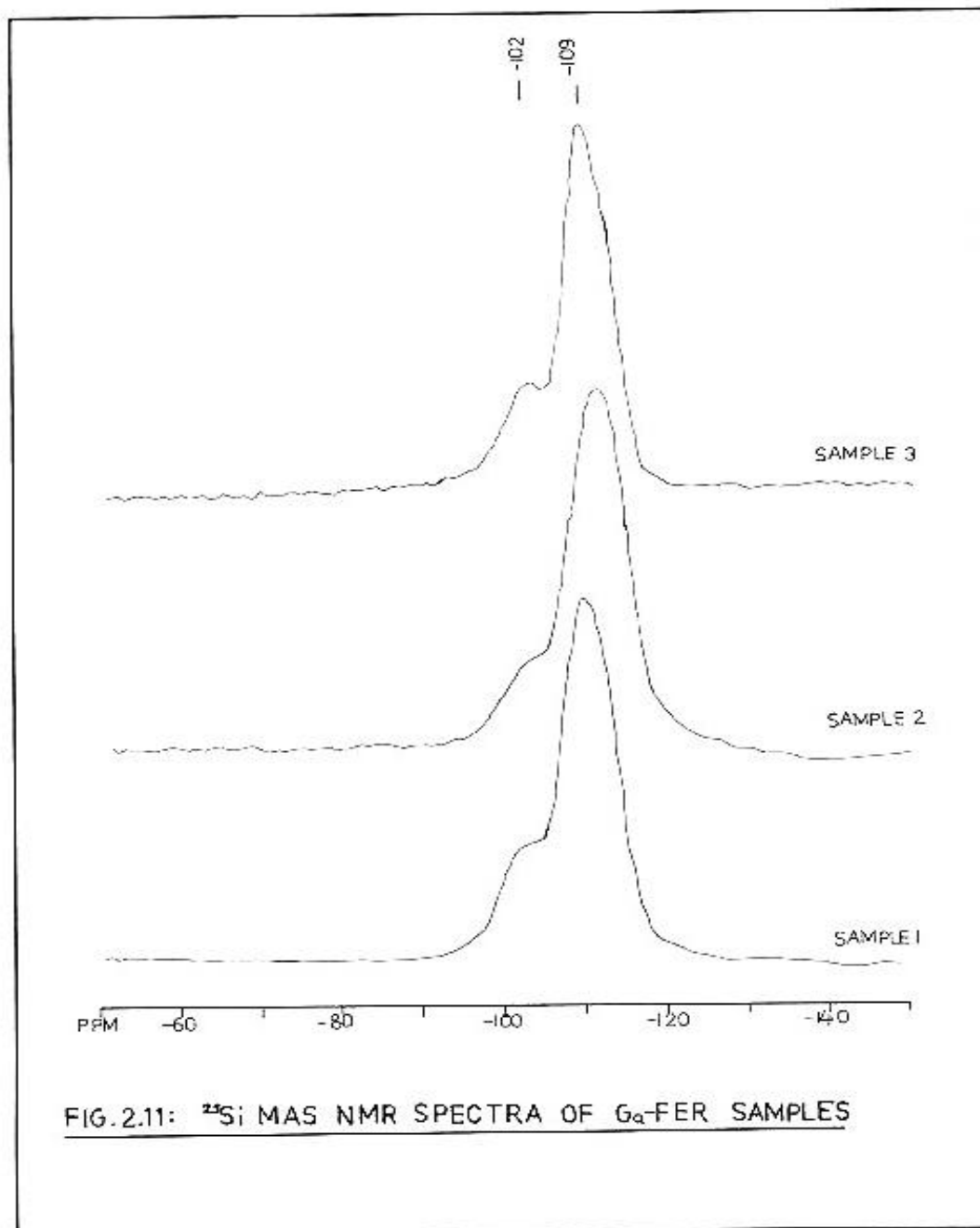
Fig. 2.9: SEM photographs of Ga-FER (sample 2)

2.3.7 Nuclear Magnetic Resonance Spectroscopy :

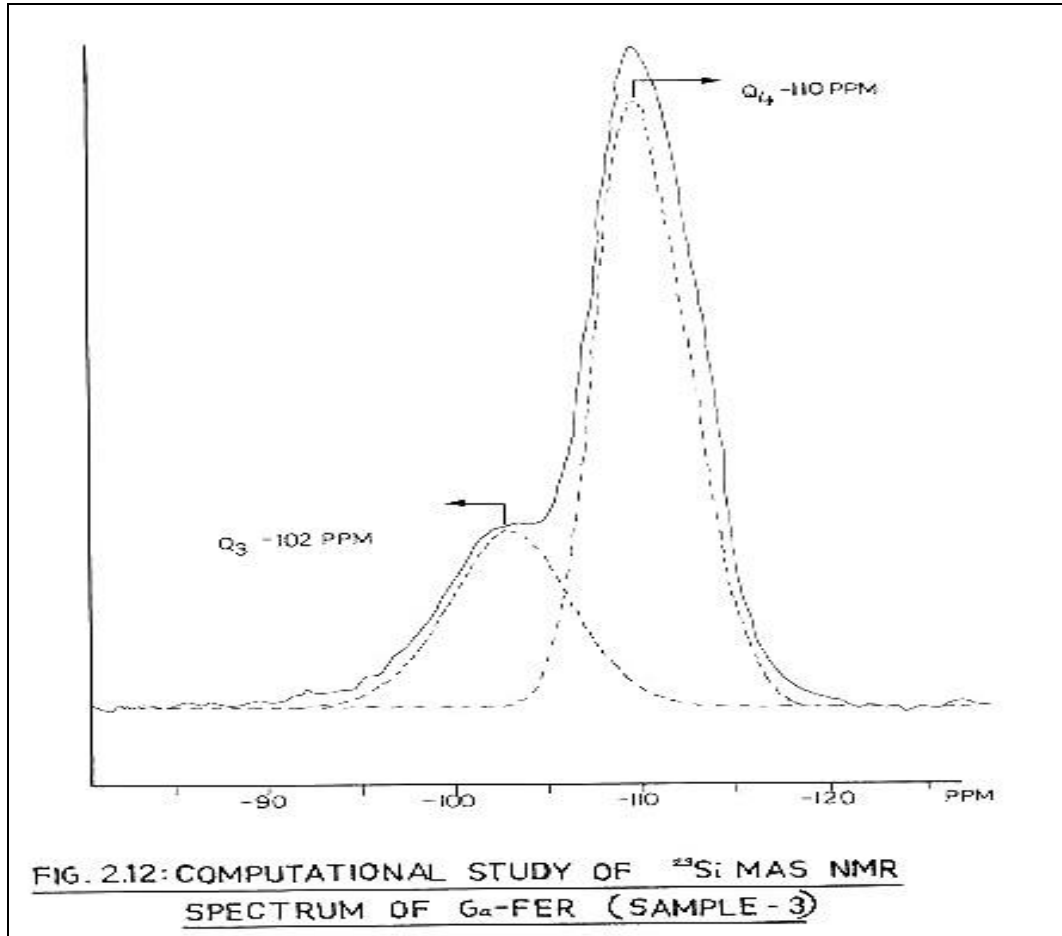
Fig 2.10 shows the ^{71}Ga MAS NMR spectra of Ga-FER samples (Sample 1, 2 and 3). The sharp peak at 150 ppm in all the three samples indicates the presence of tetrahedrally coordinated framework Ga^{+3} species [24-27]. The peak at -87 ppm was absent in all the three spectra, which is attributed for the Ga^{+3} in octahedrally coordinated form.



The Fig 2.11 shows the ^{29}Si MAS NMR of the Ga-FER samples. All the three samples are showing 2 peaks. The signal at -109 ppm is due to the Si (0 Ga 4 Si) coordinated Q_4 Silicon^{IV} species in the Ferrierite framework. The signal at -102 ppm can be assigned to the Si (1 Ga 3 Si) coordination [28] which is Q_3 silicon species with one heteroatom (Ga^{+3}) in its vicinity.

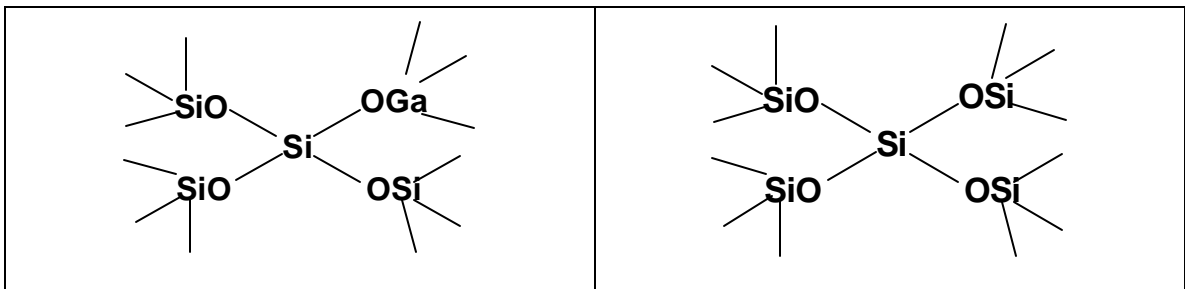


Both these MAS NMR results confirm the Ga incorporation in to the ferrierite framework which is also confirmed by unit cell expansion. The computational study of Ga-FER (Sample 3) gives quantitatively the amount of Q₄ (73.5%) and Q₃ (26.4%)species in the ²⁹Si MAS NMR (Fig. 2.12). Thus from the results, the calculated Si/Ga ratio is 15. From XRF analysis the ratio was 20.



Q₃ Species

Q₄ Species



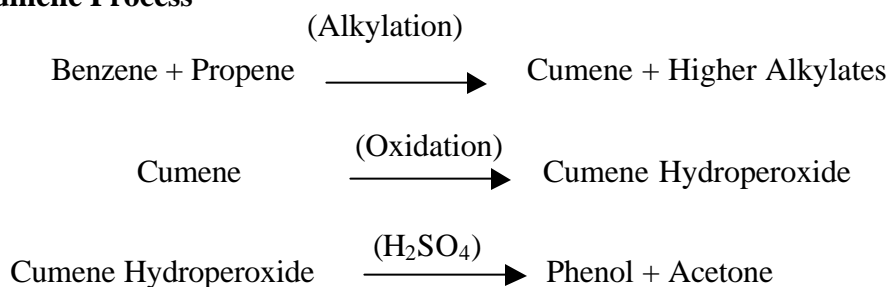
2.4 Catalysis :

The Ga-FER catalyst is having gallium in the framework of Ferrierite zeolite in place of aluminum. Due to this replacement, Ga-FER is mildly acidic than Al-FER. Gallium can show two different valence states (i.e. Ga^{+1} and Ga^{+3}) which contribute to oxidation reduction behavior [28a]. In order to investigate these properties of Ga-FER a single step Benzene Hydroxylation and Benzene Ethylation reactions were studied.

2.4.1 Benzene Hydroxylation :

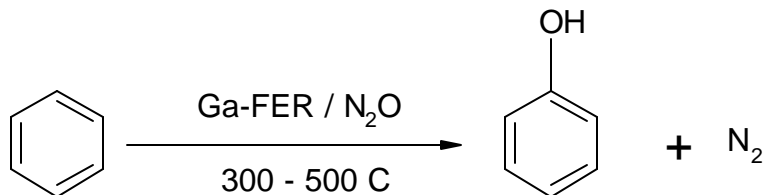
Benzene hydroxylation or partial oxidation of benzene and its derivatives to phenol and phenolic compounds is wellknown.. Due to the commercial importance of phenol, in the synthesis of various organic chemicals, in the production of Phenolic resins (used as adhesives in plywood industry), Bisphenol A (used as engineering thermoplastics), Aniline, Alkyl phenols, DPO and Polycarbonates etc., several studies have been carried out and the results are available. Holderich et.al. [30] reported liquid phase synthesis of phenol using H_2O_2 in the presence of TS-1. Iwamoto et. al. [31] followed the gas phase synthesis of phenol using N_2O in presence of a $\text{V}_2\text{O}_5/\text{SiO}_2$ catalyst. Several researchers have carried out gas phase synthesis of phenol using N_2O as oxidant and analogs of ZSM-5 zeolite as catalysts [32-51]. The most commonly used and economically competent process is the multi step cumene process [29]. In this first cumene is produced by the catalytic alkylation of benzene with propylene, followed by cumene oxidation to peroxide and finally its cleavage to phenol and acetone. A schematic diagram of cumene process is shown below :

2.4.1.1 Cumene Process



The economy of the process is due to its byproduct acetone. Even though, direct hydroxylation/partial oxidation of benzene leads to the formation of phenol, the conversions and selectivities obtained do not permit a commercially viable alternative to the cumene route. Reports on the conversion of benzene to phenol using a zeolite catalyst of MFI type and gaseous nitrous oxide as an oxidant, indicate low selectivities caused by the high exothermicity.

The worldwide phenol production (1999) was 5174×10^3 t/yr. and that in India was 61×10^3 t/yr. Herdillia Chemicals (Mumbai) and Hindustan Organic Chemicals (Cochin) are the main manufacturers of phenol in India. Ga-FER is similar to MFI type zeolite, except an eight membered ring in place of one ten membered ring. Further the acidity associated with is less than the ZSM-5, the reaction of benzene with gaseous nitrous oxide may be high in respect of the utilisation of nitrous oxide. In the gas phase reaction benzene was passed over Ga-FER catalyst at high temperature along with nitrous oxide gas (N_2O). The reaction can be shown as



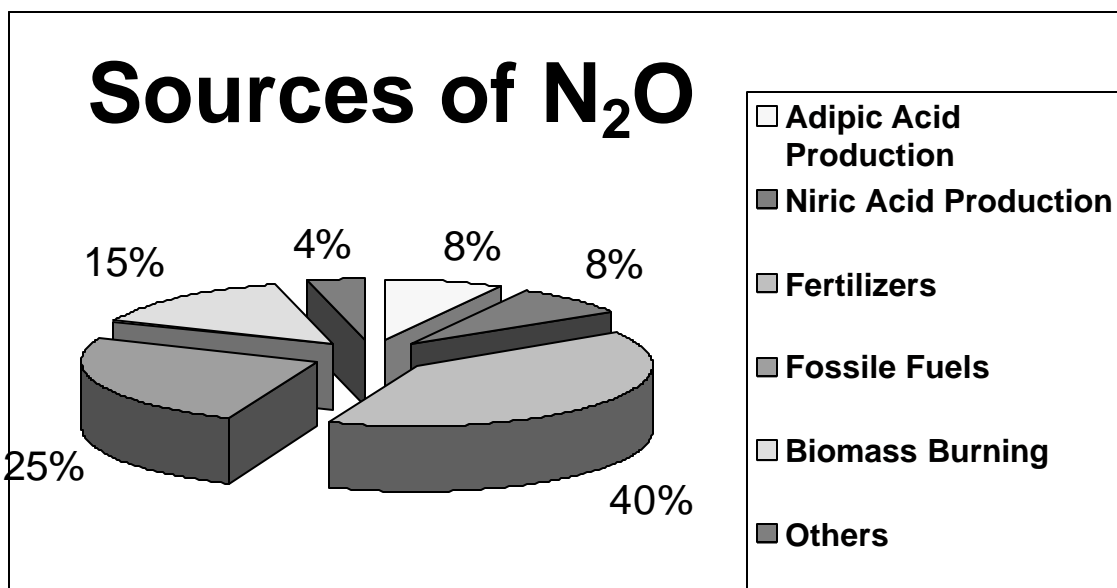
In the cumene process a total of seven steps are involved, starting with the production of cumene. During this process, corrosive and environmentally polluting catalysts like solid phosphoric acid, and H_2SO_4 are used. The handling of these materials is very hazardous and create disposal problems.

Direct hydroxylation of benzene is a single step process. Heterogeneous catalysts play an important role in this. Further byproducts like nitrous oxide produced in the adipic acid plants, fertilizer plants, causing atmospheric pollution can be utilized.

2.4.1.2 Utilization of N_2O :

Nitrous oxide (N_2O) is known as "Laughing Gas". Though it is useful for Medical Professionals as an anesthetic agent, it plays an important role in Ozone layer depletion (which is causing Global warming) in the stratosphere of the Earth. It is a very stable gas and its atmospheric life is 150 years. It is mainly produced in the reactions where Nitric acid is used as a reagent. The worldwide production of this gas is 4.7 - 7 million tones /yr (in 1999). The fragmentation of N_2O generation is shown in Fig. 2.13.

Fig. 2.13: Sources of N_2O generation

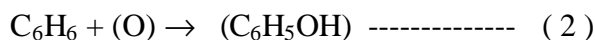


As a preventive measure, many researchers are trying to reduce N₂O by various heterogeneous catalysts like oxides, hydrotalcites, metal exchanged zeolites etc.

Our main aim to use Ga-FER catalyst for this reaction was

- To develop a single step eco-friendly synthetic route for phenol and
- To utilize a hazardous "Green house gas" N₂O, in the cause of chemical synthesis and thus developing a "Green Technology".

The gas phase hydroxylation of benzene was carried out using the above synthesized Ga-FER catalysts. Penov et.al [40,41] have suggested the following reaction mechanism :



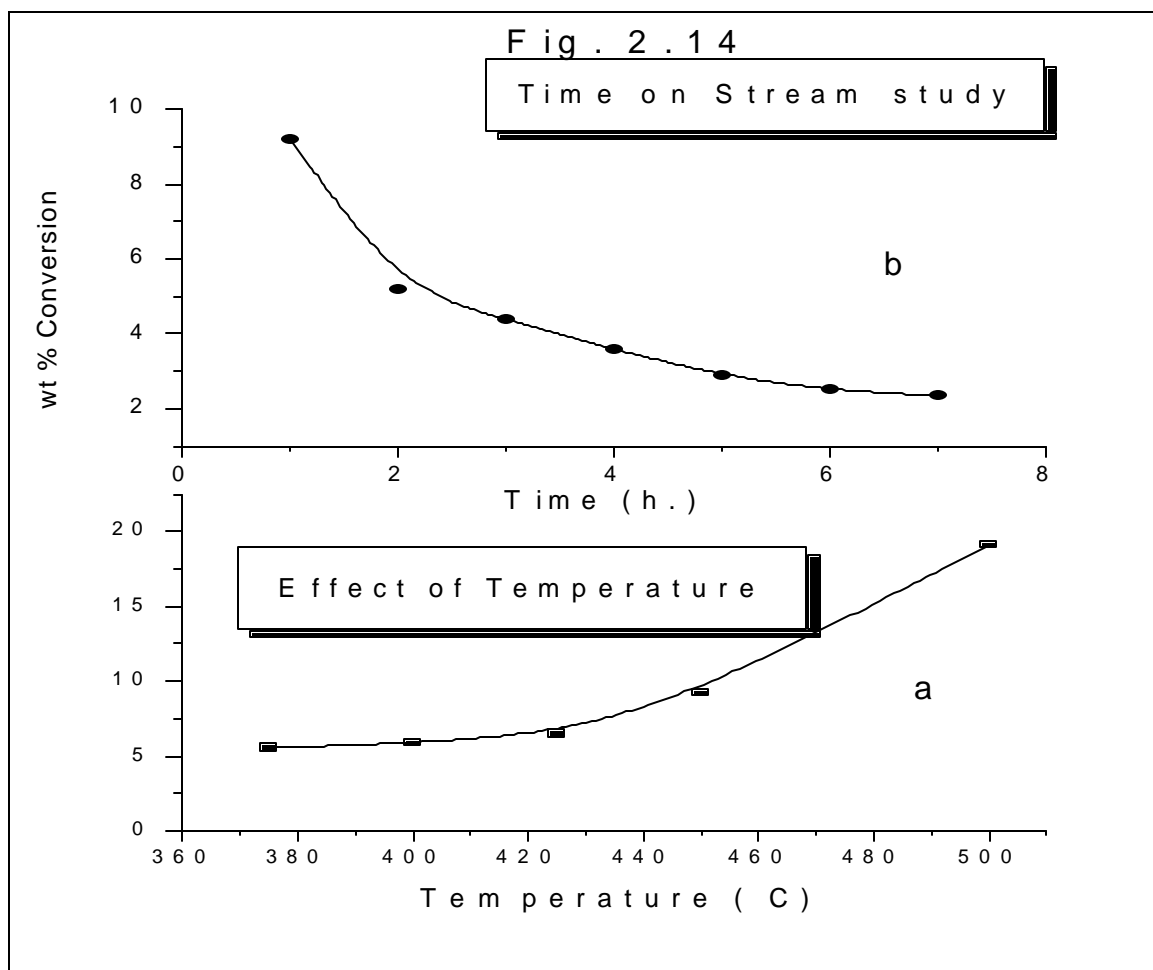
* Species in parenthesis are the active species.

The α -oxygen (O) species are acting as oxidants in the above reaction.. The (O) species are generated on the tetrahedral gallium ions of Ga-FER by the (O) obtained from the decomposition of nitrous oxide.. These sites are essential for the hydroxylation reaction [41] and hence only the catalyst with α -sites are active for this reaction. The reaction is highly exothermic. The reaction is studied as a function of temperature, space velocity and benzene to nitrous oxide mole ratio. The stability of the catalyst was studied by extending the reaction time to long hours of duration and monitoring the conversion at regular intervals of time.

2.4.1.3 Effect of temperature:

The reaction was studied at a space velocity of one and benzene to nitrous oxide mole ratio one. The reaction temperature was varied from 300°C to 500°C. The product was

collected at fixed intervals of time at each temperature and analyzed by gas chromatograph (FAPS packed column). Phenol is the only liquid product, in addition to unconverted benzene.. At high temperatures ($> 450^{\circ}\text{C}$) oxides of carbon are observed in the gas phase along with benzene. Nitrous oxide was not detected in the gas phase. The conversions are calculated on the basis of analysis of the liquid and gaseous products at each temperature. The data is presented in a graphical form in Fig.2.14a. The conversion was low in the temperature range $300 - 440^{\circ}\text{C}$ (5-7 %), and suddenly increased to 19 % at 500°C . This may be due to the diffusivity of phenol at high temperature. The utilization of nitrous oxide to the desired product phenol is 30-40% under these experimental conditions. However benzene selectivity to phenol is more than 99.5%. Further rise in temperature above 550°C lead to lower phenol selectivity. The conversion however increased steeply. The catalyst was deactivating slowly. This is due to the coke formation. The catalyst was regenerated in air and nitrogen for further experimentation.

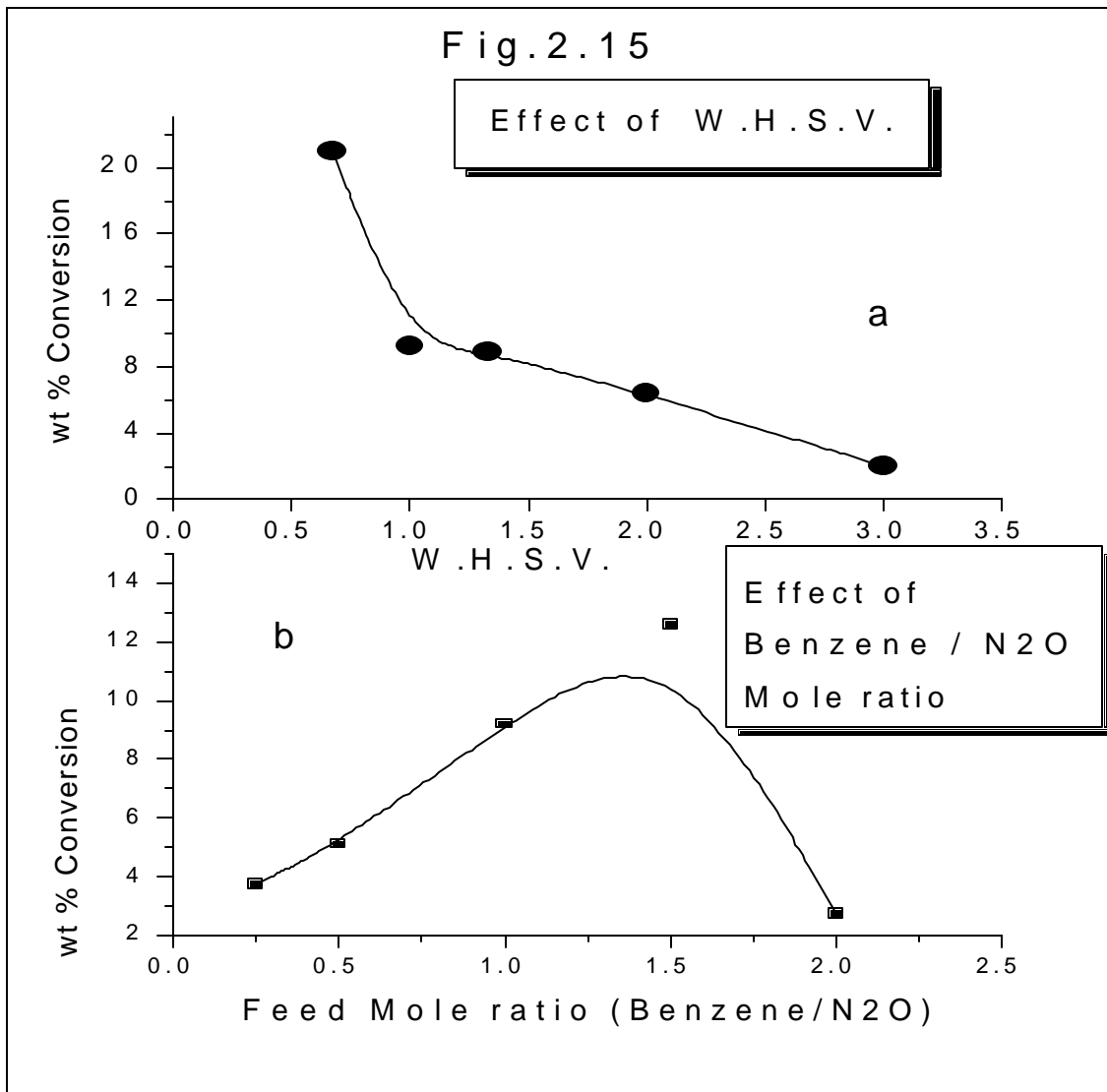


2.4.1.4 Effect of W.H.S.V. :

To further increase the utilization of nitrous oxide, influence of contact time and the variation of the amount of nitrous oxide in the feed by changing benzene to nitrous oxide mole ratio were studied. The results on the benzene conversion with contact time is included in Fig-2.15a. The other conditions are the temperature is 450°C, benzene to nitrous oxide mole ratio one. As expected at low contact time (high W.H.S.V.=3) the conversion of benzene is low (2 %) and at a W.H.S.V. of 0.7 conversion is 21%. This is purely due to the residence time of nitrous oxide. Even at high contact time no other compound than benzene and phenol were observed in the liquid product. The selectivity of phenol is very high. Unconverted nitrous oxide gas is not observed in the product.

2.4.1.5 Effect of Benzene / N₂O mole ratio :

Effect of Benzene / N₂O mole ratio is shown in Fig 2.15b. At 450°C and one W.H.S.V., the conversion of benzene is 3.7% at a benzene to nitrous oxide mole ratio 0.25. When the nitrous oxide was decreased in the feed and the ratio maintained at 1.67, the conversion increased to 12%. This is mainly due to the higher residence time of N₂O. However, when the mole ratio was further increased (2.0), the conversion of benzene was only 3%. The diffusion effects play an important role at these rates. A mole ratio of Bz/N₂O = 0.67, is optimum under these conditions.



2.4.1.6 Effect of Gallium content :

Fig 2.16a shows the effect of Ga content on the benzene conversion. The conversion of benzene is higher over sample 1 than sample 2. The Gallium content of the Sample 2 (10.14 %) was more than that of Sample 1 (5.44 %). The high activity of Sample 1 than that of 2 is due to the better dispersion of tetrahedral Ga^{+3} species acting as an active α -species. This was already shown in the MAS-NMR studies of Ga-FER wherein more amount of Ga is in tetrahedral framework in sample 1. Reaction was carried out at 450°C , W.H.S.V.=1.0 and benzene to nitrous oxide mole ratio one.

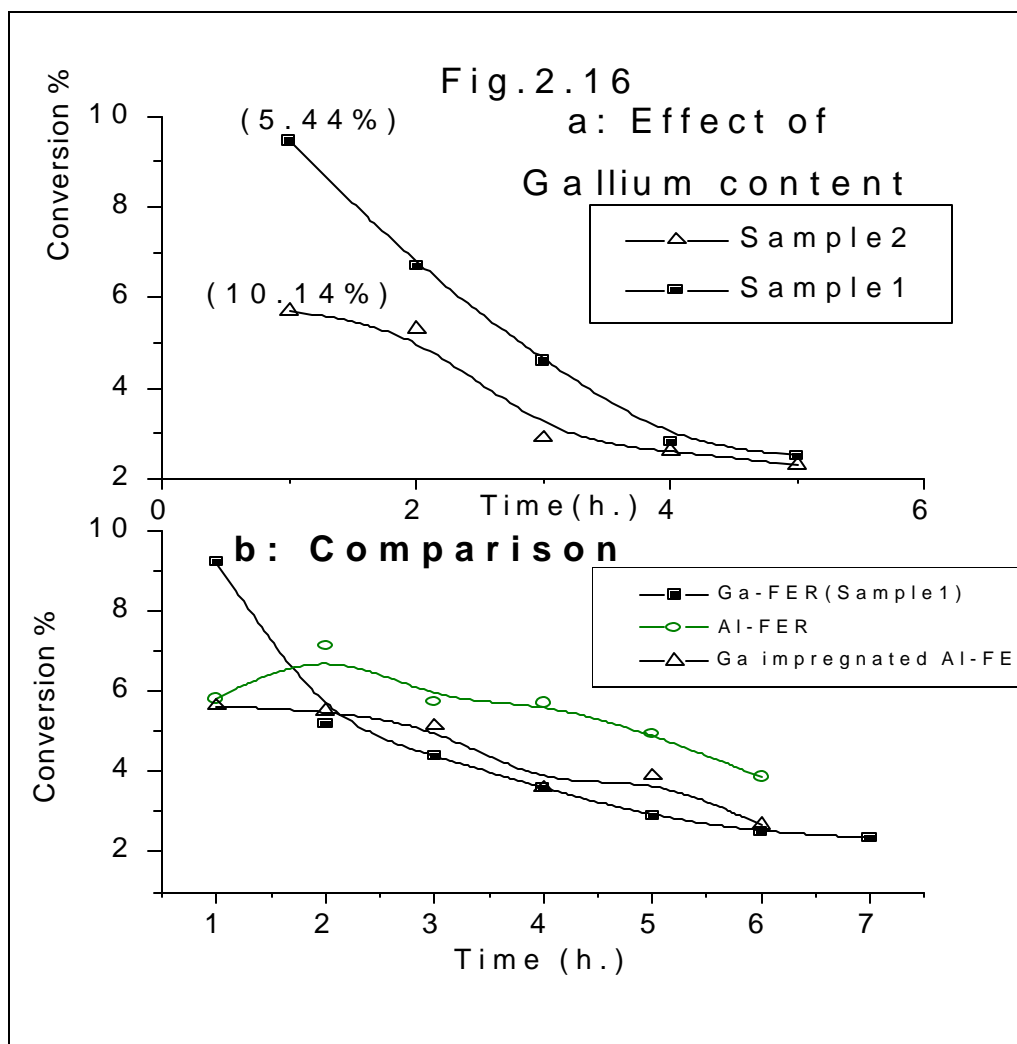
2.4.1.7 Time on stream study :

The stability of the catalyst was investigated by carrying out the reaction for longer duration with the analysis of the products at regular intervals of time. Effect of Time is shown in Fig 2.14b. The conversion of benzene decreased from 9.2% in the first hour to 2.35 % in 7 hours. The catalyst deactivation was very rapid. After the reaction the catalyst was examined. The coke content was very high which was responsible for the loss of activity. The coke formed on the catalyst surface was further examined and was found to be high boiling polymeric material, which strongly adsorbed on the catalyst, blocking the active centers for the reaction. The reaction was carried out at 450°C and at space velocity and benzene to nitrous oxide gas ratio one.

2.4.1.8 Comparison between different Ferrierites :

Fig 2.16 gives the comparison between the Ga-FER, Ga impregnated Al-FER, Fe-FER and Al-FER. Reactions were carried out at 450°C , W.H.S.V.=1.0 and benzene to nitrous oxide mole ratio one. Initially the activity of Ga-FER was more (9.2%) as compared to Al-FER (5.8 %), Ga impregnated Al-FER (5.6%) and Fe-FER (8.0%). It is due to the

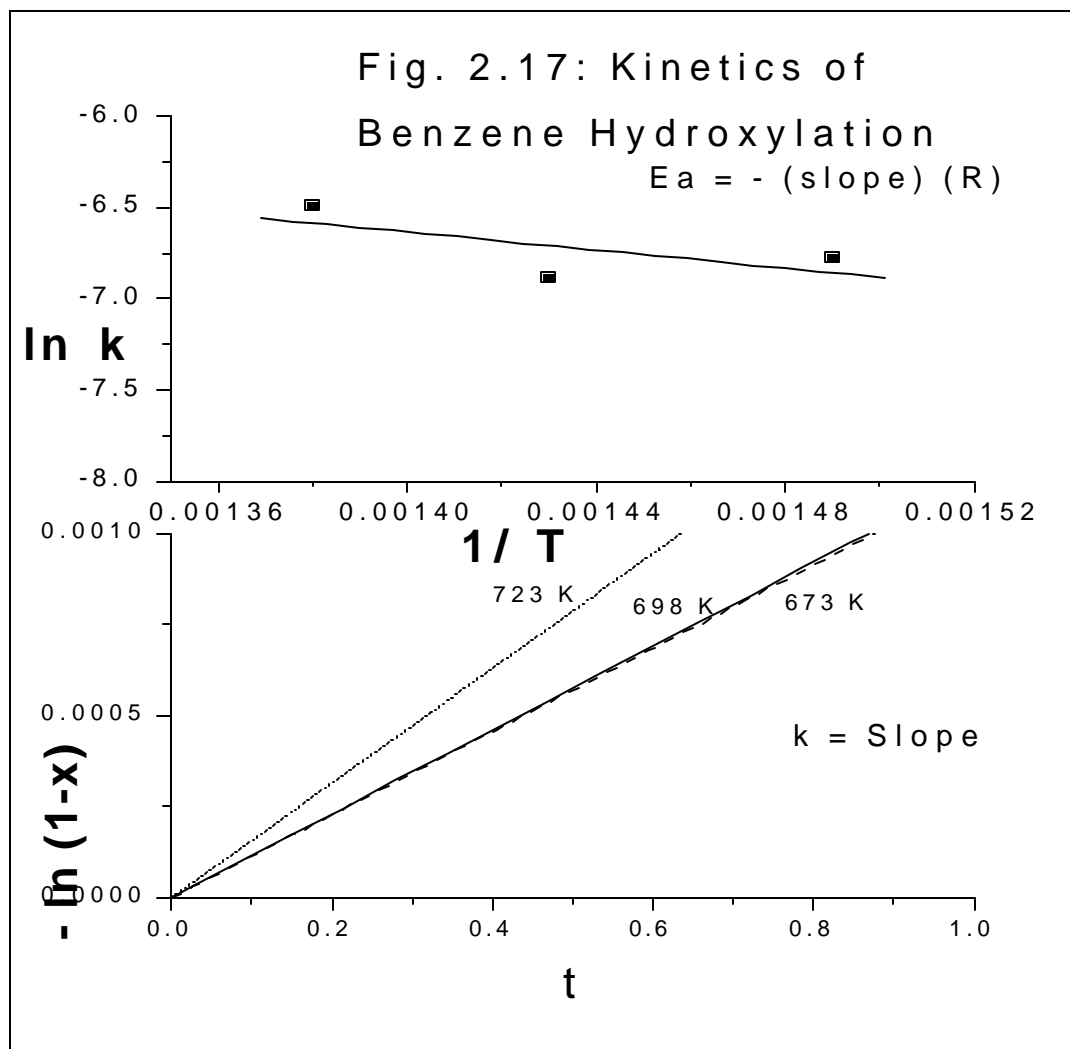
presence of a greater number of active α -species in Ga-FER (Sample 1) than in the same quantity of Gallium impregnated (5.44% Ga) Al-FER and pure Al-FER. The rate of deactivation of Ga-FER was higher as compared to that of Al-FER, and Fe-FER. However, the activity in terms of conversion of benzene was high at 450°C for Ga-FER.



2.4.1.9 Kinetic study of Benzene Hydroxylation reaction :

For the Kinetic study, the reactions were carried out at different temperatures and different contact times (W.H.S.V.). Two type of graphs are plotted [Fig.2.17]; one to calculate rate of reaction at constant temperature by varying contact time (W.H.S.V.) and the other Arrhenius plot to calculate Energy of activation (E_a). The energy of activation

for the benzene hydroxylation on Ferrierite is calculated 5.5 K.cal / mole. This seems to be slightly less than that of other bimolecular reactions [51a]. But in this case the possibility of the reaction becoming pseudounimolecular which results into reduction in activation energy.



2.4.2 Benzene alkylation :

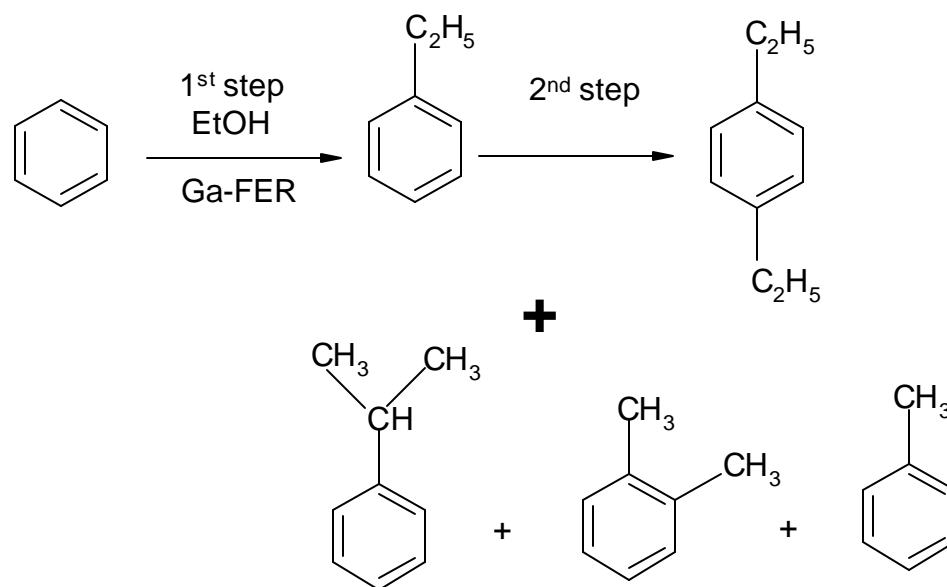
Ethyl benzene is an important petrochemical intermediate for the production of styrene. It is produced mainly by the alkylation of benzene with ethylene. Several catalysts ranging from aluminium trichloride to solid phosphoric acid are employed. Due to the corrosive and polluting nature of these substances, recent manufacturing processes

employ solid acid catalysts like zeolites. Initially protonated or rare earth exchanged faujasites were used in alkylation of benzene [52]. Other molecular sieves also have had beneficial effects in alkylation reactions as catalysts, for example, mordenite in the alkylation of benzene with C_2H_4 [53] and H-ZSM-5[54] with ethanol. However, the Mobil-Badger process employing a ZSM-5 zeolite catalyst has replaced many of the earlier processes. In some parts of the world ,due to non availability of ethylene from petrocrackers ,ethylene is generated from ethanol .The Albene technology demonstrates the use of ethyl alcohol as an alkylating agent in place of ethylene.

The ethylation of benzene with ethanol has been proved to be particularly useful for probing the catalytic properties of zeolites including hydrothermal stability and acidity [55,56]. The high electron density associated with benzene renders it susceptible to electrophilic attack by positive ion species or by positive end of a dipole or induced dipole [57]. It is now accepted generally that alkylation reactions proceed via a carbocation intermediate [58]. Both kinetic and mechanistic studies support a Rideal type mechanism [58; 59,60] in which the alkylating agent, which is strongly adsorbed at acid site, reacts with free or weakly adsorbed benzene molecule in rate determining step.

As Ga-FER catalyst is acidic in nature, the alkylation of benzene with ethanol was studied over this catalyst to investigate the product pattern due to the milder acidity inherent with Ga-FER. The activity is compared with its iron and aluminium analogs. The reaction was carried out on the H-form of the Ga-FER catalyst in down flow glass reactor system shown in Fig. 1.6 . The products were analyzed by using capillary column. The main products of the reaction are ethyl benzene and diethyl benzene. However the formation of toluene, xylene and cumene in small quantities was observed. The reaction

mechanism is shown below. During the reaction diethyl benzene is formed by the successive alkylation of the product ethylbenzene. Toluene, xylene and cumene are formed by the secondary reactions.



The catalytic activity of some of these modified FER zeolites and iron, gallium silicates are investigated in the benzene ethylation reaction. The Bronsted and Lewis acidity of these three ferrierite analoges are given in Table-2.7

Table 2.7 : Bronsted and Lewis acidity of the catalysts used for the reaction

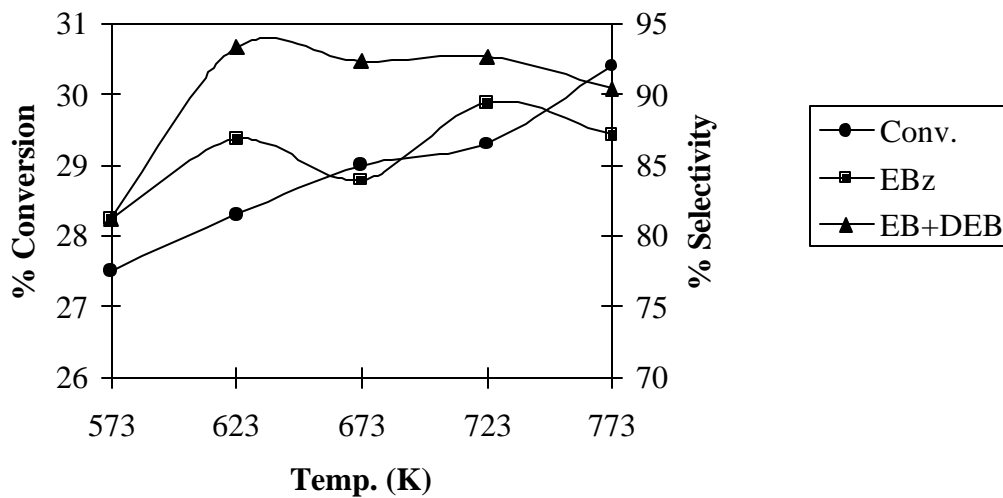
Catalyst	Si / M	L-Acidity	B-Acidity	Total Acidity
Ga-FER	9.85	0.28	0.39	0.57
Al-FER	17	0.24	0.55	0.79
Fe-FER	18.5	0.19	0.50	0.69

The reaction was studied as a function of temperature, space velocity, benzene to ethanol mole ratio.

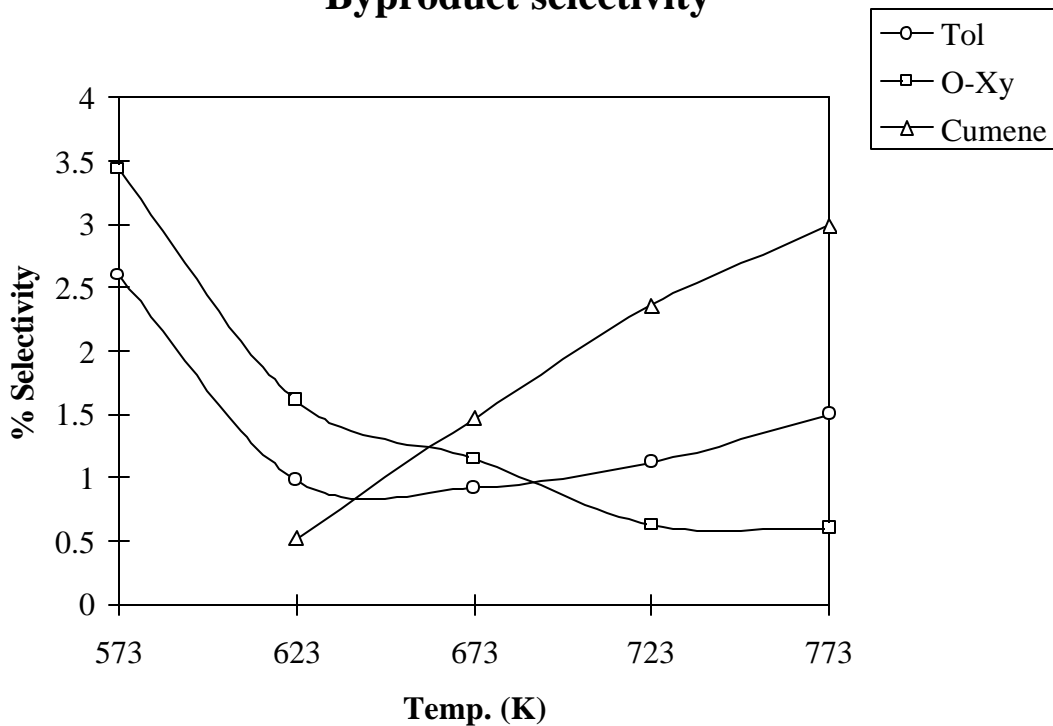
2.4.2.1 Effect of Temperature :

Figure 2.18 illustrates the effect of temperature on the conversion of benzene and selectivity of ethylbenzene in the reaction over H/Ga-FER catalyst (Sample 1). As expected, the conversion increased with the increase in reaction temperature. The formation of ethylbenzene was maximum at 723 K. Further increase of temperature lead to a fall in selectivity of both EB and DEB. At high temperatures reactions like dealkylation , disproportionation and isomerisations usually occur on acidic catalysts. Products like toluene, xylene, cumene and other methylethylbenzenes observed are by the later reactions of EB. In case of H-ZSM-5 [54] and H-Mordenite [61] these secondary reaction products are noticed even at a temperature of 673 K. As compared to zeolite beta and faujasites, the selectivity was found to be more for mono alkylated (EB) products in case of Ferrierite zeolite, which is attributed to its structure. Similar type of selectivity pattern was observed in the case of H-ZSM-5 [54].

Fig.2.18: Effect of Temperature
[6 ml/ h., 3 h., { Bz:EtOH = 4:1 }]

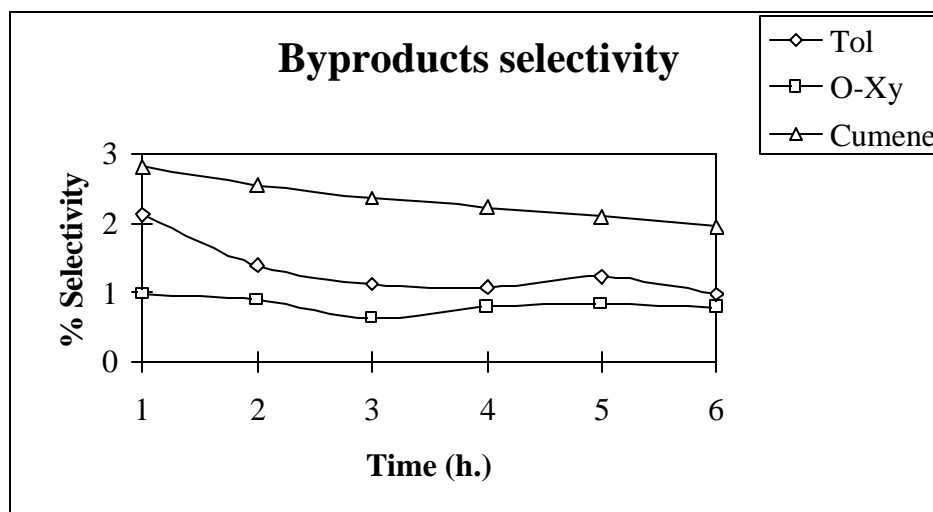
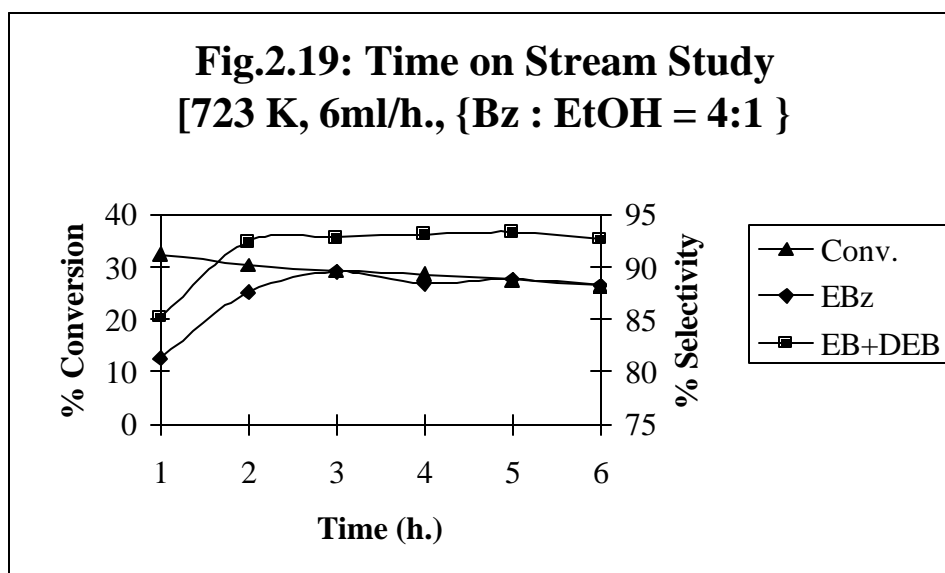


Byproduct selectivity



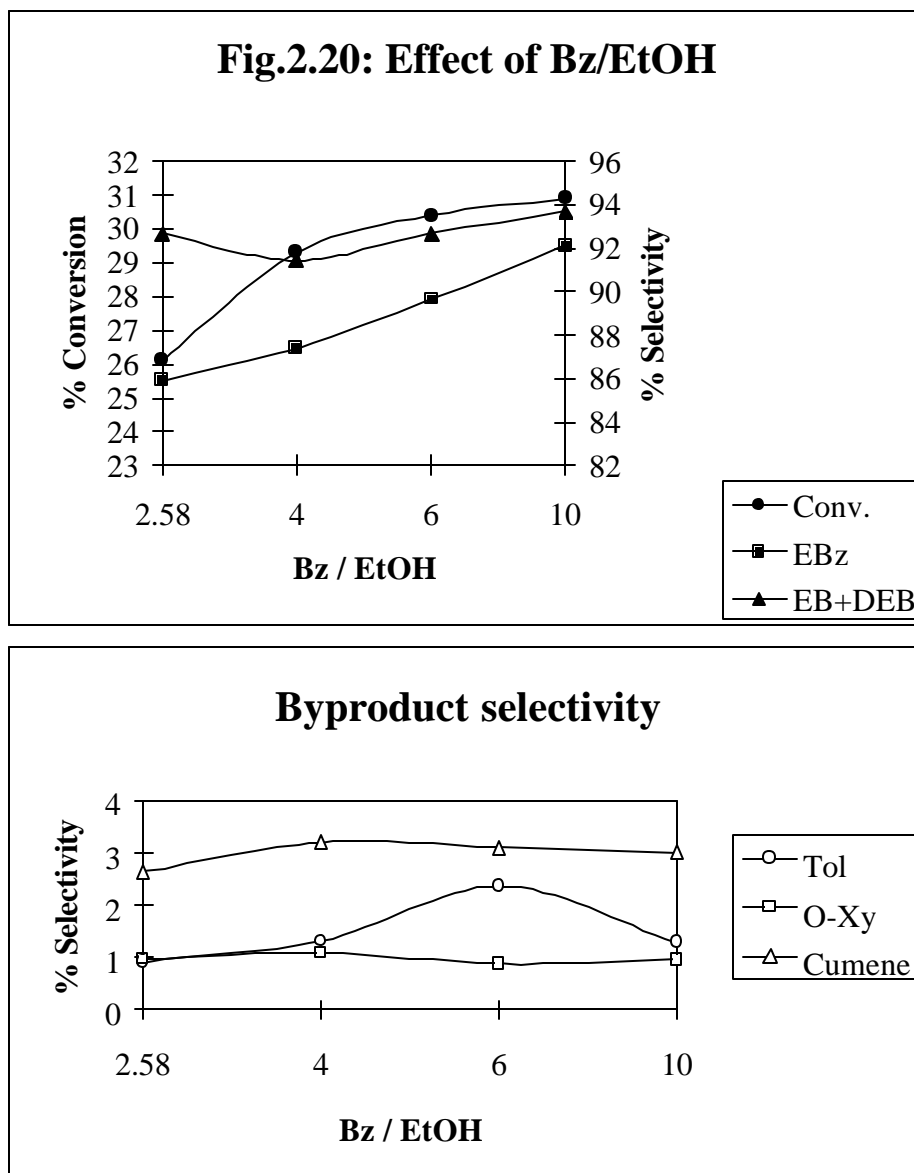
2.4.2.2 Time on stream study :

When the reaction was carried out at 723 K (450°C) to study the deactivation of the catalysts (Fig. 2.19), it was found that the conversion was decreasing with time. After 3rd hour the ethyl benzene formation remained constant and a gradual fall in the activity was observed. The bi-products also decreased with time. This is due to the passivation of surface sites which are to some extent responsible for the secondary reactions. These results suggest a gradual deactivation of Ferrierite catalyst.



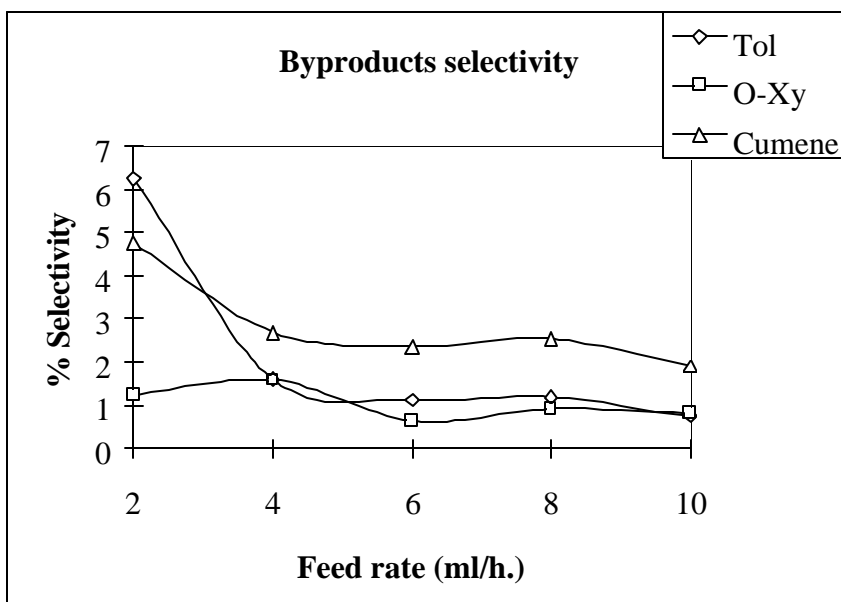
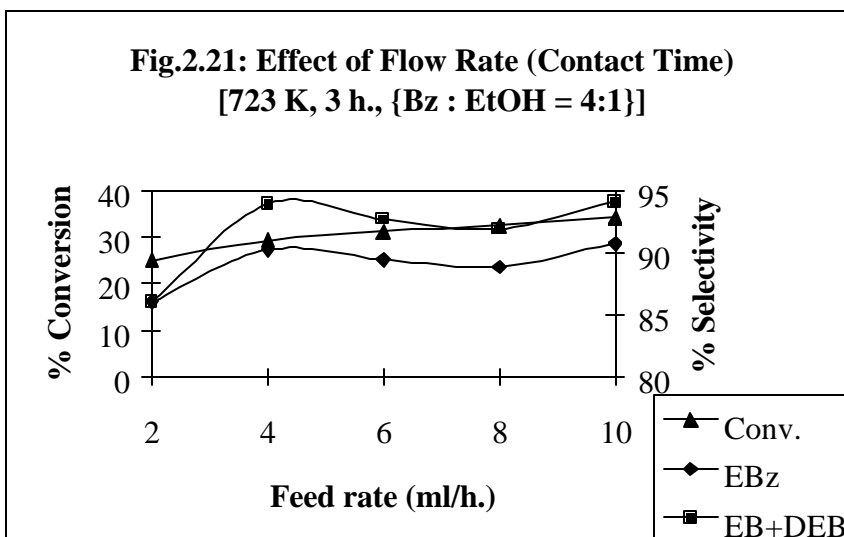
2.4.2.3 Influence of Benzene to Ethanol molar ratio:

The influence of mole ratio of Benzene to Ethanol (in the feed) on the conversion and product selectivity over H-Ga-FER is shown in Figure 2.20. The conversion was found to increase with the increase in mole ratio reaching a maxima at 10 : 1. Selectivity for EB also increased with increase in mole ratio (i.e. increase in benzene). The byproducts are remaining almost constant at all molar ratios. Reaction was carried out at 723 K and at Feed flow rate 4ml/h.. The products were collected at 3h.



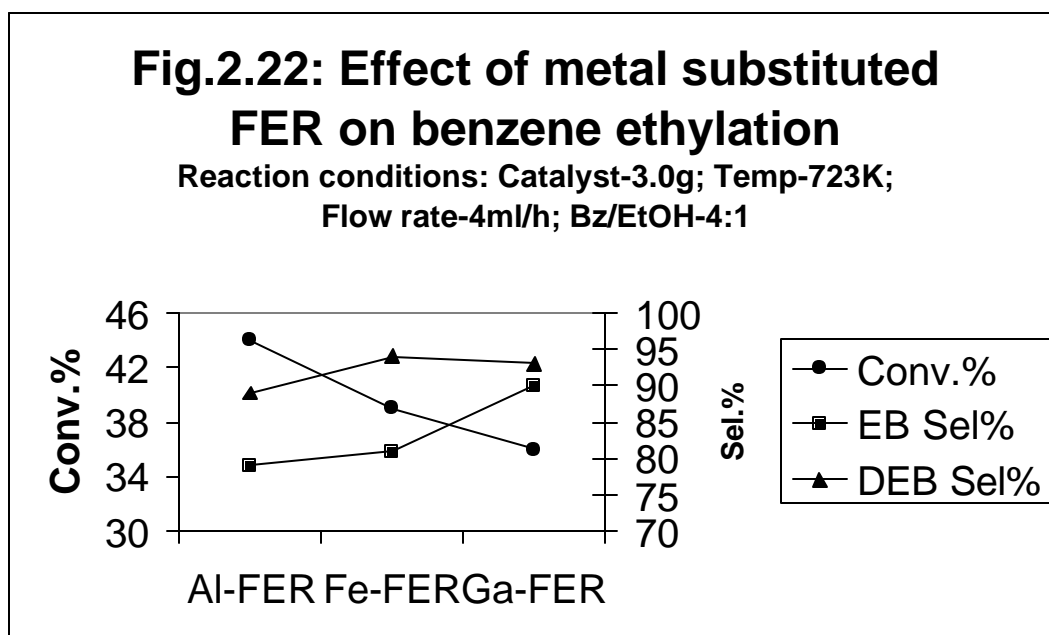
2.4.2.4 Effect of flow rate (contact time) :

Influence of contact time on EB conversion over HGa-FER is shown in Figure 2.21. Conversion with respect to benzene was found to decrease with increase in flow rate (decrease in contact time). Selectivity for Ethyl benzene increased with the increase in flow rate and is 90% at the maximum flow rate of 10 ml/h. At lower flow rate more toluene and cumene are observed. Selectivity to of DEB is almost constant over the range of flow rates studied.



2.4.2.5 Comparison of Al-FER, Fe-FER and Ga-FER:

In case of Fe-FER and Al-FER the benzene conversion showed similar behavior as that of H/Ga-FER [Fig.2.22]. The conversion with respect to benzene, increased with increase in temperature and at very high temperatures (viz. 773 K) toluene and other impurities were observed. However, in case of Fe-FER secondary alkylation viz. DEB formation was higher than Al-FER and Ga-FER. As compared to all the three catalysts toluene formation was maximum in case of H/Al-FER due to its higher acidity. All the three catalysts are selective to ethylbenzene at high mole ratios. Among the three catalysts, studied conversion decreased in the order Al-FER > Fe-FER > Ga-FER. This is due to the acidity, as total acidity is in the order; Al-FER > Fe-FER > Ga-FER. While the selectivity for ethylbenzene decreased in the order Ga-FER > Fe-FER > Al-FER. Substitution of tetrahedral aluminum in a zeolite framework by Fe^{3+} or Ga^{3+} is known to reduce the acidity [62]. Al-FER is more acidic hence it favors cracking while Ga-FER is moderately acidic it favors selective ethylbenzene formation.



CONCLUSIONS:

The Ga-FER catalysts were synthesized by using hydrothermal synthesis route using pyrrolidine as a template. Ga^{+3} ion is introduced in place of Al^{+3} ion in the Ferrierite framework. The incorporation of bulkier Ga^{+3} ion is revealed by the unit cell volume expansion in the Ga-FER samples. The tetrahedral position of the Ga^{+3} ion in the framework is confirmed by ^{71}Ga MSA-NMR spectroscopy. The acidity of the Ga-FER catalyst was found by CD_3CN adsorption followed by FTIR spectroscopy on the Ga-FER sample.

The Ga-FER catalyst is mildly acidic than Al-FER. The ethylation of benzene was studied on Al-FER, Fe-FER and Ga-FER samples. Ga-FER catalyst is also active in the hydroxylation of benzene. The presence of special type of α -surface species generated due to the tetrahedral Ga^{+3} ion in the framework is responsible for the catalysis. This reaction suggest an alternative, simpler, eco-friendly route for phenol.

References :

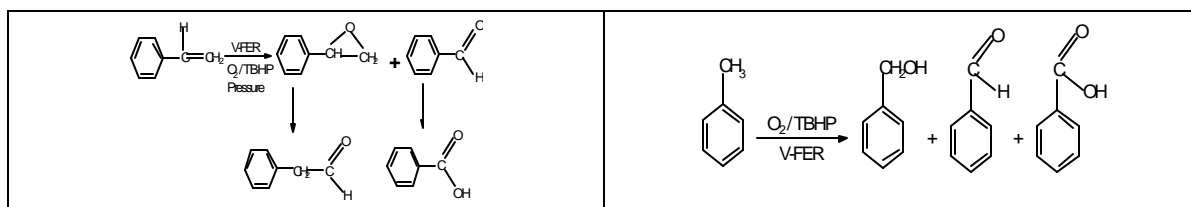
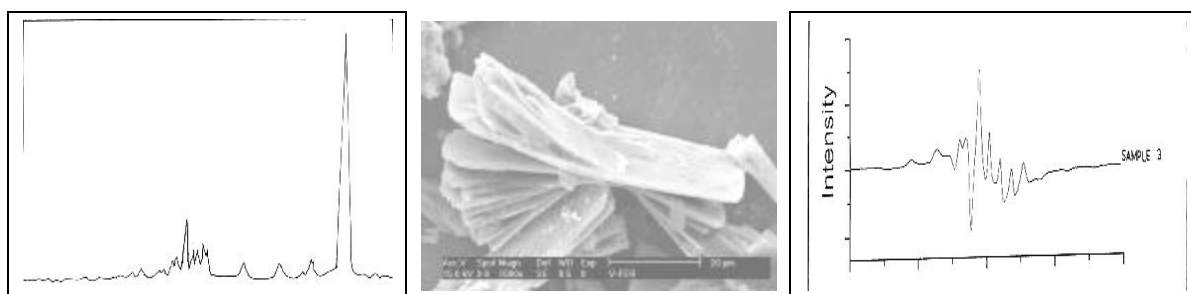
1. J.R.Goldsmith ; Miner. Mag.; 29, (1952), 952.
2. R.M.Barrer, J.W.Brynmman, F.W.Bultitude, W.M.Meier ; J.Chem. Soc.; (1959), 195.
3. J.M.Newsam, D.E.W.Vaughan; "New Developments in Zeolite Science and Technology"; Y.Mizukami et.al. Eds.; Elsevier, Amsterdam, (1986), 457.
4. Selbin; J.Inorg. Nucl. Chem.; 20, (1961), 222.
5. Kuhl; J.Inorg. Nucl. Chem.; 33, (1971), 3261.
6. Hayashi; Bull.Chem. Soc. Jpn.; 59, (1985), 52.
7. B. Sulikowersler and J. Klinnowski, J.C.S.Chem.Comm.; (1989), 1289.
8. N.E.Jacob, P.N.Joshi, R.A.Shaikh and V.P.Shiralkar; Zeolites; 13, (1993), 430.
9. Siddhesh Shevade, R.K.Ahedi, A.N.Kotasthane and B.S.Rao; "Recent Trend in Catalysis"; Eds. Murugesan et.al.; Narosa Publishig House, India; (1999), 383.
10. R.K.Iler; "The chemister of Silica"; Wiley, New York; (1979).
11. B.N.Ivanov-Emin, L.A.Nisel'son, L.E.Larionova; Russian J.Inorg.Chem.; 7, (1962), 266.
12. G.Johansson; Acta. Chim. Scand.; 14[3], (1960), 771.
13. A.Thangaraj, S.Sivasankar and P.Ratnasamy ; J.Catal., 1991, **131**, 294.
14. A.J.Avrani ; J.Chem.Phys. ; 9, 1941, 177
15. C.R.Erofeev ; Acad. Sci. U.S.S.R.; 52, 1945, 511.
16. A.N.Kotasthane, V.P.Shiralkar, S.G.Hegde and S.B.Kulkarni; Zeolites ; 6, 1986, 233.
17. S.Kannan, T.Sen, S.Shivashankar ; J.Catal.; 170(2), 1997, 304.
18. F.Cavani, F.Trifiro, K.Habersbergen, Z.Tvaruzkova ; Zeolites, 8 , 1988 , 12.
19. A.Miyamoto, T.Iwamoto, H.Matsuka, T. Inui ; Stud. Surf. Sci. Catal. ; 49B, 1989, 1233.
20. R.Szostak, "Handbook of Molecular Sieves"; Van Nastrand, New York, 1884, 201.
21. A.J.Chandawadkar, R.N.Bhal and P.Ratnasamy; Zeolites; 11, 1991, 42.
22. R.Zostak, T.L.Thomas ; J.Catal.; 101, (1986), 549.
23. B.Wichterlova, Z.Tvaruzkova, Z.Sobalik, P.Sary; Microporous and Mesoporous Mater.; 24, 1998, 223.
- 23a. A.G.Pelmenschikov, Van Santen R.A and Meijer E.; J.P.C.; **97** (1993) 11071.
24. Timken H.K.C. and Oldfield . E., J. Am. Chem. Soc. 109 (1987) 7669.
25. Beyense C.R, Van Hooff J.H.C, de Hann J.W., Vande Ven, C.J.Mand Kentgens A.P.M., Catal lett. 17 (1993) 349.
26. Bayence C.R.,Kentgens A.P.M., de Hann J.W., Vande Ven, and Van Hoof J.H.C, J.Phys. Chem. 96 (1992) 775.
27. Sulikowaski B, Olejniczak Z. Cortes Corbenan V., J.Phys. Chem, 100 (1996) 10223.
28. Kosslick H., Tuan V.A., Parlitz B., Fricke R., Pewker and Storek W. J. Chem Soc., Faraday Trans., 89 (1993) 1131.
- 28a. Cotton F.A. and Wilkinson G.; in "Advanced inorganic Chemistry"; Wiely Eastern Ltd.; Third Ed.; (1972) 279.
29. K.Weissermehl, H.J. Arpe, Industrial Organische Chemie, VCH, Weinheim, 1988.

30. W.F.Holderich in : L. Guzzi et. Al.(Ed) " New Frontiers in Catalysis " Elsevier, Amsterdam, 1993, p.127.
31. M.Iwamoto, J.Hirata, K.Matsukami, S.Kegawa, J.Phys. Chem., 87 (1993) 903.
32. Y.Ono, K.Tohmori, S.Suzuki, K.Nakashiro, E.Suzuki, in : M.Guisnet et. al. (Ed) Heterogeneous Catalysis and Fine Chemicals, Elsevier, Amsterdam, 1988, p. 75
33. M.Gubelmann, P.Tirel, EP 0341165,Rhone-Poulenc-Chemie, 1988.
34. M.Gubelmann, P.Tirel, US 5001280,Rhone-Poulenc-Chemie, 1988.
35. R.Burch, C.Howitt, Appl. Catal. A. Gen. 86 (1992) 139.
36. R.Burch, C.Howitt, Appl. Catal. A. Gen. 103 (1993) 135.
37. G.I.Penov, V.I.Sobolev, A.S.Kharitonov, J.Mol. Catal. 61 (1990) 85
38. V.I.Sobolev, G.I.Penov, A.S.Kharitonov, V.N.Romannikov, A.M.Volodin, Kinet. Catal. 34 (1993) 797.
39. V.I.Sobolev, O.N.Kovalenko, A.S.Kharitonov, G.I.Penov, Mendeleev Commun. 1 (1991) 29.
40. G.I.Penov, G.A.Shevela, A.S.Kharitonov, V.N.Romannikov, L.A.Vostrikova, Appl. Catal. A.Gen 82 (1992) 31.
41. A.S.Kharitonov, G.A.Sheveleva, G.I.Penov, V.I.Sobolev, Y.A.Paukshtis, V.N.Romannikov, Appl. Catal A Gen. 98 (1993) 33.
42. A.S.Kharitonov, G.I.Penov, K.G Ione, V.N.Romannikov, G.A.Sheveleva, L.A.Vostrikova V.I.Sobolev, US 5,110,995., (1992)
43. G.I.Penov, A.S. Kharitonov, V.I.Sobolev, Appl. Catal. A. Gen. 98 (1993) 1.
44. V.I.Sobolev, A.S.Kharitonov, Y.A. Paukshtis, G.I.Penov, J.Mol. Catal. 84 (1993) 117.
45. G.I.Penov, V.I.Sobolev, A.S.Kharitonov, E.A. Paukshtis, Meeting Phoenix 1994, poster 20.
46. V.I.Sobolev, O.N.Kovalenko, A.S.Kharitonov, Y.D. Pankratiev, G.I.Penov,. Mendeleev Commun. 1 (1991) 29.
47. V.I.Sobolev, G.I.Penov, A.S.Kharitonov, V.N.Romannikov, A.M.Volodin, K.G. Ione, J.Catal 139 (1993) 435.
48. A.S.Kharitonov, T.N.Aleksandrova, G.I.Penov ,V.I.Sobolev, G.A.Sheveleva, E.A.Paukstis, Kinet.Katal 35 (2) (1994) 296.
49. A.M.Volodin, V.A.Bolshov, G.I.Penov, J.Phys. Chem.98 (1994) 7548.
50. L.V.Piryutko, O.O.Parengo, B.V.Lunina, A.S.Kharitonov, L.G.Okkel, G.I.Penov, React. Kinet. Catal Lett. 52(1994) 275.
51. A.S.Kharitonov, V.B.BolFenelonov, T.P.Voskresensakaya, N.A.Rudina, V.V.Molchanov, L.M.Plyasova, G.I.Penov, Zeolites 15 (1995) 253
- 51a. M.G.Palekar and R.A.Rajadhyaksha; Catal. Rev.-Sci.Eng.; **28(4)** (1986) 371.
52. Venuto, P.B., Hamilton, L.A. and Landis, P.S.; (1966) *J.Catal.* **5** 484.
53. Morita, Y., Matsumato, H. , Kimura, T., Kato, F. , Takayasu, M.; (1973) *Bill. Jpn. Pet. Inst.* **15** (1) 87.
54. Chandawar, K.H., Kulkarni, S.B. and Ratnasamy, P.; (1982) *Applied Catal.* **4** 287.
55. Nunan, J., 1983, PhD thesis, National University of Ireland.
56. O' Donoghue, E., (1983) PhD thesis, National University of Ireland.
57. Venuto, P.B.; (1971) *Adv. Chem. Ser.* **102** 260.
58. Jacobs, P.A.; (1977) "*Carboniogenic activity of Zeolites*" Elsevier, Amesterdam,.

59. Coughan, B., Carroll, W.M and Nunan, J. (1983) ; *J. Chem. Soc. Faraday Trans. I* **79** 281.
60. Mukheryer, P.N. and Basu, P.K.; (1982) *Chem.Age. India* 33,202.
61. Becker K.A., Karge H.G. and Stroubel W.D.; *J.Catal.*; **28** (1973) 403.
62. Chu, C.T.W. and Chang, C.D. (1985); *J. Phys. Chem.* **89** 1569.

CHAPTER III

V-FER



3.1 Introduction :

Zeolites are crystalline, porous materials containing aluminum and silicon metals. They can impart acidity along with the molecular sieving nature. Zeolites can act as bifunctional catalysts in different types of reactions by suitable modifications.

One of them is the incorporation of metal ions. Vanadium is a transition metal having various oxidation states, -I in $\{V(CO)_6\}^-$, 0 in $\{V(CO)_6\}$, I in $\{V(bipy)_3\}^+$, II in $\{V(CN)_6\}^{-4}$, III in $\{VCl_4\}^-$, IV in $\{VCl_5\}^-$ and VO_2 , V in $VOCl_3$ and VF_5 . Some of the oxidation states are easily interchangeable with temperature, pH, air oxidation etc.. Due to that vanadium containing compounds and complexes are known for their redox properties [1] which make them as catalysts.

Modified zeolites, particularly those containing Vanadium are well known for their excellent catalytic properties in selective synthesis of various fine chemicals[2,3]. Marosi et.al. [4] have patented the first report of zeolite containing Vanadium. Xu et.al. [5] have reported the presence of three different oxidation states (III, IV, V) of vanadium in zeolites. Several reports have dealt with the synthesis, characterization and catalytic properties of vanadium containing zeolites for example ZSM-5[6,] ZSM-11[7,] ZSM-48[8,] ZSM-12[9,] NCL-1[10,] Beta[11]and MCM-41[12.]. The Vanadium analog of Ferrierite Zeolite (V-FER) was reported for the first time in our recent publication [13]. The synthesis, characterization and catalytic properties of the V-FER are included in this chapter. We also tried to investigate the various vanadium species present in the zeolite and their activity in different redox reactions.

3.2 Synthesis :

Vanadium is normally present in tetravalent state. While isomorphically substituting in Ferrierite framework it was found difficult to substitute V^{+4} in place of Al^{3+} in aqueous medium. For the synthesis of V-FER the non-aqueous organothermal route of

Si-FER[14] was followed. Teflon autoclaves are employed due to HF. The following chemicals are used .

Table 3.1 : Chemical used for the V-FER synthesis

Chemical	Used As/For	Source
SiO ₂ (Fumed Silica)	Silicon Source	Fluka, USA
VOSO ₄ , 5H ₂ O	Vanadium Source	Loba, Chemie
Propyl Amine	Structural Directing Template	E.Merck
Pyridine	Organic medium	SQ, Qualigens
HF in Pyridine	Fluride medium for better dissolution of monomeric species	70% Aldrich
Distilled water (H ₂ O)	Dissolution of Vanadium salt	

The organothermal synthesis of vanadium ferrierite was carried out using gels of the following composition:

SiO₂: (0.1-0.001)VO₂: 5.45 Propyl amine: 10.78 pyridine : 2.67 H₂O : 1.4HF

75.5g (0.955moles) of pyridine and 31.5g (0.533 moles) of propylamine were mixed under stirring. A clear blue solution of vanadyl sulfate (0.506g, 0.002 moles) in 4.8g (0.267moles) of deionised water was slowly added to the above organic solution followed by a careful addition of 3.6g (0.018moles) of HF in Pyridine. Finally 6.0g (0.1mole) of Cab-O-Sil was slowly dissolved in the above gel under vigorous stirring. The resulting solution had a pH of 11.0 ± 0.2. This liquid was then transferred to a PTFE lined autoclave (Fig. 1.4) for crystallizing at 170⁰ C for 5 to 7 days under static conditions. The crystalline V-FER was filtered, washed with water followed by acetone and dried at 100°C. The X-ray (Rigaku D max II VC) powder diffraction pattern confirmed the phase purity of the V-FER. Then this was calcined at 550°C for 12 h. to decompose the organic compounds. The product yield was 80% by wt. (5.0 g.).This sample was treated with 1 M ammonium acetate solution at room

temperature for 18 h. to remove any possible non-framework vanadium species. Vanadium silicates with four different Si:V ratios were prepared and the chemical properties are shown in Table 3.2.

Table 3.2 : Physico chemical properties of V-FER samples

Sample	Si/V		V (wt %) by XRF	Color of the sample
	Input	Output		
Sample 1	10	7.0	4.99	Dark Yellow
Sample 2	20	18	2.18	Dark Yellow
Sample 3	50	120	0.70	Pale Yellow
Sample 4	100	180	0.47	Pale Yellow

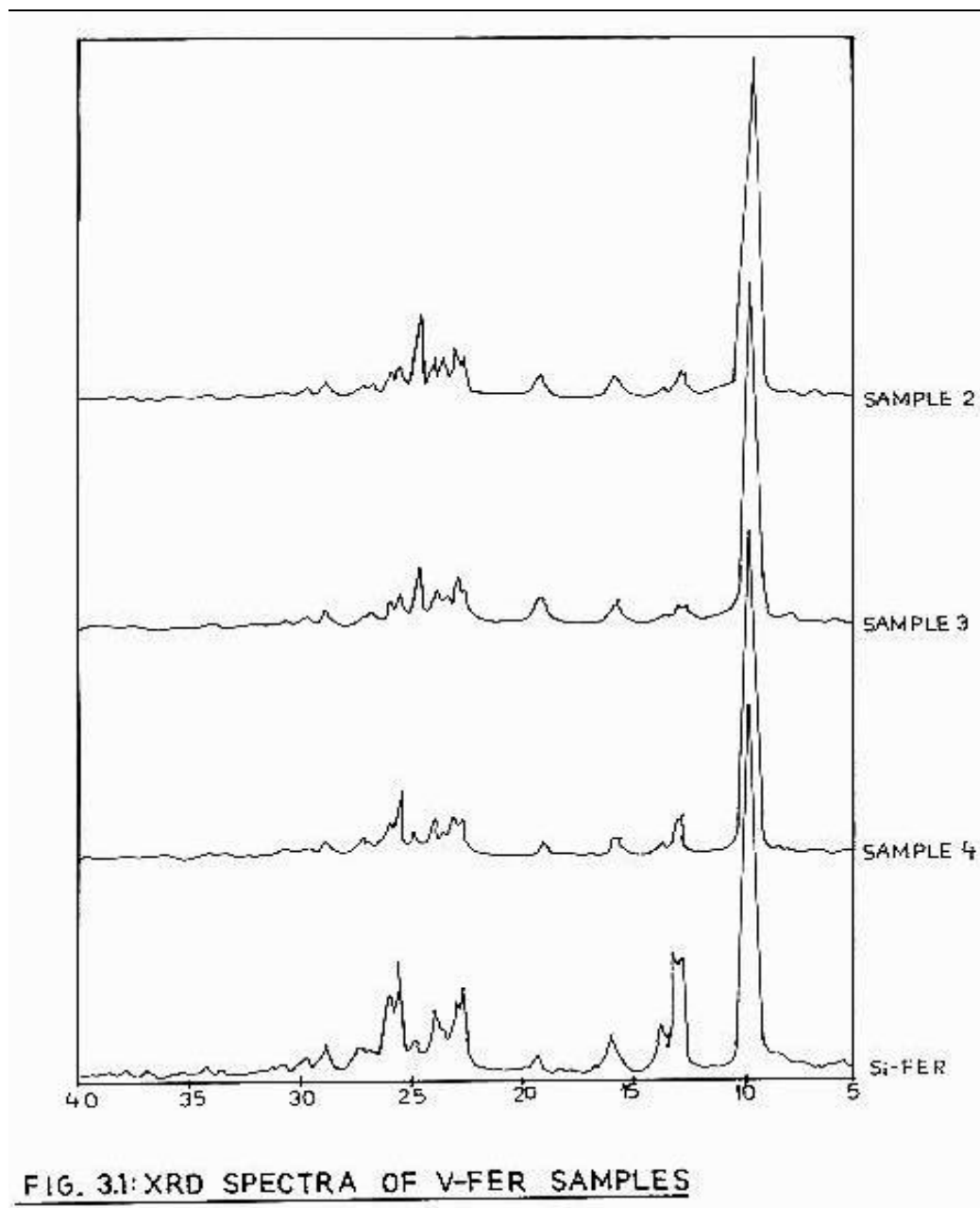
The color of the samples are actually due to the hydration of the V-FER samples. The intensity of the color depends upon the vanadium concentration in the sample.

3.3 Characterization :

The V-FER samples were characterized by using various spectroscopic and non-spectroscopic techniques. The main aim of the characterization was to find out the exact location of Vanadium Species in the V-FER zeolite.

3.3.1 X-Ray Diffraction :

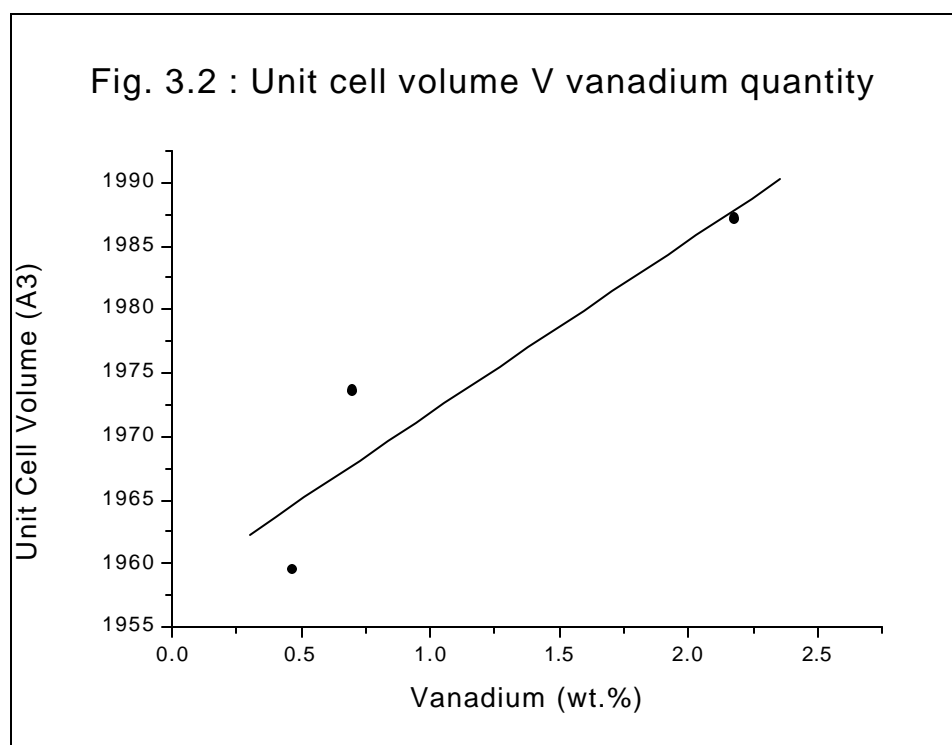
XRD was carried out on Rigaku D max II VC spectrometer to determine phase purity and percent crystallinity of the V-FER zeolites samples. Detailed analysis of the XRD patterns gave information about the Unit cell parameters of the Zeolite and possibility of Isomorphous substitution as reflected by the unit cell expansion. Three XRD patterns of different vanadium containing samples along with the Si-FER spectrum were shown in Fig3.1. The XRD patterns of the V-FER samples were similar to those of siliceous ferrierite. With the increase of the amount of vanadium, slight changes in the intensities of different peaks were seen. The positions of the peaks were not changed after vanadium incorporation , which confirms the phase purity.



As expected, the incorporation of V^{+4} ions into the framework caused an expansion in the unit cell volume [3]. In case of siliceous FER the unit cell volume was 1947.21 \AA^3 . After the incorporation, it was increased to 1959.54 \AA^3 , 1973.59 \AA^3 and 1987.12 \AA^3 for the three V-FER samples (Table 3.3). The unit cell volume increased with the increase in vanadium content (Fig. 3.2).

Table 3.3 : Unit cell parameters of various V-FER and Si-FER samples.

Sample (V-FER)	V wt% (XRF)	a_0 Å	b_0 Å	c_0 Å	unit cell volume Å ³
Sample 2	2.18	18.89	14.12	7.45	1987.12
Sample 3	0.70	18.83	14.10	7.44	1973.59
Sample 4	0.47	18.75	14.08	7.43	1959.54
Si-FER	--	18.69	14.06	7.41	1947.21



The synthesis kinetics of the V-FER zeolite is shown in the Fig. 3.3. During the synthesis, four different sets of experiments were carried out using the synthesis procedure already described. Each synthesis experiment was stopped after 24 hours of the previous experiment. Four samples with different crystallinity were obtained. The multiple plot of XRD spectra are plotted in Fig 3.3. The graph of time verses highest peak intensity is also drawn. An exact "Sigmoid" shape curve is observed which is characteristic of zeolite synthesis [15,16,17].

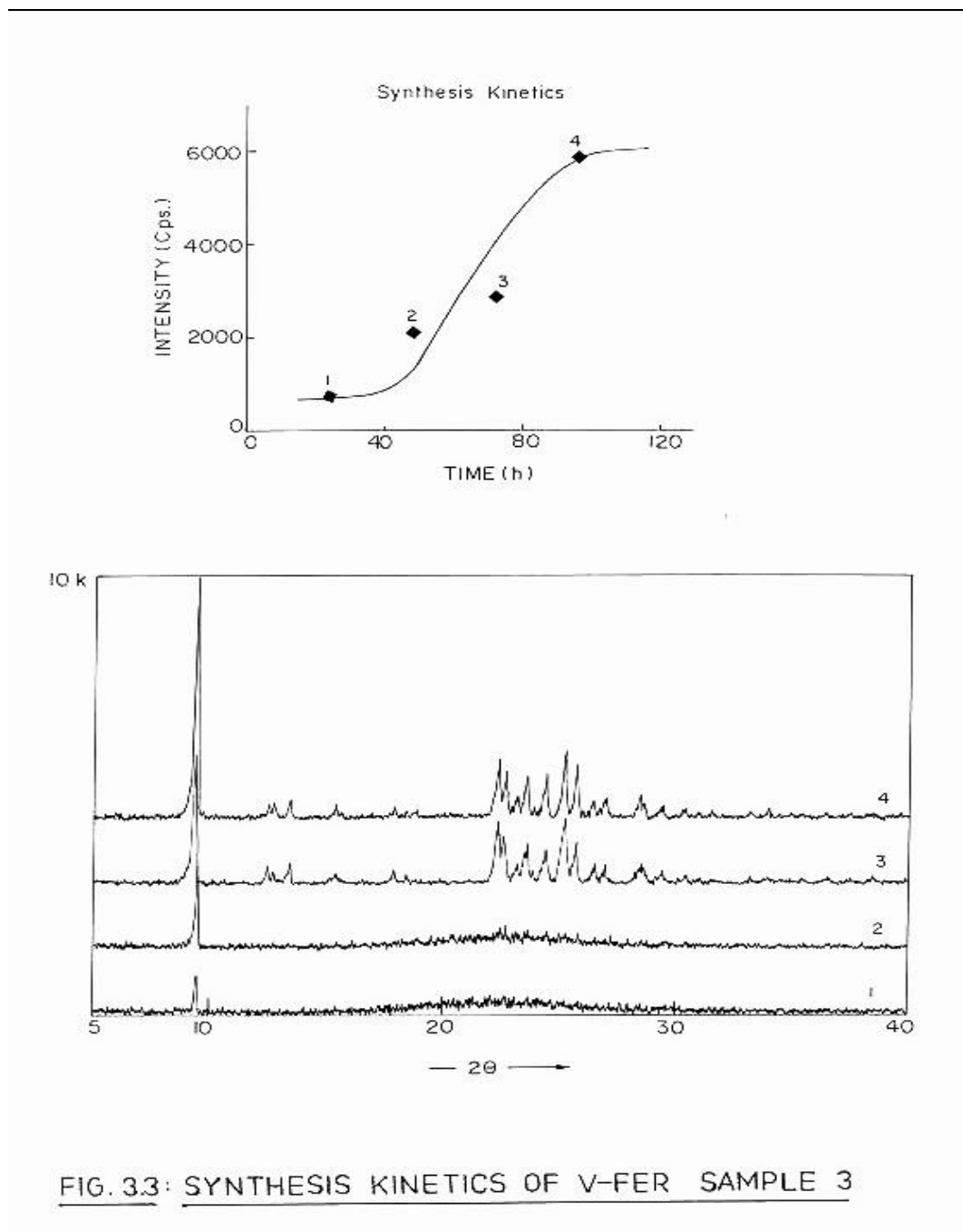


FIG. 3.3: SYNTHESIS KINETICS OF V-FER SAMPLE 3

3.3.2 Surface area measurement :

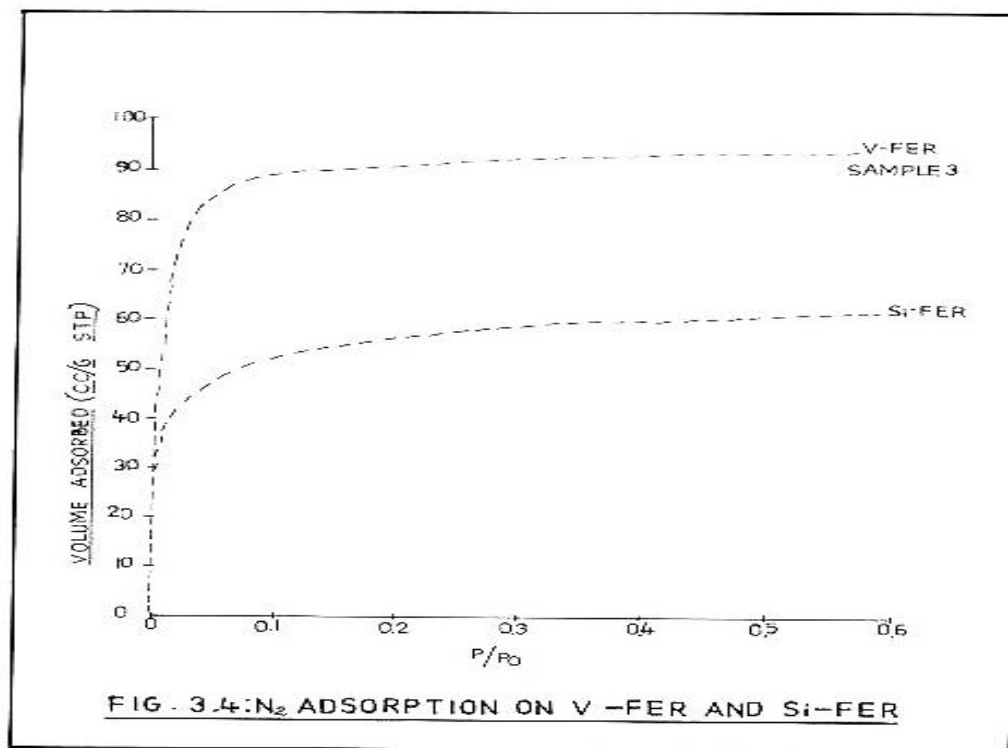
An Omnisorp 100 CX (COULTIER, USA) analyser was used for the measurement of low pressure nitrogen adsorption to determine the surface area. The sample was activated at 673 K for 2 h. in high vacuum (10^{-6} Torr). After the treatment, the

anhydrous weight of the sample was taken at room temperature. The sample was then cooled to 78 K using liquid nitrogen and then was allowed to adsorb very pure Nitrogen gas. From the amount of absorbed nitrogen, the BET surface area was calculated. Fig 3.4 shows the comparative graph of nitrogen adsorbed on Si-FER and its vanadium analog V-FER. Surface area and micro-pore volume were calculated by using BET equation in the above plotted curve and the values are given in Table 3.4 .

Table 3.4 : Surface area and Micro-pore volume of V-FER sample.

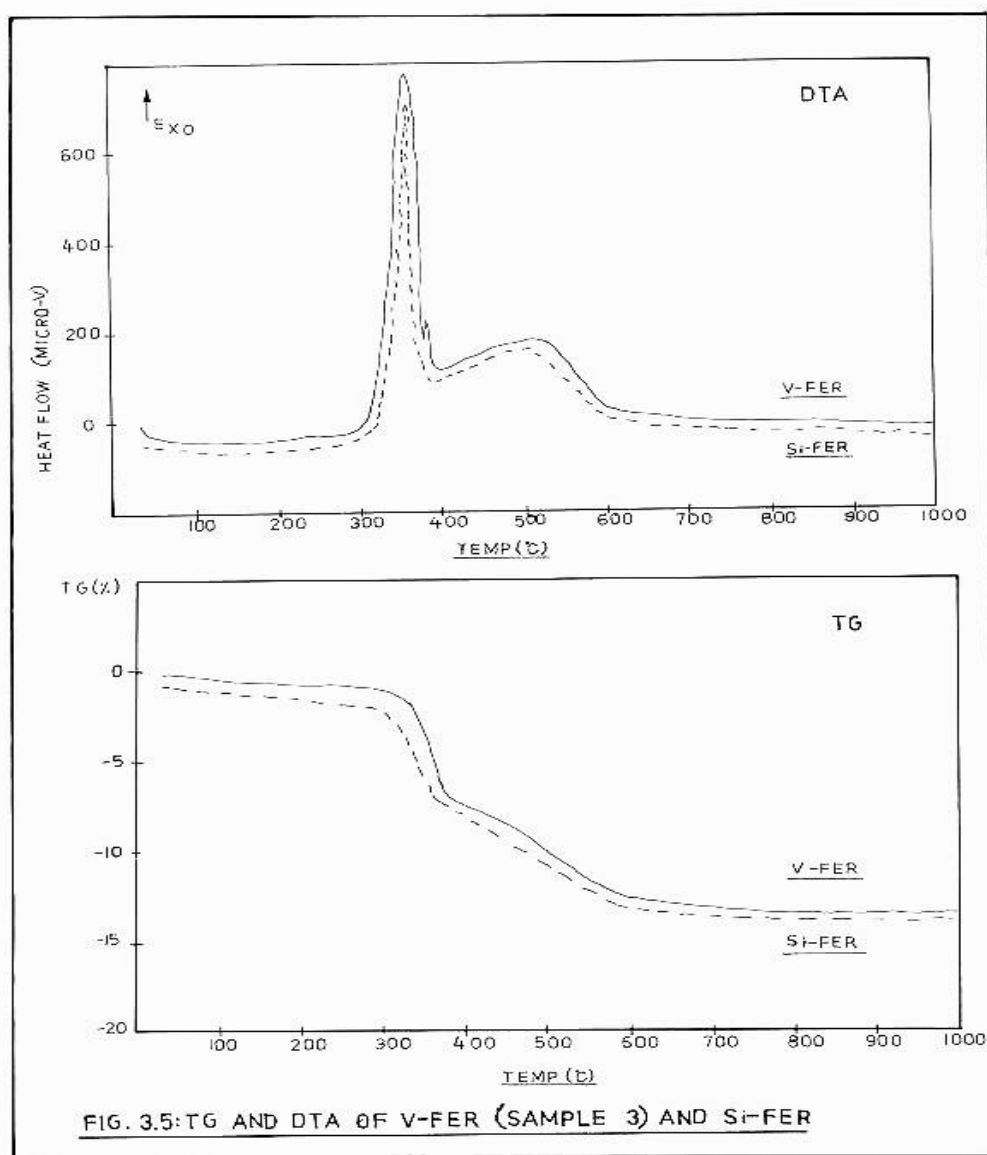
Sample	Surface Area m ² /g.	Micro-pore Volume ml/g.
V-FER (Sample 3)	366.4	0.15
Si-FER	211.0	0.08

It is observed that due to incorporation of vanadium in the ferrierite framework, the surface area and micro-pore volume increased significantly. The incorporation of vanadium is complimentary to the XRD results (unit cell expansion).



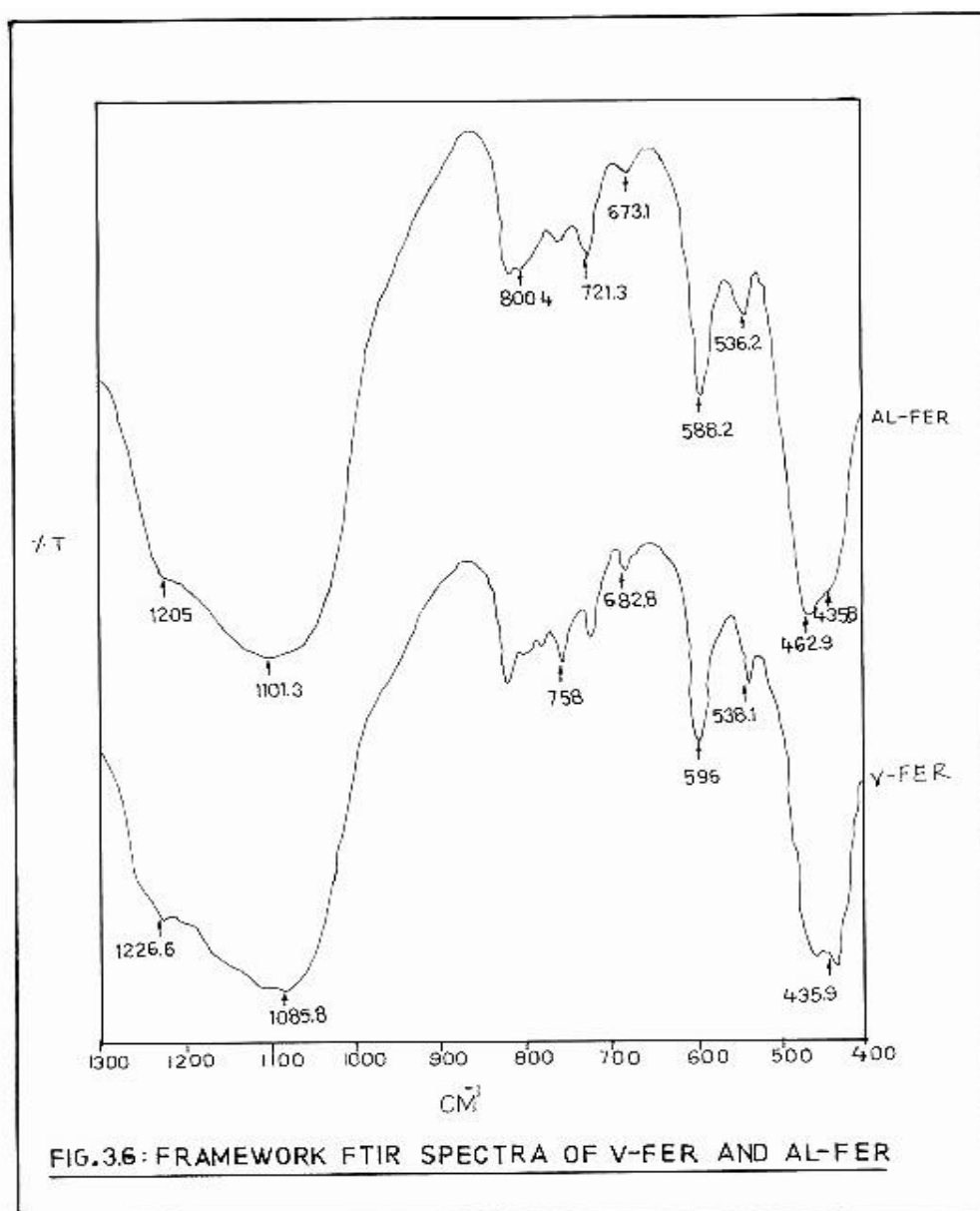
3.3.3 Thermal analysis and structural stability :

Fig. 3.5 show the TG/DTA data on the as synthesized samples of V-FER and Si-FER respectively. TG shows ~13 % weight loss in V-FER sample during the calcination. DTA revealed two exotherms at $T_{max} = \sim 375$ and 525 °C (648 and 798 K resp.), indicating the oxidative decomposition of the organic moieties. The thermoanalytical studies on V-FER samples revealed that the decomposition of occluded organic completes at 600°C (873 K) and maintains structural integrity till 1000°C (1273 K).



3.3.4 Framework IR spectra :

FTIR spectra of Ferrierite samples were recorded on wafers of thickness ca. 10 mg/cm². The Nicolet Magne-550 FTIR spectrometer was used with a DTGS KBr detector and a vacuum cell with CaF₂ windows attached to the vacuum system and a dosing arrangement for acetonitrile. The spectra were recorded in the framework region 1300-400 cm⁻¹ as Nujol mull. Figure 3.6 shows the framework region infrared spectra of V-FER (sample 3) and Al-FER samples.



V-FER spectrum shows two characteristic absorption bands around 1226 cm^{-1} and 682 cm^{-1} . These two bands can be attributed to the vibrations within the ferrierite framework [18]. The absorbance around 596 cm^{-1} confirms the presence of distorted five membered double ring (DDR-5) present in the high silica ferrierite framework. The IR spectra shows strongest band at $\sim 1085 \text{ cm}^{-1}$ due to asymmetric stretching of internal Si-O-V vibrations. The decrease in this band position from 1101 cm^{-1} was due to the introduction of heavier atom in the Ferrierite framework [19]. Table 3.5 shows the framework region vibration frequencies for V-FER system.

Table 3.5 : Framework vibration frequencies for vanadium ferrierite (V-FER) zeolite.

Wave number (cm^{-1})	Assignment
435.9	Si — O bending.
538.1, 596	Distorted double five membered rings (5-DDR).
682.8	Internal tetrahedral symmetrical stretch.
758	External link symmetric stretch.
1085.8	Internal tetrahedral asymmetric stretch.
1226.6	Internal asymmetric stretching.

3.3.5 Acidity measurements using IR spectroscopy :

Pyridine is largely used as a probe molecule to study the acid sites but due to its size it can't fully penetrate the channels of 8 and 10 membered rings of Ferrierite [20]. Nitrile has a promising functional group and is of low basicity. It is possible to determine the acidity from the wave number shift of this molecule. Acid site distribution of V-FER sample was studied by using d_3 -acetonitrile as a probe molecule. The concentration of Bronsted and Lewis acid sites was calculated by using the reported extinction coefficients [20]. The sample was activated at 670 K and adsorption of d_3 acetonitrile (Aldrich) (13 mbar) on evacuated zeolite was carried out at 298 K for 30 min., followed by evacuation for 10 min. Spectra was recorded at

ambient temperature with 2 cm^{-1} resolution by collecting 200 scans for single spectrum. IR spectra was normalized on a sample thickness of 10 mg/cm^2 . IR bands of adsorbed d_3 -acetonitrile was deconvoluted using identification of a band position in a second derivative mode of the spectrum and the least square minimization routine approximating the band by a gaussian profile. Extinction coefficients of Bronsted and Lewis acid sites of Al-FER were used for calculating acid sites. Fig. 3.7 shows the FTIR spectra in the hydroxyl stretching region ($4000\text{-}2800\text{ cm}^{-1}$). The intensity of the 2 bands at 3740 and 3603 cm^{-1} are very low in V-FER as compared with Al-FER catalyst. The 3740 cm^{-1} band can be ascribed to isolated silanol groups present in the channels and at the external surface. The second band at 3603 cm^{-1} can be assigned to Bronsted sites associated with framework. With Si-FER sample it is not possible to observe any of the above mentioned bands.

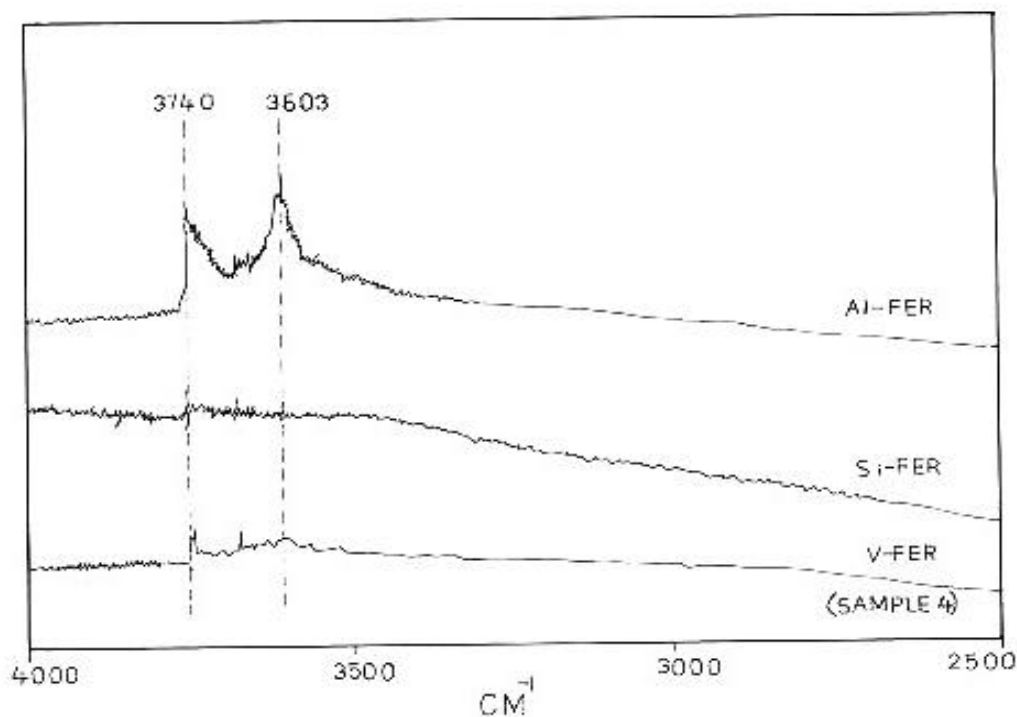


FIG. 3.7: HYDROXYL REGION (OH) OF V-FER, Si-FER AND Al-FER SAMPLES

Fig.3.8 shows the spectra of d_3 -acetonitrile adsorbed on the V-FER sample. The bands at 2322 cm^{-1} and 2296 cm^{-1} correspond to Lewis sites and Bronsted sites resp. (Table 3.6). In V-FER the amount of Lewis and Bronsted acid sites are comparable to Al-FER in spite of low concentration of the Vanadium. The concentration of OH^- is very less. This may be explained by reversible disruption of the V-OH-Si bridge after evacuation and it's reconstruction in the acetonitrile. Si-FER didn't show any d_3 -Acetonitrile adsorption.

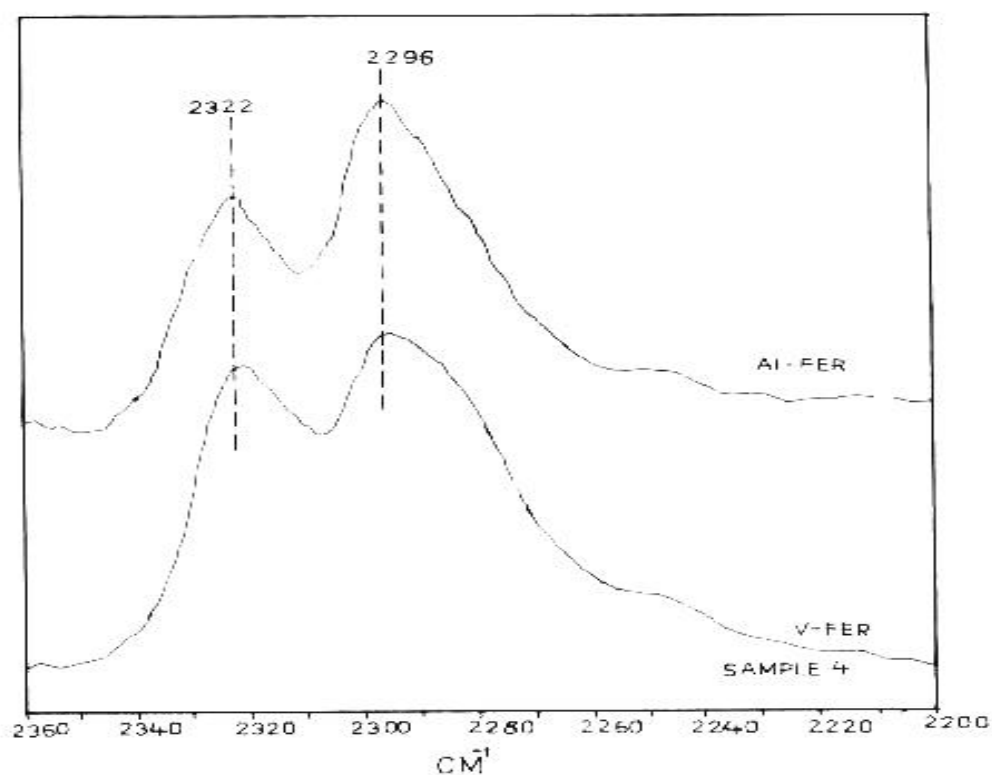


FIG.3.8: IR SPECTRA OF D-ACETONITRILE ADSORBED ON V-FER AND Al-FER SAMPLES

Table 3.6 : d_3 -Acetonitrile Adsorption (cm^{-1})

Sample	Position	Area	Position	Area	Conc.	
	(cm^{-1})		(cm^{-1})		(mmol/g)	
	L-site	L-site	B-site	B-site	L-site	B-site
Al-FER	2323	8.5	2296	11.4	0.24	0.55
V-FER	2322	7.7	2296	9.3	0.21	0.45

3.3.6 Scanning Electron Micrographs :

Fig. 3.9 displays the scanning electron micrographs of V-FER sample 3. The crystals are large in size (~ 30 to $40 \mu\text{m}$), exhibiting rectangular plate type morphology. The large size is due to the synthesis in fluoride medium . The isolated particles are of the size $10 \mu\text{m} \times 50 \mu\text{m}$. These particles form a bunch of rectangular plates.

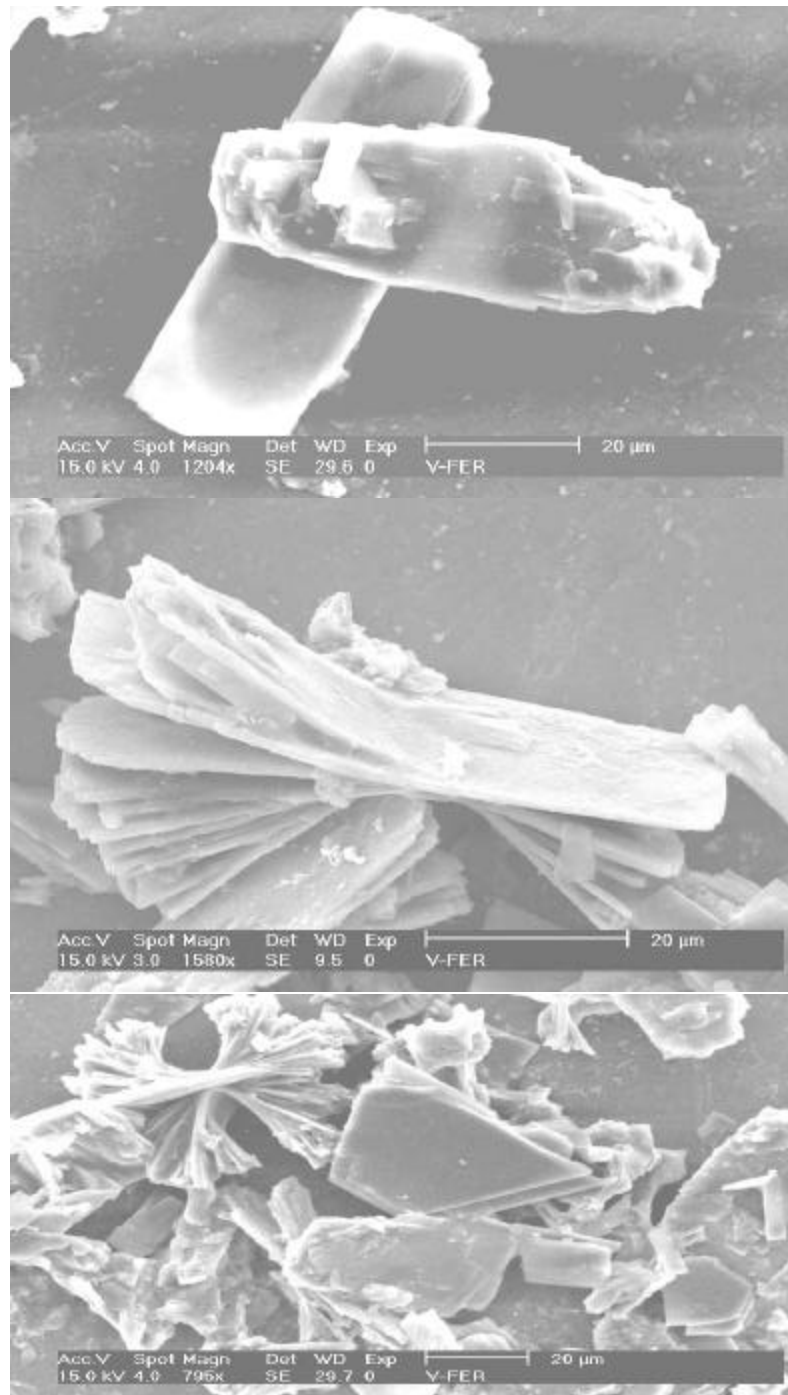
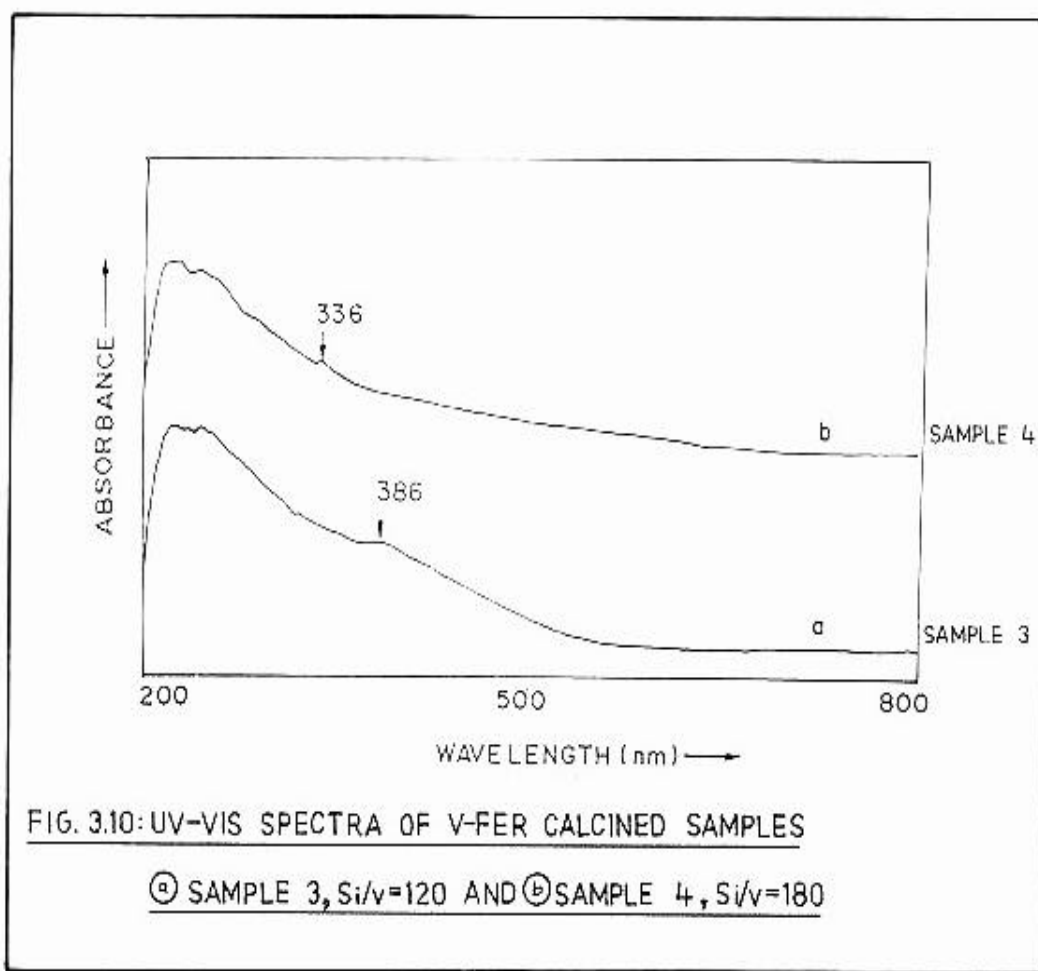


Fig. 3.9: SEM photographs of V-FER (sample 3)

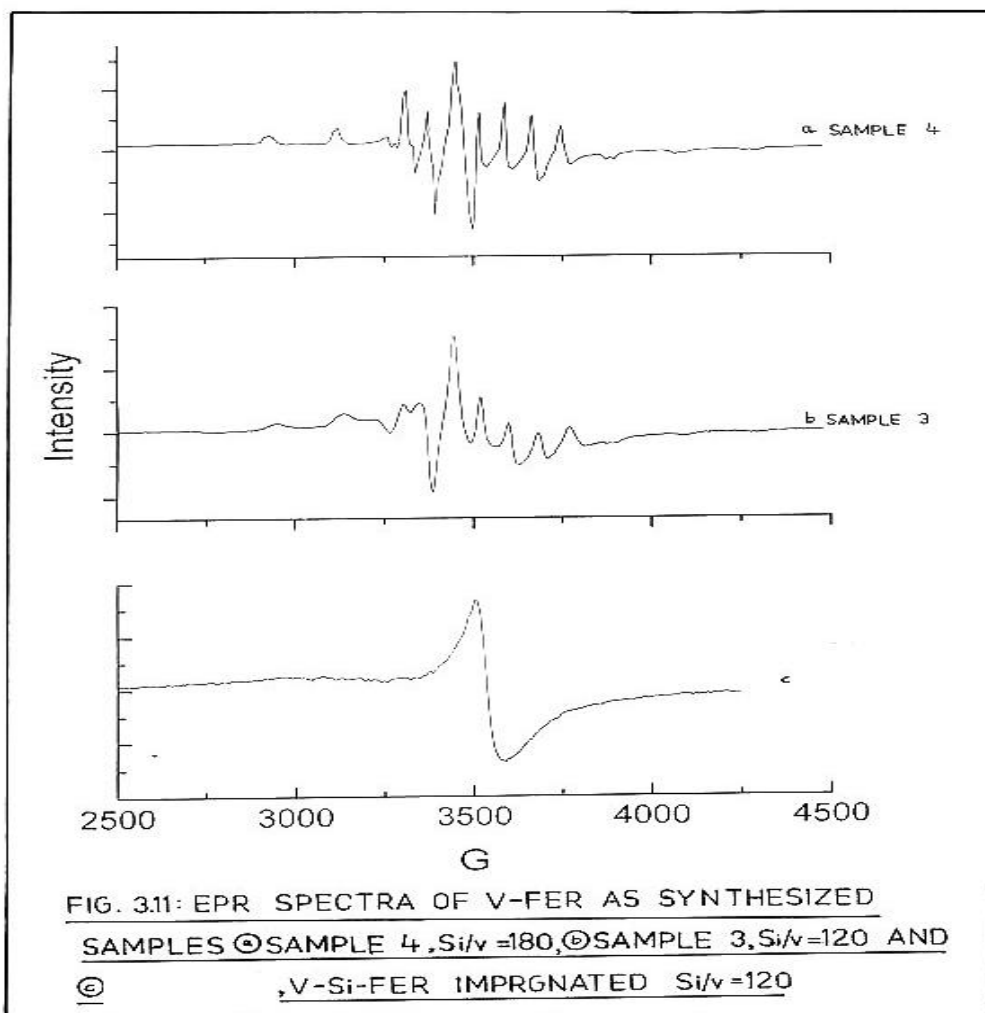
3.3.7 UV-VIS spectroscopy :

Diffuse reflectance UV-VIS is an efficient technique to evaluate qualitatively the presence of vanadium species in the Ferrierite framework [6]. The UV-VIS spectrum (Shimadzu UV-VIS spectrophotometer 2101Pc) of calcined V-FER catalyst shows high intense charge transfer bands in the range 225-250 nm due to V-O bonding (Fig 3.10). The absorption band at 386nm can be assigned to V^{+5} species having V=O bond [6] (Sample 3, Si/V = 120, Fig. 3.10[a]). The 336nm band indicates presence of V^{+5} species in tetrahedral environment (Sample 4, Si/V = 180 , Fig. 3.10[b]). It was observed that as Si/V ratio increased (decrease in vanadium quantity) , the number of vanadium ions in the tetrahedral environment also increased.



3.3.8 Electron Spin Resonance spectroscopy :

In the characterization of vanadium species, ESR spectroscopy plays a very important role in determining its exact oxidation state and position [6]. In zeolite framework vanadium can exist in 3 different oxidation states (eg. III, IV, V). Out of that only V^{IV} is paramagnetic and ESR active, The other 2 states are inactive. The "g" values of the vanadium species are changing according to its co-ordination which helps to locate the exact position of the vanadium species, Fig. 3.11 shows three different ESR spectra of V-FER (Sample 3, 4) and vanadium impregnated Si-FER (Bruker EMX EPR).



The spectra of as-synthesized V-FER (Fig. 3.11; a, b) consists, an anisotropic signal with eight equally spaced hyperfine splittings indicating the presence of paramagnetic atomically dispersed and immobile V^{4+} ions [6,21,22]. The absence of superimposed broad singlet indicates absence of clusters of extraframework vanadium species. The ‘g’ values and hyperfine splitting constants are given in Table 3.7

Table 3. 7 : ‘g’ values and hyperfine splitting constants of the V-FER samples.

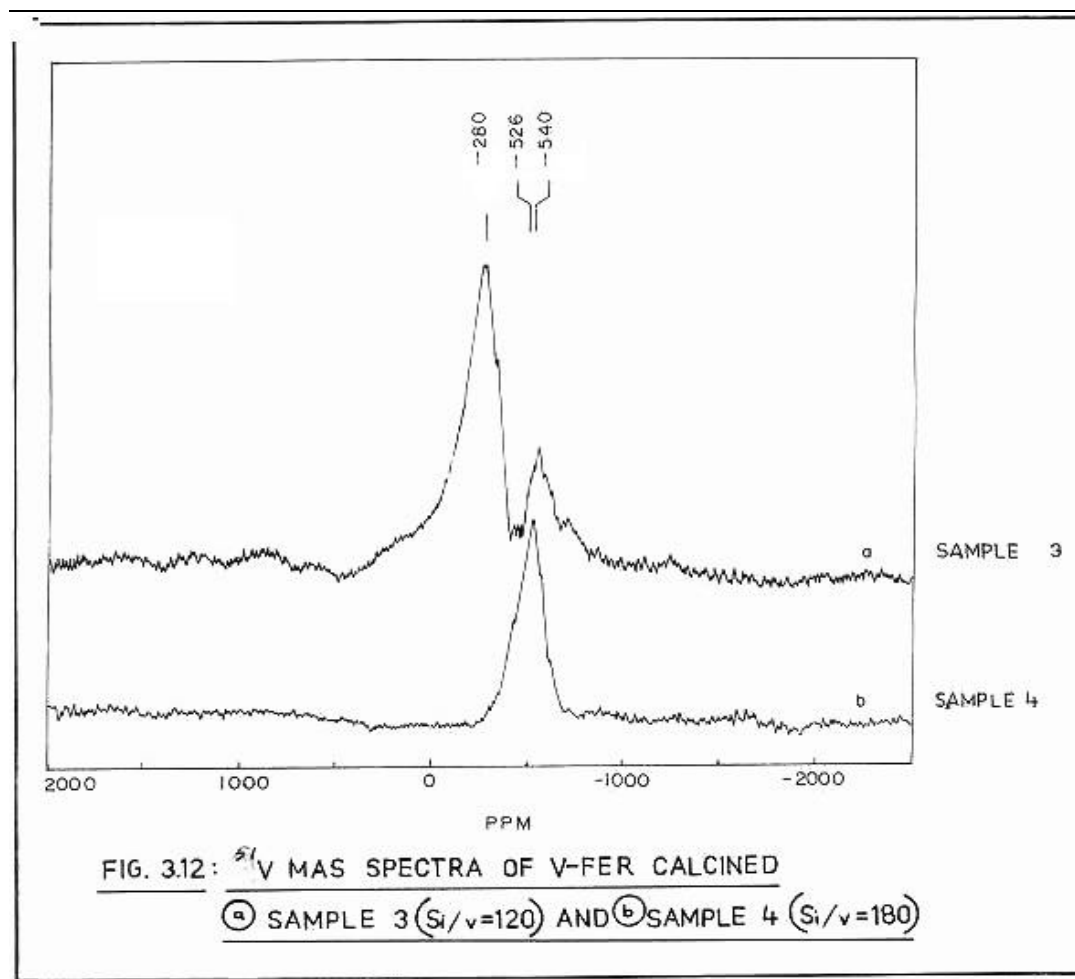
Sample (V-FER)	Si/V	$g_{1/2}$	g_{\perp}	$A_{1/2}$ (G)	A_{\perp} (G)
3	120	1.938	2.000	197.7	69.7
4	180	1.935	1.975	186.8	76

These values are characteristic of vanadyl VO^{+2} species [6,21,22].It indicates that the V^{4+} species in the zeolite may be present in distorted octahedral environment. The spectrum of vanadium impregnated Si-FER (Fig.3.11, c) is totally different from the two V-FER spectra, indicating the extraframework clusters of vanadium species.

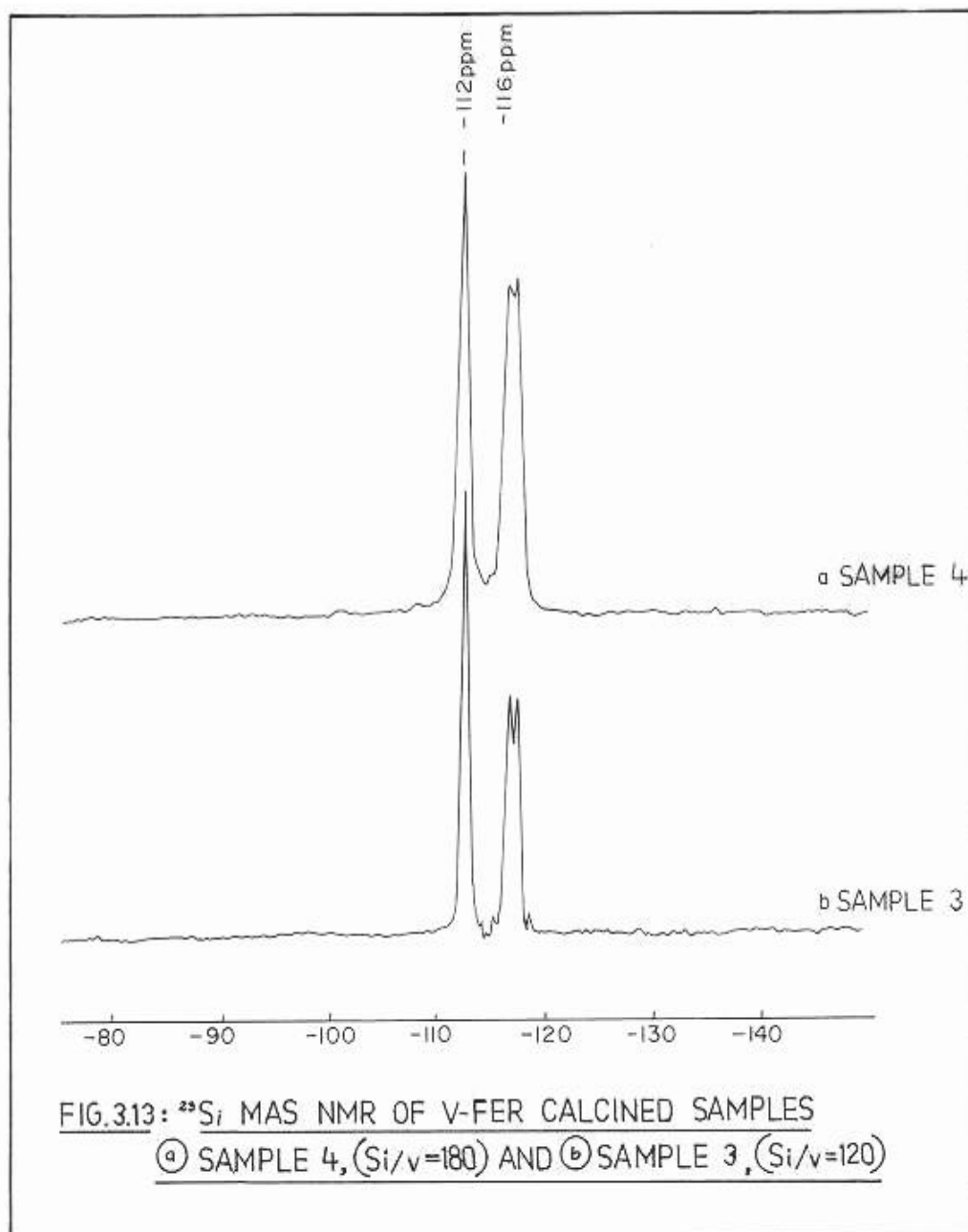
3.3.9 Nuclear Magnetic Resonance spectroscopy :

NMR spectroscopy gives exact idea about all the metal nuclei present in the matter. In the present study, it has been used to identify the nature of the Vanadium and Silicon species in the V-FER zeolite. The spectra for both the elements were recorded with magic angle spinning (MAS) by Bruker MSL-300 NMR spectrometer. The solid state MAS ^{51}V NMR spectra of calcined V-FER samples were recorded. The samples show two different peak positions, one at ~ -300 ppm, which corresponds to V^{5+} in square pyramidal environment [6,22] and the second peak at ~ -530 ppm corresponds to V^{5+} species in tetrahedral position. In Fig. 3.12, the spectra of samples 3 and 4 are shown. Sample with high vanadium content (Sample 3, Si/V = 120, Fig. 3.12[a]) reveals the V^{5+} species present in the structure are mostly in the square pyramidal environment along with small amount in tetrahedral environment. When the

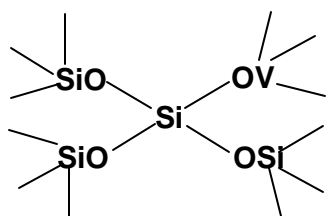
vanadium content was low (Sample 4, Si/V= 180, Fig. 3.12[b]), all the V^{5+} species were present in tetrahedral environment. This confirms that as the vanadium content in FER was reduced, the probability of vanadium ion in tetrahedral co-ordination in the framework is increased. These results are complementary to those obtained from UV studies.



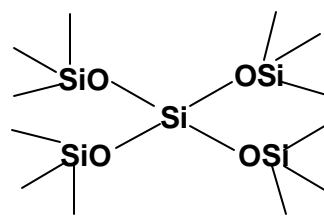
^{29}Si MAS NMR of sample 1 and 2 are shown in the Fig.3.13. The doublet at -116 ppm corresponds to Q_4 species and the sharp single peak at -112 ppm corresponds to Q_3 species. It was observed that the intensity of Q_4 species band in the sample 4 (Si/V = 180) was more than that of Sample 3 (Si/V = 120). This was due to increased vanadium (tetrahedral or square pyramidal) content in case of sample 3 than 4.



Q₃ Species



Q₄ Species



From all these characterization studies, the presence of vanadium in the framework was confirmed (XRD → unit cell expansion; UV → tetrahedral vanadium species and NMR → square pyramidal vanadium species). Moudrakovski et.al.[22]and Kornatowski et.al. [23] have suggested one 'V=O' species which are in the framework in distorted octahedral form but not exactly in the tetrahedral form. However, in the impregnated sample the extraframework vanadium species are totally different (ESR spectra).

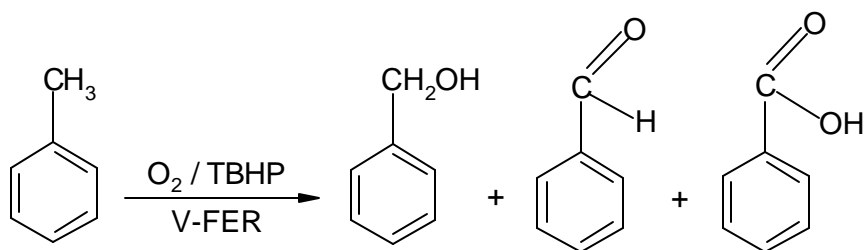
3.4 Catalysis :

Vanadium Zeolites are wellknown for the ir redox properties. It is due to the reversible change in the oxidation states of vanadium species in the zeolites. The liquid phase oxidation of various organic molecules such as the oxyfunctionalization of n-alkanes and cyclohexane, hydroxylation of benzene and phenol, oxidation of toluene, aniline have been reported over VS-2 catalyst [7,24,25,26]. V-Mordenite is highly active in the oxidation of H₂S to sulfur dioxide [27]. Different Vanadium zeolites are active in propane oxidation with molecular Oxygen [28]. VS-1 has been utilized in oxidative dehydrogenation of ethanol [29], selective ammoxidation of xylenes & propane [30,31] and oxidation of butadiene to furan [32].

We have studied 3 different reactions using V-FER as a catalyst.

In the first reaction toluene oxidation was carried out to investigate the oxidative property of the V-FER catalyst. The oxidative property along with the shape selectivity of the V-FER catalyst was tested by the styrene epoxidation reaction. As already mentioned, the vanadium species are redox in nature in the vanadium zeolites. The reducing property of V-FER catalyst was evaluated in gas phase nitrobenzene reduction.

3.4.1 Toluene Oxidation reaction :



Catalytic oxidation of hydrocarbons by heterogeneous catalysts are preferred over conventional routes [33]. Important intermediates, like benzaldehyde and benzoic acid, used in perfumery, pharmaceutical and food industries are obtained by the partial oxidation of toluene. Several catalysts, homogeneous and heterogeneous are reported. Due to the high exothermicity of the reaction some times complete oxidation of the products and reactants occur leading to low selectivities and high conversions. The use of vanadium ferrierite as catalyst with an initiator like TBHP and molecular oxygen from air is described in this study.

3.4.1.1 Experimental :

The experiments were carried out in a batch process containing a stainless steel autoclave. In a typical experimental run, 0.1g of solid catalyst(V-FER) was added to 2.0 ml of toluene (AR grade, S.D.Fine chemicals, India) in 5.0 ml of suitable solvent (e.g. acetone). Then this mixture was placed in a steel autoclave (Parr 4842, 300 ml Fig. 1.4) and about 0.5ml of TBHP [Tertiary butyl hydro peroxide (AR, 70%, S.d.Fine, India)] was added. The autoclave after closing and pressurizing with air to 200 psi was placed in a heater and heated to the desired temperature slowly. The reaction was studied by keeping the autoclave at this temperature for a period of 1.0 h. After the reaction was over, the vessel was cooled, depressurized and then the product was separated by centrifuging it from the solid catalyst. The liquid product was analyzed separately and the catalyst was reused.

3.4.1.2 Product analysis :

The product of the oxidation reaction was analyzed by a gas chromatograph (Shimadzu GC-15A) equipped with packed column (SE-30). The identity of the products was further confirmed by GC-MS (Shimadzu QCMC-QP 2000A)

3.4.1.3 Results and Discussion :

The V-FER samples were catalytically active in the oxidation of toluene. The chemical analysis before and after the reaction of the catalyst showed that there was no leaching of the Vanadium from the framework of the Ferrierite.

Table 3.8 : Chemical compositions of the catalysts before and after the reaction.

Catalyst	Si/V before reaction (By XRF)	Si/V after reaction. (By XRF)
V-FER [Sample 3]	120	122
V-FER [Sample 4]	180	183
V-impregnated Si-FER	120	124

During the reaction benzaldehyde, benzyl alcohol, and benzoic acid were formed. The results at different reaction conditions are summarized in Table 3.9 .

3.4.1.4 Effect of Temperature :

As the temperature of the reaction was increased from 60 to 90 °C the conversion increased from 1.4 % to 7.9 %. Further rise in temperature lead to a decrease of conversion (5.2%). At low temperatures (up to 90°C) almost 50% of the product contained compounds other than benzyl alcohol, benzaldehyde and benzoic acid. At temperatures around 110° C the products other than these three are only 29%. This decrease in selectivity of the other products at high temperature is due to complete oxidation to oxides of carbon. The primary product in the oxidation is benzyl alcohol which on further oxidation converts to benza ldehyde. The benzaldehyde on further

reaction forms benzoic acid. However depending on the experimental conditions and the availability of the oxidant, toluene oxidizes to carbon dioxide and carbon monoxide if the exothermicity is not controlled.

3.4.1.5 Effect of Solvents :

The influence of polar and non-polar solvents on the activity of the catalyst is studied. The activity (conversion of toluene) in polar solvent like acetone was higher as compared to the non -polar solvents. In acetonitrile, the high boiling products are less. But even with solvents like hexane also high concentration of products other than the three are observed. At a temperature of 90°C and in presence of acetonitrile as solvent, the selectivity of partially oxidized products is high. The selectivity to benzyl alcohol and benzaldehyde is about 65%.

The conversion as well as the product distribution varies with the quantity of TBHP. At high TBHP content, the conversion was 3 folds. The secondary oxidation product Benzoic acid was more in that case.

3.4.1.6 Effect of the amount of vanadium :

The conversion also varies with the amount of vanadium present in the catalyst. The vanadium impregnated sample [V-Si-FER (Si/V=120)] has lesser activity as compared to the sample containing same quantity of vanadium in the zeolite framework [sample 3]. The high activity with vanado silicates may be due to the oxy functionalization of toluene only by those vanadium species which are in the framework position. Similar results have been observed in the case of titanosilicates and Vanadosilicates by Tatsmul et.al.[23]and Rao et.al.[25] resp.

3.4.2 Styrene Epoxidation reaction :

The epoxidation of alkenes constitutes one of the most useful reactions in organic synthesis, as the epoxide group is an active intermediate, which can be readily transformed to required functionality in a stereo specific manner. Styrene oxide (obtained by epoxidation of styrene) is commercially important material used for UV-absorbers, drugs, perfumes, sweeteners, etc. Moreover it can also be used as one of the epoxy resin reactive diluents as chain terminating agents to reduce cross-linking density. A number of reports [35-43] on the preparation of styrene oxide using various metal complexes and encapsulated zeolites as catalysts in homogeneous medium are cited in the literature. However, the selectivity towards styrene oxide is lower (5-35%) and the major product is benzaldehyde. High conversion of styrene was reported on TS-1 catalyst [41], a metallosilicate. V-FER being a metallosilicate, with different structure than TS-1; we explore the oxidative properties, epoxidation of styrene using molecular oxygen as oxidant and TBHP as initiator. Styrene oxidation over the V-FER towards styrene epoxide shows higher selectivity than that of homogeneous complexes and encapsulated zeolites.

3.4.2.1 Experimental

The experiments were carried out in the stirred autoclave (Sec. 1.). The catalyst used for the present study was activated in a flow of air at 573 K for 3-5h. Typical reaction procedure include addition of acetone (6.96g, 0.12moles) to styrene (0.502g, 5mmol) followed by addition of TBHP (0.05g, 70% s.d fine chemicals Ltd.). Finally activated V-FER catalyst (0.05g) was added to the solution. The total mass was then transferred into a closed high-pressure stirred autoclave [(Parr 4842, USA) Fig. 1.4]. The autoclave was pressurized to 200 PSI by air and the content of the autoclave is heated from ambient to the desired temperature (time taken to reach the desired

temperature was approximately 15-20 min.) and maintained for 30 min. Finally, the autoclave was quenched with cold water. The contents of the autoclave were subjected to product analysis after separation of the catalyst. Similar procedure was followed for all the other runs.

3.4.2.2 Product analysis:

The product was analyzed by GC (Shimadzu GC-15 A, packed column SE-30 and FID as detector). The components of the product were confirmed by GC-MS (Shimadzu GCMS-QP 2000A, SC-52 column) and GC-FTIR (Perkin Elmer, FTIR spectrometer spectrum 2000).

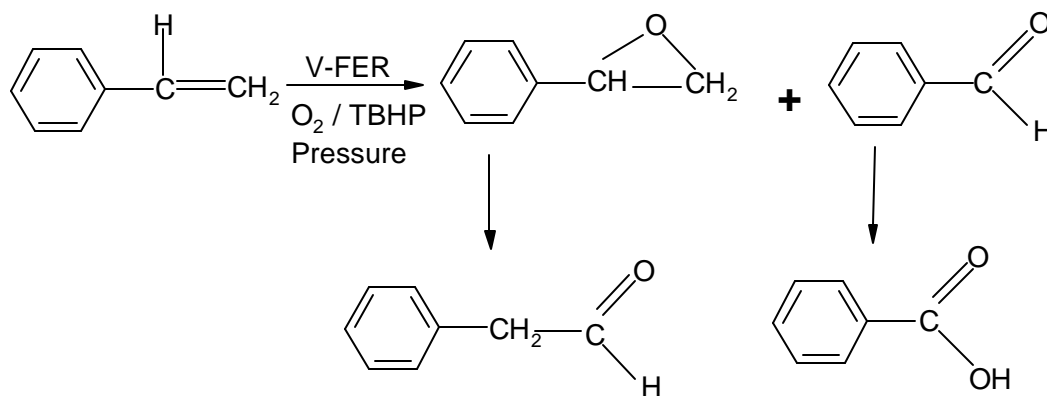
3.4.2.3 Results and Discussion

In the case of V-FER, there was no indication of Vanadium leaching from the catalyst as confirmed by XRF analysis (Table 3.10).

Table 3.10 : Chemical compositions of the catalysts under study.

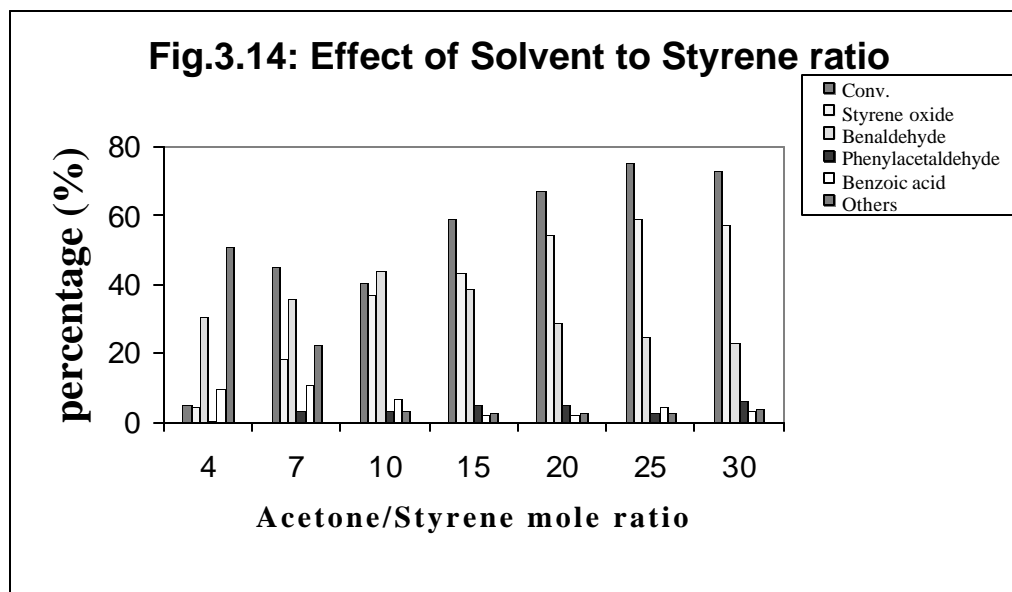
Catalyst	Si/M before reaction (By XRF)	Si/M After reaction. (By XRF)
V-FER(HR) [Sample 3]	120	122
V-FER(LR) [Sample 2]	18	19
TS-FER [44]	114	115
TS-1 [41]		
Fe-FER [45]	16	17
V-impregnated Si-FER		

The primary products of the reaction were styrene oxide and benzaldehyde. Under our reaction conditions it is believed that part of styrene oxide formed was isomerized to phenylacetaldehyde. The formation of benzoic acid was due to the successive oxidation of benzaldehyde. The higher regioselectivity towards phenylacetaldehyde than acetophenone during the isomerization of styrene oxide is due to the formation of more stable α cation adjacent to phenyl ring [46].



3.4.2.4 Effect of solvent to styrene ratio

Fig. 3.14 highlights the influence of acetone to styrene molar ratio on the conversion and the selectivity for styrene epoxide. Solvent dilution was found to have a profound effect on the reaction. When acetone to styrene molar ratio was increased to 25, the conversion increased significantly along with increase in selectivity for styrene epoxide with decrease in formation of benzaldehyde. However, further increase in acetone to styrene molar ratio did not exhibit any significant change both in styrene conversion and selectivity for styrene oxide. Dilution reduces the polymerization of styrene monomer favoring the epoxidation.



3.4.2.5 Effect of solvent polarity

Table 3.11 summarizes the effect of solvent polarity on the styrene epoxidation reaction. It was observed that with the increase in solvent polarity the conversion and selectivity for epoxide increased. Non-polar solvent like cyclohexane showed lower conversion and selectivity as compared to polar solvent such as acetone. Furthermore, it is known [41] that aprotic solvent like acetone, acetonitrile, etc. favors this reaction.

Table 3.11 : Effect of solvents on styrene epoxidation.

Solvent	Styrene Conv. %	Product Distribution Selectivity (%)				
		B	S.O	P.A	B.A	O*
Cyclohexane	57.0	45.44	48.07	4.74	1.23	0.52
Acetonitrile	58.0	38.62	51.38	3.03	2.17	4.80
Acetone	75.3	24.57	59.18	2.92	4.72	8.61

Reaction Conditions: Time = 30 min; Styrene / TBHP (mole ratio)= 12; Solvent/Styrene (mole ratio)= 25;

Catalyst (V-FER) = 0.05g (Si/V=18); Temperature = 373K, Pressure = 200 psi

B = Benzaldehyde; S.O = Styrene Oxide; P.A = Phenylacetaldehyde; B.A = Benzoic acid; O = Other unidentified high boilers and polymers.

3.4.2.6 Effect of Temperature and pressure on Styrene epoxidation

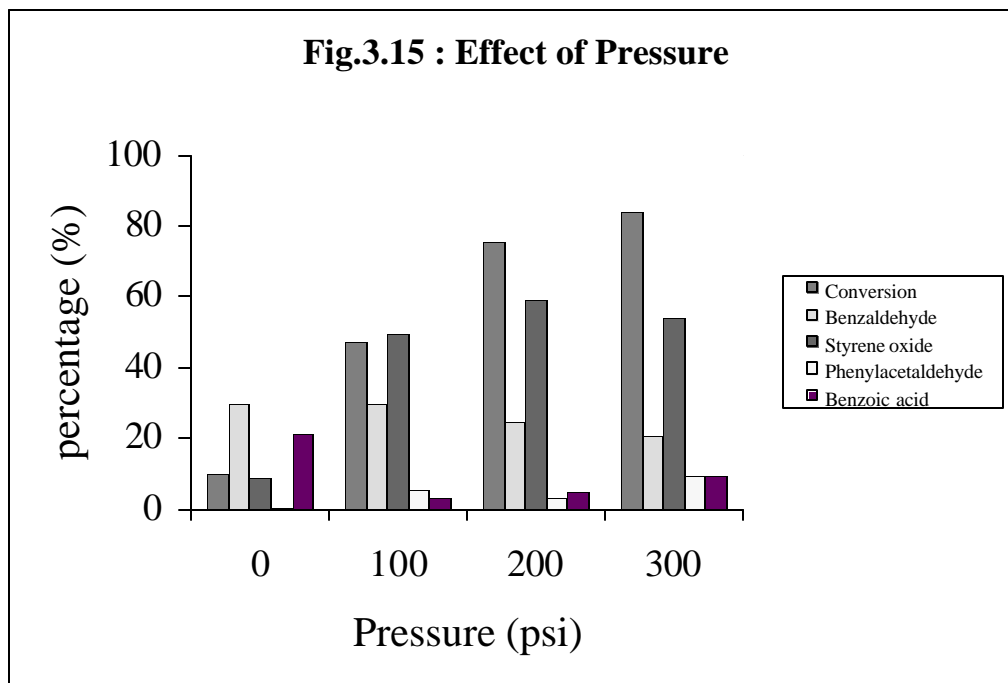
Table 3.12 describes the effect of temperature on styrene epoxidation. As expected the conversion increased with the increase in temperature, however, the increase in selectivity of styrene epoxide was not linear. When the temperature was increased from 353 K to 373 K (at 200 psi), selectivity of styrene oxide increased, but on further increase of temperature (i.e. to 393 K) the selectivity for benzaldehyde and phenylacetaldehyde increased at the expense of styrene oxide. According to Reddy *et al.*[46] at lower temperature cleavage of olefinic (C = C) was higher while at higher temperature formation of epoxide seems to be favored.

Table 3.12 : Effect of temperature on styrene epoxidation

Temperature °C	Styrene Conv. (%)	Product Distribution Selectivity (%)				
		B	S.O	P.A	B.A	O
353	63.9	30.05	49.14	5.01	1.41	14.30
373	75.3	24.57	59.18	2.92	4.72	8.61
393	82.1	43.01	33.01	5.85	9.78	8.35

Reaction Conditions: Pressure = 200 psi; Time = 30 min; Styrene/ TBHP (mole ratio) = 12; Solvent/Styrene (mole ratio) = 25; Catalyst (V-FER) = 0.05g (Si/V=18); (Solvent = Acetone)
 B = Benzaldehyde; S.O = Styrene Oxide; P.A = Phenylacetaldehyde; B.A = Benzoic acid and O= Other unidentified high boilers and polymers.

Figure 3.15 displays the influence of pressure at 373 K. The conversion increased with the increase in pressure. When the pressure was increased from 100 to 300 psi the selectivity for styrene oxide remained nearly constant however, selectivity for phenylacetaldehyde as well as others increased and that for benzaldehyde decreased. At high pressure the styrene oxide formed may be rapidly isomerizing to phenylacetaldehyde.



3.4.2.7 Effect of different transition metal substituted molecular sieves on styrene epoxidation :

Table 3.13 summarizes the effect of different metals and their amount in the substituted metallosilicate molecular sieves for styrene epoxidation. Vanadosilicates with two different Si/V ratio were investigated. The conversion of styrene increased with the increase in Si/V ratio. This may be due to well-dispersed vanadium ions in FER structure, in the case of V-FER (HR). Even though V-FER (HR) with $\text{SiO}_2/\text{V}_2\text{O}_5 = 120$ was found to give higher conversion, Ti-FER ($\text{SiO}_2/\text{TiO}_2 = 114$) exhibited higher selectivity for styrene oxide. Under similar reaction conditions, TS-1 was found to give benzaldehyde as major product along with low styrene oxide, however, Ti-FER exhibited better selectivity for styrene oxide. This may be related to structural differences of FER and TS-1 type molecular sieves. In the case of Vanadium impregnated sample, increase in conversion was observed, however, the selectivity for styrene oxide decreased significantly, yielding higher amount of low and high boilers including polymers. This indicates that surface vanadium is not selective. Fe-FER showed higher conversion but poor selectivity for styrene oxide and the major product being benzaldehyde, high boilers and polymers, indicating Fe-FER is active but not selective for epoxidation. It is known that styrene epoxidation with molecular oxygen alone gives 50% conversion with selectivity ratio for benzaldehyde and styrene oxide as 1:1 [47]. When the reaction was carried out in nitrogen atmosphere with TBHP as oxidant the conversion was about 60% with lower boilers as major constituent (~34 %). The above results indicate that molecular oxygen plays an important role in this reaction. Further when the above reaction was carried out in the absence of a catalyst the conversion decreased (~ 23 %) and benzaldehyde and polymers are the major products. The reaction is also carried out in the presence of

air and in the absence of catalyst (373 K, 200 psi). In this case conversion is almost complete with 50% as polymeric material. This shows that the presence of catalyst increases the selectivity for styrene oxide and reduces polymeric materials.

Table 3.13 : Effect of different transition metal substituted metallocate molecular sieve zeolites for styrene epoxidation

Catalyst	Styrene Conv. (%)	Product Distribution Selectivity (%)				
		B	S.O	P.A	B.A	O
V-FER(LR)	75.3	24.57	59.18	2.92	4.72	2.52
V-FER(HR)	85.5	27.75	52.43	9.32	3.57	2.4
Ti-FER	76.5	24.31	57.42	7.97	2.48	1.83
TS-1	84.7	38.02	24.56	27.86	3.78	2.48
V-impregnated Si-FER	94.7	45.13	7.39	7.91	5.43	29.99 ^a
Fe-FER	87.0	33.79	17.25	13.46	7.64	20.85
V-FER ^b	60.0	37.5	10.17	3.5	7.83	36.67 ^a
C	23.3	40.77	3.61	3.43	9.58	41.46
D	99.2	26.21	3.33	0.71	12.1	50.32

Reaction Conditions:

Temperature = 373 K; Pressure = 200 psi; Time = 30 min; Styrene/TBHP (mole ratio)= 12;

Acetone /Styrene (mole ratio) = 25; Catalyst = 0.05g

B = Benzaldehyde; S.O = Styrene Oxide; P.A = Phenylacetaldehyde; B.A = Benzoic acid and O = Other unidentified high boilers and polymers.

a = lower boilers benzene, toluene. ; b = Reaction carried out in the presence of N₂ atm and catalyst.

C = Reaction carried out in the absence of catalyst and in presence of N₂ atm.

D = Reaction carried out in the absence of catalyst and in presence of air.

3.4.3 Hydrogenation of Nitrobenzene :

Hydrogenation of Nitrobenzene is a well-known reaction for testing the reducing property of the catalyst. This reaction had been reported on various Homogeneous [48] and Heterogeneous catalysts [49]. The gas phase hydrogenation of Nitrobenzene

has been studied on V-FER catalysts. Four major products are forming. The product contains aniline, nitrosobenzene, azobenzene and azoxybenzene. During the reaction the catalyst was first reduced to lower oxidation state of Vanadium by hydrogen treatment and then reacted with Nitrobenzene.

3.4.3.1 Experimental :

Catalytic studies were carried out at atmospheric pressure, in a fixed bed, down flow, integral silica reactor.[F ig.1.6] About 3.0 g. of V-FER catalyst (10-20 mesh, Sample 3, Si/V = 120) was placed at the center of the silica reactor, which was placed vertical in the electric furnace (Geomechanique, France). Hydrogen gas was passed through the reactor at 400 °C at the rate of 20 ml/min to reduce the catalyst for 3 hours. The temperature was brought to the desired reaction temperature in presence of hydrogen flow. Nitrobenzene at the rate of 3 ml per hour was then fed with a syringe pump (Sage instruments, USA). Hydrogen flow was adjusted in such a way that the hydrogen to nitrobenzene mole ratio is three to four. Reaction products were condensed by passing through cold water and samples were collected at various intervals of time. Reaction parameters such as feed flow rate, time, temperature of the reaction were varied and the data was collected.

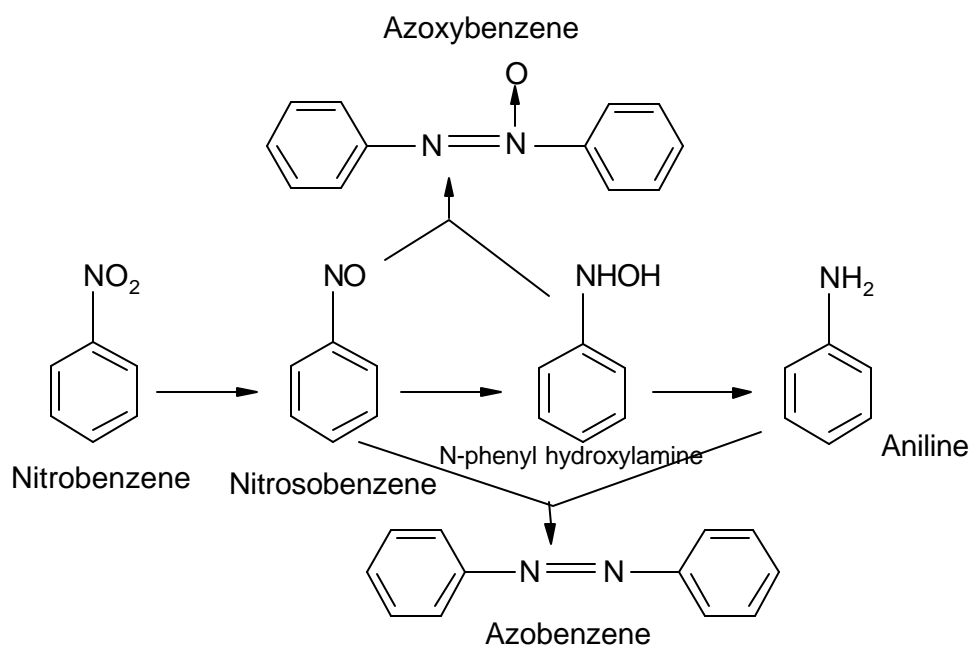
3.4.3.2 Product analysis:

The product was analyzed by GC (Shimadzu GC-15 A, packed column SE-30 and FID as detector). The products were also confirmed by GC-MS (Shimadzu GCMS-QP 2000A, SC-52 column) and GC-FTIR (Perkin Elmer, FTIR spectrometer spectrum 2000).

3.4.3.3 Results and Discussion :

Four major products were identified in the reaction. Nitrosobenzene and aniline are the primary hydrogenation products while azobenzene and azoxybenzene the secondary products. The possible reaction mechanism is shown in Fig. 3.16 .

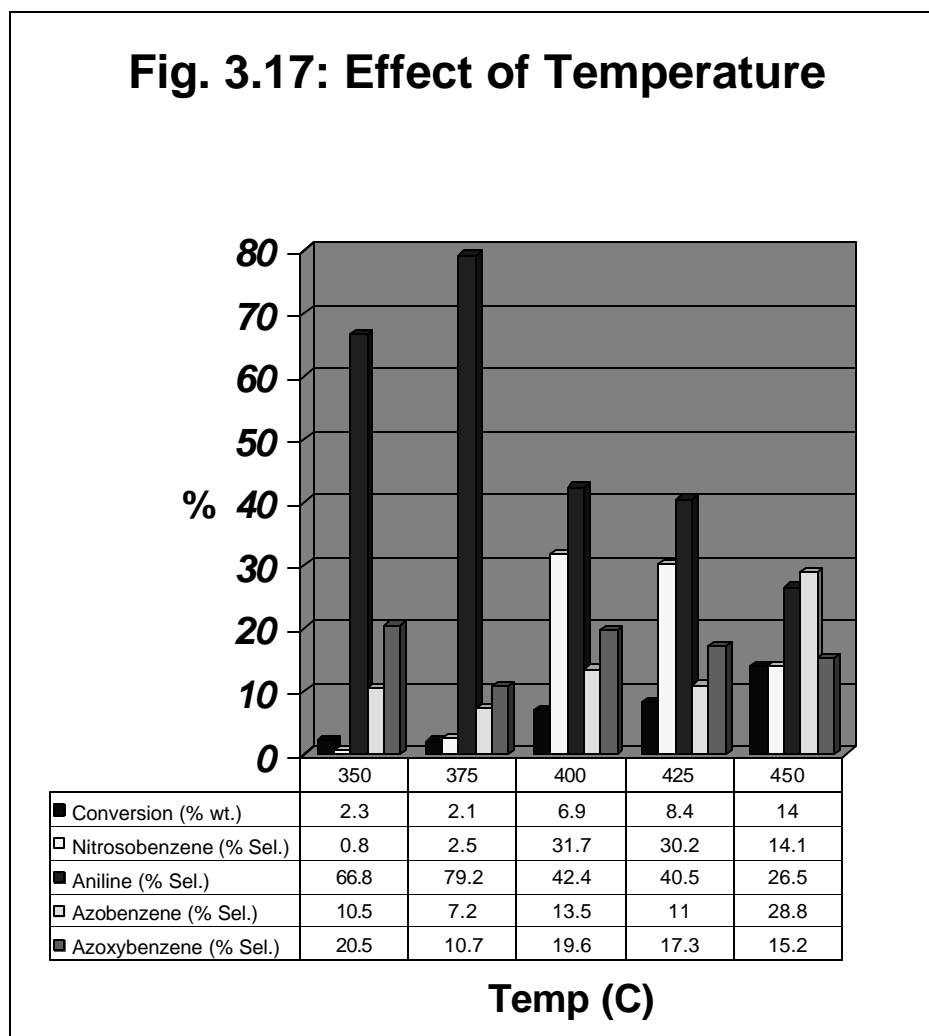
Fig.3.16: Mechanism of Nitrobenzene hydrogenation.



3.4.3.4 Effect of Temperature :

The reaction was studied in between the temperature range 350 to 450°C. The conversion of nitrobenzene was increasing with the increase of temperature. Four compound were observed in the product in addition to unconverted nitrobenzene. At low temperatures (below 400 C) the formation of nitrosobenzene and azobenzene are less. However, the aniline selectivity was around 80 % at 375 C. Further increase in temperature led to the formation of more nitrosobenzene and more azobenzene. However, azoxybenzene selectivity is in between 15-20 percent at all temperatures.

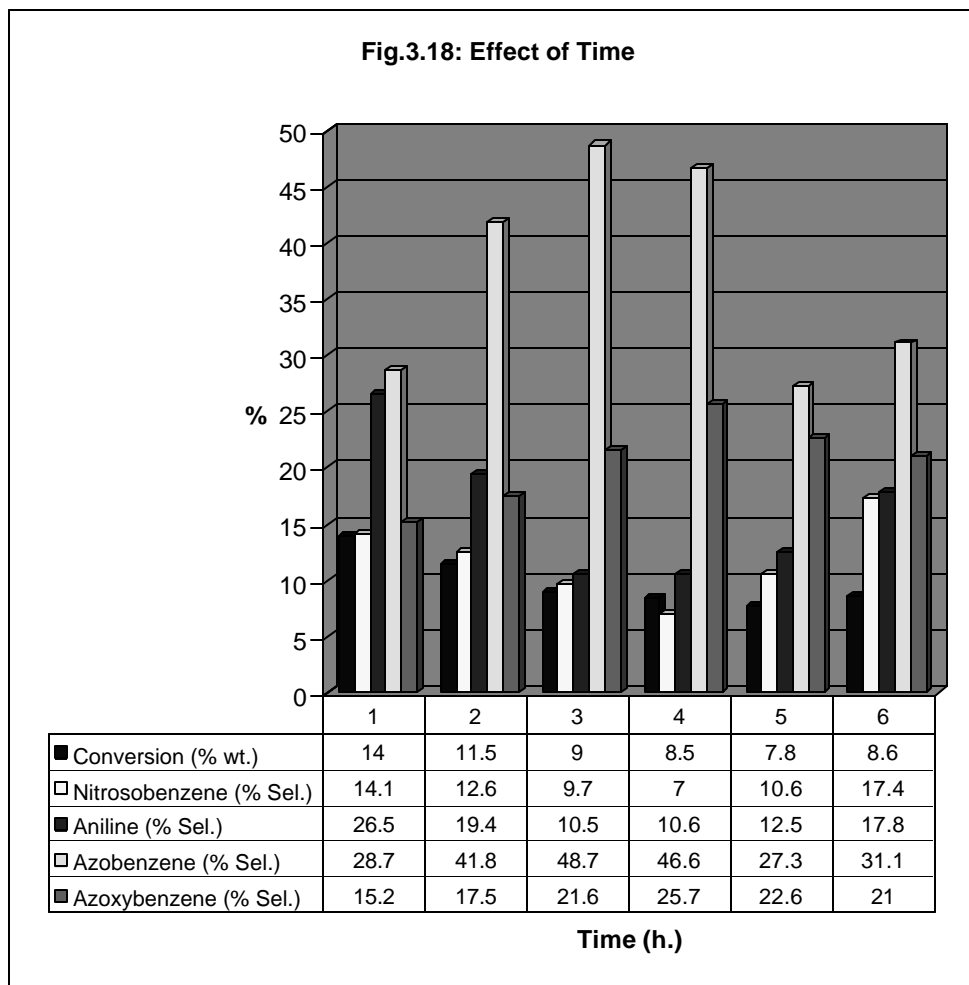
The effect of temperature is shown in Fig. 3.17 . The other reaction conditions are as follows : Time =1.0h.; W.H.S.V.= 1.0; H₂/nitrobenzene = 4.0



3.4.3.5 Time on stream study :

When the reaction is carried out for longer time the conversion goes on decreasing, indicating the deactivation of the catalyst. The aniline formation also decreased. However, the formation of azobenzene and azoxybenzene has a marginal increase. For the formation of aniline, hydrogenation activity of the catalyst is important where as azobenzene and azoxybenzene are formed by the reaction of aniline and nitrosobenzene on any acidic catalyst. When the reaction took place for the longer hours, the hydrogenation activity was reduced due to the strong adsorption of the

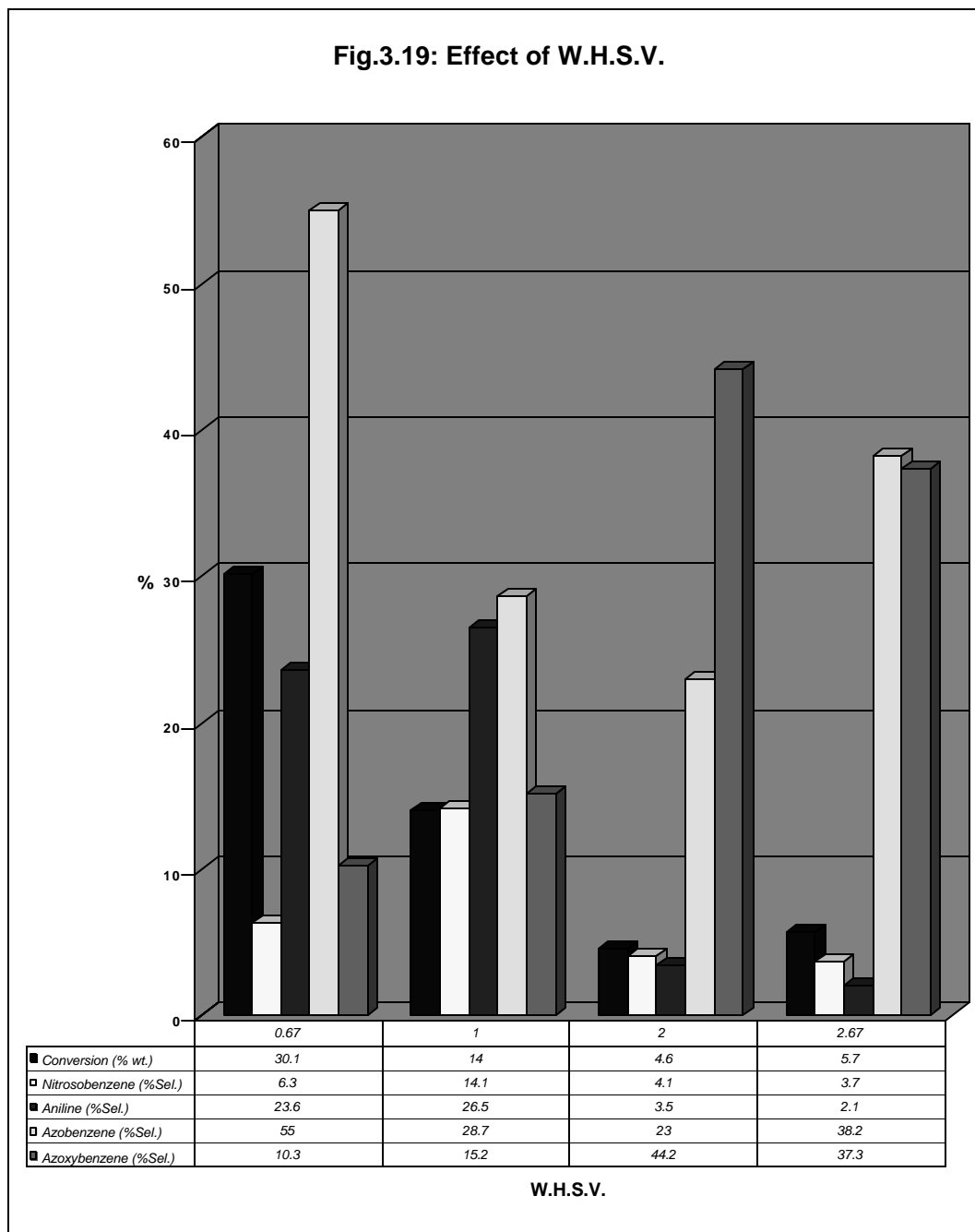
formed products on the active sites. This is represented in Fig. 3.18. The other reaction conditions are as follows : Temp =450°C; W.H.S.V.= 1.0; H₂/nitrobenzene = 4.0



3.4.3.6 Effect of W.H.S.V. :

At very low W.H.S.V. the conversion of nitrobenzene was very high. The nitrosobenzene formation was almost same at all space velocities. At higher space velocities, aniline concentration in the product is less. This is due to the formation of azoxybenzene as a secondary reaction. The primary product of the reaction was nitrosobenzene which converts to N-phenyl hydroxylamine and subsequently to aniline depending the concentration of hydrogen and the active sites. However, the

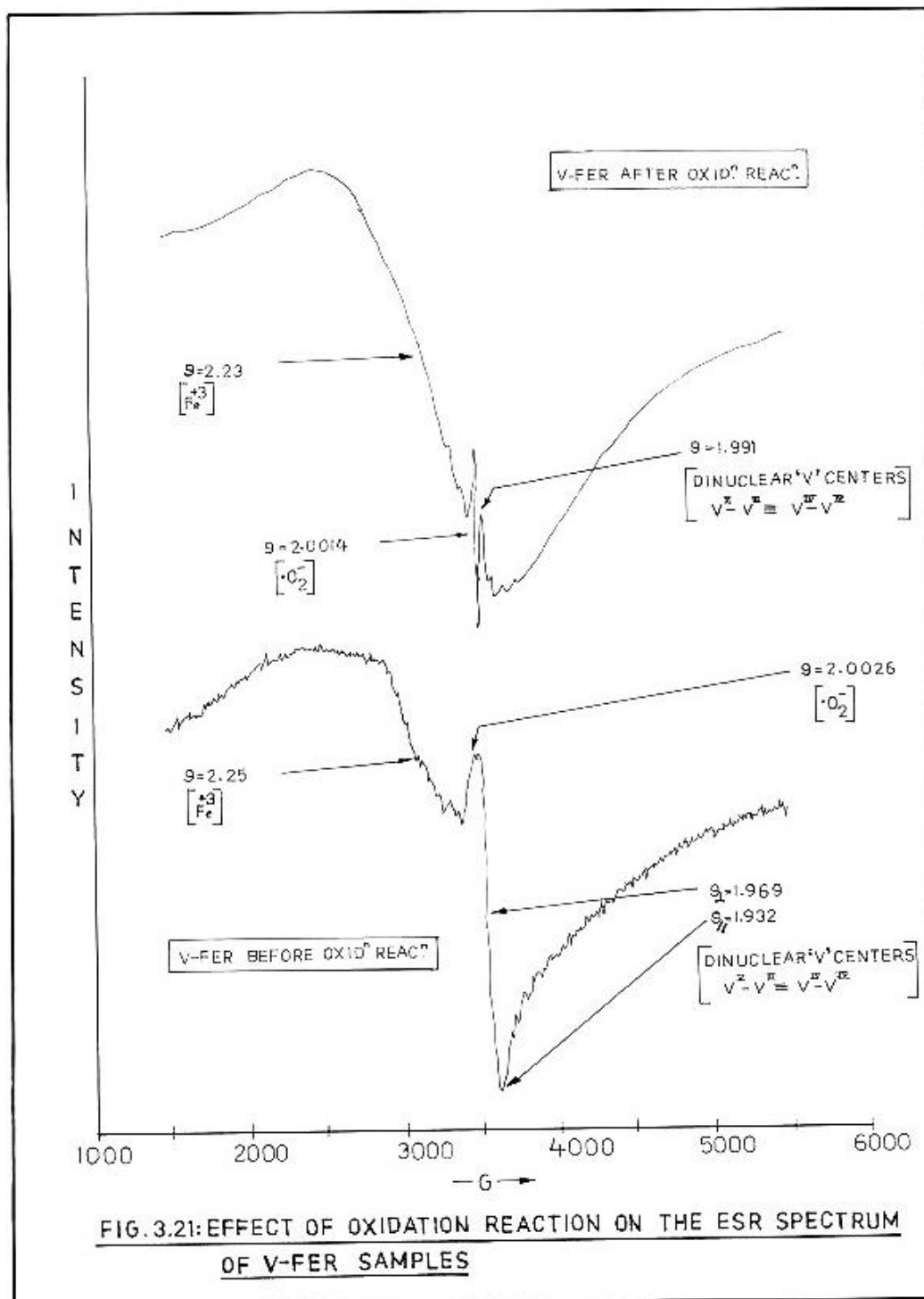
secondary reactions in which the formation of azoxybenzene and azobenzene can take place between final product aniline and the intermediate products which needs an acidic sites. Since this zeolite is acidic, these products are formed in large quantities. This is explained in Fig 3.19. The other reaction conditions are as follows : Time =1.0h.; Temp=450°C; H₂/nitrobenzene = 4.0



3.5 ESR spectroscopy of the redox behavior of vanadium species in V-FER :

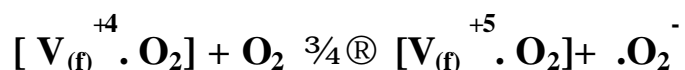
It has been demonstrated that vanadium in the ferrierite structure V-FER is present in a distorted octahedral geometry (3.3.8). It is well known that vanadium as vanadyl ion " VO^{+2} " acts as a redox catalyst. The V-FER catalyst oxidizes toluene to benzyl alcohol, benzaldehyde and benzoic acid (3.4.1) using molecular oxygen as an oxidant and a small amount of tetra butyl hydrogen peroxide (TBHP) as an initiator. It is also shown that V-FER catalyses the hydrogenation reaction of Nitrobenzene to Nitrosobenzene, Aniline, Azobenzene and Azoxybenzene (3.4.3). In the later reaction, the catalyst was initially treated with a flow of hydrogen gas (20 ml / min. at 450 C for 2h.). ESR spectroscopy is used to investigate the active vanadium species in the redox reactions.

Calcined sample of V-FER were yellow and showed a broad asymmetric ESR signal with $g_{||} = 1.932$ and $g_{\perp} = 1.968$ (Fig.3.21).

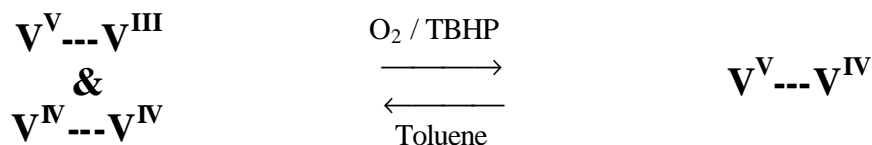


Unlike those of as-synthesized samples (Fig.3.11), the calcined V-FER did not show hyperfine coupling features due to vanadium. During the process of calcinations dinuclear vanadium species of the type $V^{IV} \cdots V^{III}$ and $V^{IV} \cdots V^{IV}$ are formed [50,51]. As

a consequence of a spin-spin interactions within the dimer species, ESR signals are broad. During the oxidation reaction with O₂/ TBHP the signals due to V^V---V^{III} and V^{IV}---V^{IV} disappeared, instead a weak signal due to V^{IV} ion showing resolved hyperfine features [g_{av} = 1.991] along with a sharp signal at g = 2.0014. The later signal is assigned to a super oxide radical ion [O₂⁻] formed during the process of oxidation reaction as described below[51].



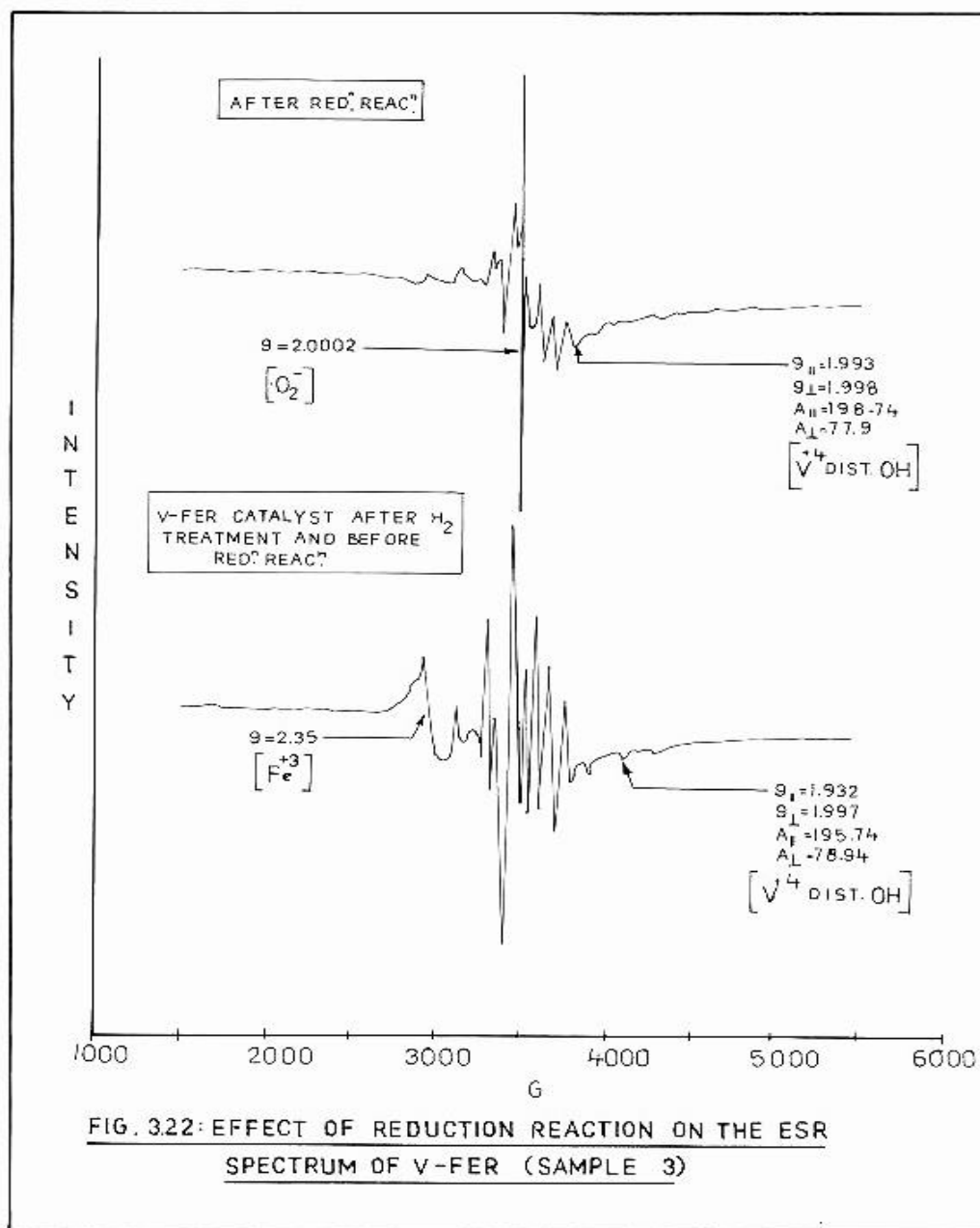
The signal at g = 1.991 is attributed to oxidized form of the vanadium species [V^V---V^{IV}].



The signal at g = 2.23 is a Fe⁺³ impurity in V-FER samples which does not take part in the redox reaction [52].

Reaction with hydrogen showed a spectrum with resolved vanadium hyperfine features in both parallel and perpendicular regions [Fig. 3.22 A]. The ESR parameters [g_{||} = 1.932, g_⊥ = 1.997 and hyperfine splitting constants A_{||} = 195.74G, A_⊥ = 78.94G] of the reduced samples corresponds to that of monomeric vanadyl ions with a octahedral geometry. Before hydrogen treatment these species are probably present as V^V ions. Upon treating the reduced catalyst with Nitrobenzene, the intensity of the signals have decreased. Also the formation of a radical species at g = 2.002 was observed. The reduction in the intensity of V^V signal is due to their re-oxidation to V^V ions after participating in the hydrogenation reaction. The dinuclear species originally present in the V-FER catalyst [V^V---V^{III} and V^{IV}---V^{IV}] got reduced

to an inactive $V^{II} \rightarrow V^{III}$ species which do not participate in the hydrogenation reaction.



All the above study confirms the presence of three different vanadium species in the samples.

1] V^{+4} in the framework position

2] Dimer like $V^V \cdots V^{III}$ OR $V^{IV} \cdots V^{IV}$ and

3] V^{+4} in distorted octahedral coordination.

The ESR studies of the reactions revealed that the di nuclear vanadium centers which are present probably in extraframework locations participate in the oxidation reaction while the dispersed vanadium species in the framework structure are responsible for the hydrogenation reaction.

3.6 Conclusion :

A novel medium pore vanadium silicate with FER structure has been synthesized for the first time. Unit cell volume and XRD pattern confirmed the phase purity and incorporation of vanadium in the framework. ESR technique confirmed that some of the V^{+4} are present in distorted octahedral position in Ferrierite framework. UV-vis and NMR confirmed the presence of V^{+5} (tetrahedral) species in the framework.

It was also observed that as vanadium content in the catalyst increased the non tetrahedral framework species increased. All these spectroscopic information indicated the presence of isolated, well-dispersed vanadium ions are stabilized within the zeolitic lattice.

V-FER acts as good oxidation catalyst in Toluene Oxidation reactions . The activity of the catalyst was found to be better in polar solvents like acetone. The vanadium quantity affect the product formation and the vanadium species in the catalyst affect the selectivity of the product. The oxidation reaction occurred due to the $V(V) \cdots V(III)$ OR $V(IV) \cdots V(IV)$ dimer vanadium species present in the catalyst.

V-FER is a highly selective catalyst in styrene epoxidation reaction to synthesize important styrene oxide.

Nitrobenzene Hydrogenation reaction was carried out on V-FER to test the reducing property of the catalyst. The well dispersed V(IV) species in distorted octahedral environment acted as reducing agent in this reaction.

References :

1. F.A.Cotton and G.Wilkinson in " Advanced Inorganic Chemistry ", Wiley Eastern ; 1972, 818.
2. A.Thangaraj, S.Sivasankar and P.Ratnasamy ; J.Catal., 1991, **131**, 294.
3. P.R.H.Prasad Rao, A.V.Ramaswamy and P.Ratnasamy ; J.Catal., 1992, **137**, 225.
4. C.Marosi, J.Sttaberow, M.Schwarzmann; Ger. Pat. 2831631, 1978.
5. R.Xu and W.Pang ; stud. Surf. Sci. Catal.; 24, 1985, 27.
6. G.Centi, S.Perathoner, F.Trifiro, A.Aboukais, C.F. Aissi and M.Guelton ; J.Phys. Chem., 1992, **96**, 2617.
7. P.R.H.Prasad Rao, A.A.Belhekar, S.G.Hegde, A.V.Ramaswamy and P.Ratnasamy; J.Catal., 1993, **141**, 595.
8. A.Tuel and Y.Ben Taarit; Zeolites; 1994, **14**, 18.
9. K.M.Reddy, I.Moudrakovski and Sayari, J.C.S.Chem. Comm., 1994, 1491.
10. K.R.Reddy, A.V.Ramaswamy, and P.Ratnasamy; J.Catal., 1993, **143**, 275.
11. Chen, Shu-Hua, Ho, Jan-Cheng, Mon, Shine-Su; Zeolites, 1997, **18(2/3)**, 182.
12. Chao K.J., Wu C.N., Chang. H., Lee L.J, Hu., Shufen.; J.Phys. Chem., 1997, **101**, 6341.
13. Siddhesh Shevade and B.S.Rao; J.Mater. Chem.; 9, 1999, 2459.
14. A.Kuperman, S.Nadami, S.Oliver, G.A.Qzin, J.M.Graces and M.M.Olken, Nature, 1993, 365, 239.
15. A.J.Avrami ; J.Chem.Phys. ; 9, 1941, 177
16. C.R.Erofeev ; Acad. Sci. U.S.S.R.; 52, 1945, 511.
17. A.N.Kotasthane, V.P.Shiralkar, S.G.Hegde and S.B.Kulkarni; Zeolites ; 6, 1986, 233.
18. R.Szostak, "Handbook of Molecular Sieves"; Van Nastrand, New York, 1884, 201.
19. A.J.Chandawadkar, R.N.Bhal and P.Ratnasamy; Zeolites; 11, 1991, 42.
20. B.Wichterlova, Z.Tvaruzkova, Z.Sobalík, P.Sarv; Microporous and Mesoporous Mater.; 24, 1998, 223.
21. M.Narayana and L.Kevan ; J.Phys.C: Solid state Phys., 1983, **16**, 1-863.
22. I.L.Moudrakovski, A.Sayari, C.L.Ratcliffe, J.A.Ripmeester and K.F.Preston ; J.Phys. Chem., 1994, **98**, 10895.
23. T.Tatsumi, M. Nakamura, S.Negishi and H.Tominaga; J.Chem.Soc.,Chem Commun, 1990, 476.
24. J.Kornatowski, B.Wichterlova, M.Rozwdowski and W.H.Baur; Stud. Surf. Sci. Catal.; 1994, **84**, 117.
25. P.R.H.Prasad Rao, A.V.Ramaswamy, P.Ratnasamy ; J.Catal.; 141(2), 1993, 604.
26. P.R.H.Prasad Rao, A.V.Ramaswamy, P.Ratnasamy ; Appl. Catal. A.; 93(2), 1993, 123.
27. R.H.Hass, R.C.Hansford, H.Henning; U.S.Pat. 4,088,743 , 1978.
28. G.Centi and F.Trifiro; Appl. Catal. A; 143(1), 1996, 3.
29. S.Kannan, T.Sen, S.Shivashankar ; J.Catal.; 170(2), 1997, 304.
30. F.Cavani, F.Trifiro, K.Habersbergen, Z.Tvaruzkova ; Zeolites, 8 , 1988 , 12.
31. A.Miyamoto, T.Iwamoto, H.Matsuka, T. Inui ; Stud. Surf. Sci. Catal. ; 49B, 1989, 1233.
32. Z.Tvaruzkova, G.Centi, P.Jiru, F.Trifiro ; Appl. Catal. ; 19, 1985, 307
33. M.Suzuki, K.Tsutsumi, H.Takahashi and Y.Saito ; Zeolites ; 8(5), 1988, 387.
34. P.R.H.P.Rao and A.V.Ramaswamy; J.Chem. Soc. Chem. Commun., 1992, 1245.
35. Park, Yuchul; Kim, Seong Su. Bull. Korean Chem. Soc. 13(5), (1992) 458.

36. Shum, Wilfred P.; Kesling, Ha ven S., Jr. US Patent 5103027 (1992).
37. Varkey, Saji P.; Ratnasamy, Chandra; Ratnasamy, Paul J. Mol. Catal. A: Chem., 135(3), 295-306 1998
38. Kanai, Hiroyoshi; Hayashi, Hirokatsu; Koike, Tatsuya; Ohsuga, Makoto; Matsumoto, Masakatsu J. Catal., 138(2), 611-16 1992.
39. Xu, Cheng-Hua; Lu, Shao-Jie; Qiu, Fa-Li Hecheng Huaxue, 6(3), 283-286 1998.
40. Neri, C. and Buonomo, F., Eur Pat. 102, 097 (1984).
41. Sujit B. Kumar, S.P.Mirajkar, Godwin C.G. Pais, Pradeep Kumar , Rajiv Kumar J. Catal. 156, (1995) 163.
42. Suprun, Wladimir Chem. Tech 49(2), (1997) 67.
43. Hata,Eiichiro ; Takahashi, Katsuya; Isauama, Shigem Jpn. Pat. 05025149 (1993).
44. R.K.Ahedi and A.N.Kotasthane J.Mater.Chem., 8 (1998) 1685.
45. S.S.Shevde, R.K.Ahedi and A.N.Kotasthane Catalysis Lett. 49 (1997) 69.
46. Reddy, J.S., Khire,U.R. Ratnasamy.P and Mitra,R.B., J.Chem.Soc. Chem.Comm. (1992) 1234 .
47. Rueffer,Ljudmila; Hoefft, Euan. Chem. Tech 43(9) (1991) 300.
48. T.Banerjee, T.Mondal, C.R.Saha; Chem. Ind.; 6 (1979) 212
49. N.J.Jebarathinam, M.Eswaramoorthy and V.Krishnasamy, Stud. Surf. Sci. Catal.; 113, 1998, 1039.
50. B.I.Whittington and J.R.Anderson ; J.Phys. Chem.; 97, 1993, 1032.
51. P.Fejes, I.Marsi, I.Kiricsi, J.Halasz, I.Hannus, A.Rockenbauer, G.Tasi, L.Korecz and G.Schobel; in " Zeolite Chemistry and Catalysis " Eds. P.A.Jacobs., 1991, 173.
52. A.Bruckner, P.Luck, W.Wieker, B.Fahlke and H.Mehner ; Zeolites, 12 1992, 380.

CHAPTER IV

SUMMARY

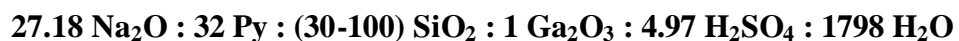
: SUMMARY :

Natural and synthetic forms of ferrierite zeolite contain framework structure comprising of aluminum (Al^{+3}) and silicon (Si^{+4}) ions in the tetrahedral coordination. During synthesis of gallium ferrierite (Ga-FER) by hydrothermal route, substitution of Ga^{+3} ion in place of Al^{+3} , in the framework position, is achieved. Vanadium ferrierite (V-FER) contains some vanadium ions in place of silicon ions. For the incorporation of V^{+4} ions in place of framework Si^{+4} ions, the non-aqueous synthetic route; i.e. organothermal synthesis similar to silicon ferrierite, was followed. The synthesis of the silicon analog of ferrierite is not reported in aqueous medium. The details of the synthesis, characterization and catalytic applications of these gallium and vanadium modified zeolites, are described

.4.1 Gallium ferrierite(Ga-FER) :

4.1.1 SYNTHESIS:

The Ga-FER was synthesized by using pyrrolidine as a template in hydrothermal synthesis route. The molar composition used is:



where : Py is pyrrolidine.

Three Ga-FER samples were synthesized with three different Si/Ga molar input ratios. Precautions were taken in autoclave cleanliness and maintenance of pH during the synthesis. Otherwise ferrierite phase may change into α -Quartz or ZSM-5 etc. The synthesis kinetics followed the sigmoid curve.

4.1.2 CHARACTERIZATION:

The main objective of the characterization was to locate the exact position of incorporated Ga^{+3} ion.

The phase purity of the modified ferrierite is detected by XRD technique. The incorporation of bulkier Ga^{+3} ion in ferrierite framework results in the increase of unit cell volume, as evidenced by the XRD pattern of the Ga-FER samples.

The tetrahedral position of the Ga^{+3} ion in the framework is further confirmed by ^{71}Ga MAS-NMR spectroscopy which indicates a single peak at ~ 150 ppm. These results were supported by ^{29}Si MAS NMR. All the 3 samples show 2 peaks in ^{29}Si NMR which are assigned to Q_3 and Q_4 silicon species. It means that the concentration of Q_3 species corresponds to the Ga^{+3} tetrahedral ions bound with Si^{+4} ions. This quantitative analysis is also comparable with the chemical analysis.

The acidity of the Ga-FER catalyst was found by CD_3CN adsorption on the sample followed by FTIR spectroscopic measurements. It was found that Ga-FER is moderately acidic compared to Al-FER and Fe-FER. The acidity trend is in the order : Al-FER > Fe-FER > Ga-FER.

The Ga-FER sample is highly stable till 1000°C , according to Thermal Analysis.

SEM results reveal the morphology of the Ga-FER samples. The photographs indicate plate like shape having non-uniform crystals of size 2-5 μm .

4.1.3 CATALYTIC REACTIONS :

Ga-FER catalyst is active and highly selective in the hydroxylation of benzene using nitrous oxide as an oxidant. The main objective in doing this reaction is to find an alternative route for the production of phenol by a single step process by avoiding the

present multi step cumene route utilizing corrosive and polluting catalytic systems. The utilization of the hazardous "Green House Gas " N_2O for this will be an eco-benign and economically viable process. The activity of the catalyst is due to the presence of special type of α -surface species generated by the tetrahedral Ga^{+3} ions in the zeolite framework. Ga-FER catalysts deactivate very fast in both the above mentioned reactions. This may be due to the pore blocking by the reactants and products in the small '8 MR' channels of the medium pore ferrierite zeolite restricting the molecular traffic control phenomenon observed in the medium pore zeolites..

The Ga-FER catalyst is less acidic than Al-FER. It is tested in the alkylation reaction of benzene with ethanol. The conversion of ethanol is around 90% ,but secondary products contributing to lower selectivity are more as compared to ZSM-5. Loss in activity is noticed with time. The activity in terms of conversion increases with increase of temperature. However, the byproducts like toluene, xylene ,cumene and other higher aromatics are more at higher reaction temperatures. These are mainly due to the structural differences between ZSM-5 and ferrierite, the former ,contributing to the molecular traffic control. Due to lower ethanol conversions and high by product formation it can't be considered as an alternative to ZSM- 5.

4.2 Vanadium ferrierite (V-FER) :

4.2.1 SYNTHESIS:

A novel medium pore vanadium silicate with FER structure has been synthesized for the first time. The synthesis was carried out in nonaqueous pyridine medium with HF as dissolving agent, which increases solubility of V^{+4} ion in the system and thus supporting

the zeolite nucleation. Four V-FER samples with different Si/V ratio have been synthesized.

4.2.2 CHARACTERIZATION:

XRD patterns confirmed the phase purity, unit cell volume information confirms incorporation of vanadium in the framework. The unit cell volume increases with increase in the vanadium content in the zeolite but not exactly proportional.

ESR technique (at $g_{\parallel}=1.935$, $g_{\perp}=1.975$ and $A_{\parallel}=186.8$, $A_{\perp}=76$ G) confirmed that some of the V^{+4} ion are present in distorted octahedral position in ferrierite framework.

UV-VIS (peak at 336 nm) and ^{51}V MAS NMR (peak at -530 ppm) confirmed the presence of V^{+5} (tetrahedral) species in the framework. ^{29}Si MAS NMR (peak at -112 ppm) supports the presence of heteroatom attached with the Si^{+4} ion in the V-FER framework.

It was also observed that as vanadium content in the catalyst increased the non tetrahedral framework species increased. The spectroscopic information indicated the presence of isolated, well-dispersed vanadium ions, stabilized within the zeolitic lattice.

The crystal size of the V-FER catalyst is much more than normal Al-FER. The morphology is plate like and crystallites varied in size between 20-50 μm . The large size is due to the effect of synthesis medium HF.

4.2.3 CATALYSIS :

V-FER acts as good catalyst in toluene oxidation reaction. The activity of the catalyst was found to be better in polar solvents like acetone. The quantity of vanadium influence the product formation and the vanadium species in the catalyst affect the selectivity of the product.

V-FER is a highly selective oxidizing agent for the epoxidation of styrene to styrene oxide reaction. In this case it was more active than the conventional homogeneous and heterogeneous catalysts like TS-1 etc.

Nitrobenzene hydrogenation reaction was carried out on V-FER to investigate the reducing property of the catalyst.

When the catalysts(V-FER) after the oxidation and reduction reactions were examined by ESR spectroscopy, surprising results were observed. Three types of vanadium species were present in the samples.

- 1] V^{+4} in the framework position
- 2] Dimer like $V^V\text{---}V^{III}$ OR $V^{IV}\text{---}V^{IV}$ and
- 3] V^{+4} in distorted octahedral coordination.

Out of these 3 species the oxidation reaction occurred only due to the $V^V\text{---}V^{III}$ OR $V^{IV}\text{---}V^{IV}$ dimer vanadium species.

The well dispersed V^{IV} species in distorted octahedral environment was responsible for the reducing action.

This study indicated that the $V^{IV}(Td)$ in the framework is not contributing to the redox nature of the V-FER catalyst.

The detailed studies on the gallium and vanadium ferrierites are included in the chapters two and three respectively. Introductory chapter contains the general methods of zeolite synthesis, characterization techniques and the application of zeolites. Also the available data on ferrierite, both patented and published in open literature is included in this chapter. Chapter one also includes the aim and objectives of this work.

This summary of the work is presented in the last chapter.

: List of Publication :

1. "Synthesis and characterization of ferrisilicate analogs of ferrierite(Fe-FER) zeolite"
S.S.Shevade, R.K.Ahedi and A.N.Kotasthane
Catalysis letters , 49 (1997) 69-75.
2. "Copper (II) phthalocyanines entrapped in MFI zeolite catalysts and their application in phenol hydroxylation"
S.S.Shevade, Robert Raja and A.N.Kotasthane
Applied Catalysis A: General, 178 (2) [1999] Pg. 243-249
3. " Synthesis of vanadium analog of silicious FER "
S.S.Shevade and B.S.Rao
J. Mat. Chemistry, 1999, 9, 2459-2462
4. "Titanosilicate derivative of NU-1 framework zeolites (TS-NU-1)"
R.K.Ahedi, **S.S.Shevade** and A.N.Kotasthane
Zeolites , 18 (1997) 361.
5. "Interpreting the oxidative catalytic activity in Iron substituted Ferrierite using in-situ Mössbauer spectroscopy"
K.Lazar, G.Leieune, R.K.Ahedi, **S.S.Shevade** and A.N.Kotasthane
Journal of Physical Chemistry B 102 (1998) 4865.
6. " Anovel titanium analog of NU-1 framework zeolite (TS-NU-1)"
R.K.Ahedi, **S.S.Shevade** and A.N.Kotasthane
Stud. Surf. Sci. Catal. 113 (1997) 201
7. "Benzene Alkylation with ethanol on FER type zeolites"
Siddhesh Shevade, R.K.Ahedi, A.N.Kotasthane and B.S.Rao
"Recent Trend in Catalysis", Ed. Murugesan et.al.; Narosa Publishig House, 1999
p.383
8. "Epoxidation of styrene with TBHP/O₂ over Ferrierite (FER) type molecular sieves"
R.Anand, **Siddhesh Shevade**, R.K.Ahedi and B.S.Rao
Catalysis Letters 62 (1999) 209-13
9. "Gas phase Hydroxylation of Benzene over H-Ga-FER Zeolite."
Siddhesh S. Shevade and B.S.Rao
Accepted in '*Catalysis Letters*'
10. " Study of redox behavior of vanadium species in V-FER by ESR spectroscopy "
S.S.Shevade, D.Srinivasan and B.S.Rao
Submitted to '*Mesoporous and Microporous Materials*'
11. " Effect of acid sites of metal analogs of Ferrierite on m-Xylene isomerization."
S.S.Shevade, R.K.Ahedi, Satish Kuriyaware, Sobalik, B.S.Rao and A.A.Belhekar
Submitted to '*Catalysis Letters*'

: List of Papers presented at Symposia :

1. " Non-templated synthesis of Ferrierite (FER) type zeolites "
R.K.Ahedi, **S.S.Shevade** and A.N.Kotasthane
Presented at 12th Workshop on Catalysis, Bhavnagar' 1995.
2. "Synthesis and characterization of a new Fe-FER zeolite"
S.S.Shevade, R.K.Ahedi and A.N.Kotasthane
Presented at 13th Workshop on Catalysis, Thiruanantpuram' 1997.
3. "Synthesis, characterization and catalysis of a new V-FER zeolite"
S.S.Shevade, N.R.Shiju and B.S.Rao
Presented at 14th Workshop on Catalysis, Hyderabad' 2000.
4. " Synthesis of ϵ -Caprolactam over Ferrierite (FER) type zeolite "
R.Anand, **S.S.Shevade**, R.K.Ahedi and B.S.Rao
Presented at NCL Golden Jubilee Symposium on Catalysis, 1999.
5. " Utilization of Nitrous oxide gas in phenol preparation "
S.S.Shevade and B.S.Rao
Presented at 87th session of Indian Science Congress; 2000.

: List of Patents :

1. " A process for the preparation of a novel titanium rich NU-1 zeolites "
A.N.Kotasthane, R.K.Ahedi, **S.S.Shevade** and A.V.Ramaswamy
IP 3515/DEL/97 (dt. 8th Dec.,97)
2. " A process for the preparation of encapsulated metal phthalocyanine silicates designated as encilite-En "
A.N.Kotasthane, R.Raja and **S.S.Shevade**
NF-148/97
3. " Process for the preparation of crystalline ferrisilicate ferrierite type zeolite "
A.N.Kotasthane, R.K.Ahedi, **S.S.Shevade** and A.V.Ramaswamy
NF-202/97
4. " Process for the preparation of crystalline ferrierite type aluminosilicate "
A.N.Kotasthane, R.K.Ahedi, **S.S.Shevade** and A.V.Ramaswamy
NF-201/97
5. " Process for the preparation of crystalline titanosilicate ferrierite (TS-FER) from non-aqueous medium "
A.N.Kotasthane, R.K.Ahedi, **S.S.Shevade** and A.V.Ramaswamy
NF-203/97.
6. " A process for the preparation of Phenol "
B.S.Rao and **S.S.Shevade**
NF-261/99
7. " Process for the preparation of ultrathin films of molecular sieves "
S.D.Sathye, K.R.Patil, D.V.Paranjape, **S.S.Shevade** and P.N.Joshi
NF-328/99

